Impact of neuronal CPEB2 on the translation of mRNAs involved in synaptic plasticity

Dissertation

zur

Erlangung des Doktorgrades (Dr. rer. nat)

der

Mathematisch-Naturwissenschaftlichen Fakultät

der

Rheinischen Friedrich-Wilhelms-Universität Bonn

vorgelegt von

Sada Lakshmi Turimella

aus

Guntur, Indien

Bonn, January 2013

Angefertigt mit Genehmigung der Mathematisch-Naturwissenschaftlichen Fakultät der Rheinischen Friedrich-Wilhelms-Universität Bonn

1. Gutachter Prof. Dr. Martin Theis

2. Gutachter Prof. Dr. Klaus Willecke

Tag der Promotion: 02.05.2013

Erscheinungjahr: 2013

Declaration

I solemnly declare that the work submitted here is result of my own investigation except where otherwise stated. This work has not been submitted to any other university or institute towards the partial fulfilment of any degree.

Bonn, January 2013

Sada Lakshmi Turimella

Acknowledgements

I would like to thank **Prof. Dr. Martin Theis** for giving me the opportunity to perform my doctoral studies in his laboratory at the Institute of Cellular Neurosciences, Bonn. I would like to extend my gratitude towards him for supervising my project and giving valuable suggestions and support and also for consistent encouragement throughout my project.

I owe my sincere gratitude to **Prof. Dr. Christian Steinhäuser** for his constructive discussions throughout my project work.

I would like to thank **Prof. Dr. Klaus Willecke, Prof. Dr. Walter Witke and Dr. Andreas Waha** for kindly accepting my request to be in the doctoral committee.

I am especially grateful to **Dr. Gerald Seifert, Dr. Peter Bedner and Mr. Vamshidhar Reddy Vangoor** for their help regarding Single cell RT-PCR experiments.

I would like to thank **Prof. Dr. Georg Zoidl** for giving me an opportunity to perform experiments with the primary hippocampal cultures in his laboratory at the Ruhr University, Bochum.

I would like to thank **Joana Fischer** and **Anja Matijevic** for technical assistance and also for their support. I thank the members from the Institute of Cellular Neurosciences for their support. I would like to thank **Mrs. Yvette Simons** and **Dr. Ines Nauroth** for helping me with the administrative things.

I would like to thank the **people from House for Experimental Therapy (HET),** Bonn for maintaining various transgenic mice lines and providing them whenever in need.

I would like to express my deepest gratitude towards **my mother, father and brother;** especially **my parents**, whose unwavering love and blessings, their continuous support and encouragement made me feel confident always in all times. I would like to thank my beloved husband **Vamshi** for his constant encouragement and incredible moral support. I would like to thank all my friends for making my stay in Germany a memorable one.

Table of Contents

Abbreviations ..... **I**

1 Introduction **1**

1.1 Synaptic plasticity 1

1.2 Synapse-specific local protein synthesis 4

1.3 Mechanisms of translational regulation 4
1.3.1 RNA binding proteins 5

1.4 The CPEB family 5
1.4.1 Mechanism of CPEB regulation 8
1.4.2 Role of CPEBs in different cell types 9
1.4.3 CPEBs in synaptic plasticity, learning and memory 10
1.4.4 CPEBs in Epilepsy 11

1.5 CPEB2 11
1.5.1 Putative targets of CPEB2 12
1.5.1.1 β-catenin 12
1.5.1.2 GluR2 14
1.5.1.3 GluR2 interacting partners 16
1.5.1.4 EphA4 18

1.6 Conditional transgenic systems to study gene function in vivo 20

2 Aim of the thesis **23**

3 Materials and Methods **24**

3.1 Materials 24

3.1.1 Chemicals 24
3.1.2 Buffers for Western blotting 24
3.1.3 Buffers for RNA Co-immunoprecipitation 26
3.1.4 Solutions for Genotyping 27
3.1.5 Solutions for Immunocytochemistry (ICC) 28
3.1.6 Solutions for Immunohistochemistry (IHC) 28
3.1.7 Ready-to-use solutions 29
3.1.8 Antibiotics 30
3.1.9 Restriction Enzymes 30
3.1.10 DNA Polymerases 30
3.1.11 Antibodies 31
3.1.11.1 Primary Antibodies 31
3.1.11.2 Secondary Antibodies 32
3.1.12 Kits used 32
3.1.13 Competent E. *coli* 33
3.1.14 Molecular weight markers 33

3.1.15 General lab materials 33
3.1.16 Laboratory Equipment 34
3.1.17 Softwares used 35

3.2 Methods 36

3.2.1 RT-PCR of rat/human hippocampus 36
3.2.2 Immunocytochemistry 37
3.2.3 Single cell RT-PCR 38
3.2.3.1 Harvesting cytoplasm from neurons, astrocytes, NG2 glia and microglia 38
3.2.3.2 Reverse transcription of RNA to first strand cDNA 39
3.2.3.3 Two round multiplex PCR 39
3.2.3.4 Analysis of the PCR products 42
3.2.4 Generation of vectors for generation of transgenic mice 43
3.2.4.1 Restriction digestion of pMM403-400 vector 43
3.2.4.2 Amplification of insert (CPEB2-EGFP/CPEB2ΔZn-EGFP) 43
3.2.4.3 Infusion cloning 44
3.2.4.4 Analysis of clones 45
3.2.5 Generation of transgenic mice with overexpression of CPEB2/CPEB2ΔZn in pyramidal neurons of mouse hippocampus 45
3.2.6 Screening of newborn mice for transgene expression 46
3.2.6.1 Lysis of tail tips from mice and isolation of DNA 46
3.2.6.2 Genotyping (tTA and *tet*O PCRs) 46
3.2.6.3 Breeding of *tet*O-CPEB2/*tet*O-CPEB2ΔZn mice with CamKII-tTA mice 47
3.2.7 Analysis of transgenic mice 47
3.2.7.1 Perfusion and cryosectioning 47
3.2.7.2 Immunohistochemistry 48
3.2.8 Analysis of target protein levels in CPEB2/CPEB2ΔZn transgenic mice 48
3.2.8.1 Isolation of mouse hippocampus 48
3.2.8.2 Preparation of hippocampal protein lysates 49
3.2.8.3 Western blotting 49
3.2.8.4 Quantification of blots 50
3.2.9 Analysis of transcript levels of different targets in CPEB2/CPEB2ΔZn transgenic mice 50
3.2.9.1 Isolation of RNA from mouse hippocampus 50
3.2.9.2 Reverse transcription of RNA into cDNA 51
3.2.9.3 Estimating the efficiencies of real time PCR primers 52
3.2.9.4 Quantitative real time PCR 52
3.2.10 RNA Co-immunoprecipitation 53
3.2.10.1 Generation of CPEB2-FLAG construct 53
3.2.10.2 Generation of EphA4 3'UTR-PGL construct 53
3.2.10.3 Transfection of HeLa cells 54
3.2.10.4 Co-immunoprecipitation 54
3.2.10.5 Isolation of RNA from co-immunoprecipitated samples 55
3.2.10.6 Quantitative real time PCR 55
3.2.11 Dual luciferase reporter assay 56
3.2.12 Rapid Amplification of cDNA Ends (3' RACE) of CPEB2 57

4 Results 59

4.1 CPEBs in rat and human brain hippocampus 59
4.2 CPEBs in PHCs 60
4.3 Single-cell RT-PCR: Expression of CPEBs in neurons and glia 61
4.4 In-fusion cloning of CPEB2/CPEB2ΔZn into pMM403-400 65
4.4.1 Cloning 65
4.4.2 Verification of clones 65
4.5 Generation of CPEB2/CPEB2ΔZn transgenic mice 66
4.6 Screening of newborn mice for the presence of the transgene 67
4.7 Screening of lines for transgene expression 68
4.7.1 Screening different lines for CPEB2 transgene expression 68
4.7.2 Screening different lines for CPEB2ΔZn transgene expression 68
4.8 Analysis of transgenic mice 69
4.8.1 Immunofluorescence of CPEB2-EGFP 69
4.8.2 Immunofluorescence of CPEB2ΔZn-EGFP 72
4.9 Analysis of protein levels of putative targets in CPEB2/CPEB2ΔZn mice 73
4.9.1 CPEB2 represses the basal translation of β-catenin in neurons 74
4.9.1.1 β-catenin downregulation *in situ* 74
4.9.1.2 Decreased β-catenin protein levels in CPEB2 overexpressing mice 75
4.9.1.3 CPEB2- β-catenin co-immunoprecipitation 76
4.9.2 CPEB2 represses the basal translation of GluR2 in neurons 77
4.9.3 GluR1 protein levels were unaltered in CPEB2 overexpressing mice 78
4.9.4 The protein levels of GluR2 interacting proteins were not altered in CPEB2 overexpressing mice 79
4.9.5 CPEB2 represses basal translation of EphA4 (a new CPEB target) in neurons 80
4.9.5.1 Decreased EphA4 protein levels in CPEB2 overexpressing mice 80
4.9.5.2 CPEB2 interacts with EphA4 *in vitro* 81
4.9.6 Synaptophysin protein levels were unaltered in CPEB2 overexpressing mice 82
4.9.7 No change in basal protein levels of β-catenin/GluR2/EphA4 in CPEB2ΔZn overexpressing mice 83
4.10 Estimating the efficiencies for Real Time PCR primers 83
4.11 Analyzing the transcript levels of putative targets by real time PCR 85
4.12 Interaction of CPEBs with other target mRNAs 86
4.12.1 CPEB2 interacts with the CamKIIα 3'UTR 86
4.12.2 CPEB2 interacts with Cx36 3'UTR 86
4.13 Rapid Amplification of cDNA ends (3' RACE) of CPEB2 87
5 Discussion 89

5.1 Cell type specific expression of CPEBs: Single-cell RT-PCR 89
5.2 CPEB2/CPEB2ΔZn overexpressing mice 90
5.3 CPEB2 regulates β-catenin translation in neurons 91
5.4 CPEB2 might participate in Ca^{2+} permeability by regulating GluR2 translation in neurons 92
5.5 CPEB2 does not regulate the translation of GluR1, an AMPA receptor subunit 93
5.6 The GluR2 interacting partners are unaffected by CPEB2 in neurons 93
5.7 CPEB2 might participate in neuron to glia communication by regulating EphA4 protein levels 94
5.8 CPEB2 regulates each target mRNA differentially 95
5.9 The presence of the zinc finger is essential for CPEB2 mediated translational regulation 97
5.10 CPEB2 might be a putative target for other CPEBs 98

6 Future directions 99

7 Summary 101

8 References 104

9 Appendix 116

A 9.1 Preparation of TOP10 chemically competent E. coli 116

A 9.2 Single-cell RT-PCR 117
A 9.2.1 Expression of CPEB1 in neurons 117
A 9.2.2 Expression of CPEB3 in neurons (A), astrocytes (B), NG2 glia (C) and microglia (D) 117
A 9.2.3 Expression of CPEB4 in neurons (A), astrocytes (B), NG2 glia (C) and microglia (D) 118

List of Figures 119

List of tables 121

Curriculum Vitae 122

Abbreviations

^{o}C	degree Celsius
α-tubulin	alpha tubulin
β-actin	beta actin
β-catenin	beta catenin
µg	microgram
µl	microlitre
µM	micromolar
ABP	AMPA receptor Binding Protein
ACSF	Artificial CerebroSpinal fluid
AJ	Adherens Junction
ALS	Amyotrophic Lateral Sclerosis
AMPA	2-amino-3-hydroxy-5-methyl-4-isoxazole propionic acid
AMPAR	AMPA receptors
ADAR2	Adenosine Deaminase
AP	Adaptor Primer
AP-2	Adaptor Protein-2
APS	Ammonium PerSulphate
Arc	Activity related cytoskeletal protein
ARE	AU-Rich Elements
BCA	Bicinchonic Acid
BDNF	Brain Derived Neurotrophic Factor
bp	base pairs
BSA	Bovine Serum Albumin
cAMP	cyclic Adenosine MonoPhosphate
CamKIIα	Calcium-calmodulin dependent protein Kinase II, α subunit
CCD	Charge-Coupled Device
cDNA	Complimentary DNA
CNS	Central Nervous System
CPE	Cytoplasmic Polyadenylation Element
CPEB	CPE Binding protein
CPSF	Cleavage and Polyadenylation Specificity Factor
CREB	cAMP Response Binding element
Cx30	Connexin30
Cx43	Connexin43
DEPC	Diethyl Pyrocarbonate
DG	Dentate Gyrus
DIV	days *in vitro*
Dlg-A	Discs-large
DMEM	Dulbecco's Modified Eagle's Medium
DMSO	Dimethyl Sulfoxide
DN	Dominant Negative
dNTPs	deoxy Ribonucleotide Phosphates
Dox	Doxycycline
DT	Double Transgenic
DTT	Dithiothreitol
E	Efficiency
E. *coli*	Escherichia *coli*
EDTA	Ethylene Diamine Tetra Acetic acid

EGFP	Enhanced Green Fluorescent Protein
eIF4E	eukaryotic Initiation Factor 4E
eIF4G	eukaryotic Initiation Factor 4G
E-LTP	Early phase of Long Term Potentiation
EphA4	Ephrin receptor A4
EPSP	Excitatory Post Synaptic Potential
ER	Endoplasmic Reticulum
EYFP	Enhanced Yellow Fluorescent Protein
FAM	Fluorescein Amidite
FCS	Foetal Calf Serum
FMRP	Fragile X Mental Retardation Protein
g	grams
G	Gauge
GAPDH	Glyceraldehyde 3-Phosphate Dehydrogenase
GFP	Green Fluorescent Protein
GFAP	Glial fibrillary acidic Protein
GLAST	Glutamate aspartate transporter
GLT-1	Glutamate Transporter-1
GluR2	Glutamate Receptor 2
GPI	Glycosyl Phosphatidyl Inositol
GRIP1	Glutamate Receptor Interacting Protein1
GS	Glutamine Synthetase
GSK 3β	Glycogen Synthase Kinase 3β
h	hours
HEPES	4-(2-hydroxyethyl)-1-piperazineethanesulfonic acid
Hif-1α	Hypoxia inducible factor-1α
HRP	Horse Radish Peroxidase
HuR	Hu antigen R
Iba-I	Ionized calcium binding adapter I
ICC	Immunocytochemistry
IgG	Immunoglobulin G
IHC	Immunohistochemistry
IR	immunoreactivity
IR-DIC	Infrared Differential Interference Contrast
KA	Kainic Acid
KO	Knock Out
Kb	Kilobase
KDa	kilo Dalton
ki	knockin
L	Litre
LB	Luria Bertani
LEF	Lymphoid Enhancer Factor
LTD	Long Term Depression
LTF	Long Term Facilitation
L-TLE	Lateral Temporal Lobe Epilepsy
LTP	Long Term Potentiation
L-LTP	Late phase of LTP
M	Molar
MAP2	Microtubule Associated Protein 2
MEF	Mouse Embryonic Fibroblasts

min	minutes
miRNA	micro RNA
ml	milliliter
mM	millimolar
MTLE	Mesial Temporal Lobe Epilepsy
ng	nanogram
NGS	Normal Goat Serum
NMDA	N-Methyl-D-Aspartate
NO	Nitric Oxide
NP-40	Nonidet P-40
NSF	N-ethylamide Sensitive Fusion protein
NT3	Neurotrophin-3
NTC	No Template Control
ORF	Open Reading Frame
pA	polyadenylation
PABP	Poly(A)-Binding Protein
PAGE	PolyAcrylamide Gel Electrophoresis
PAP	Poly(A) Polymerase
PAS	Protein A-Sepharose
PBGD	PorphoBilinogen Deaminase
PBS	Phosphate Buffered Saline
PDZ	PSD-95/Dlg-A/ZO-1
PFA	Paraformaldehyde
PGDB	Protein-G Dynabeads
PHC	Primary Hippocampal Cultures
PICK1	Protein Interacting with C-kinase 1
PKA	Protein Kinase-A
PKC	Protein Kinase-C
pmol	picomol
PSD	Post Synaptic Density
PVDF	PolyVinylidene Fluoride
RACE	Rapid Amplification of cDNA Ends
RIPA	RNA ImmunoPrecipitation Assay
rpm	rotations per minute
RRM	RNA Recognition Motif
RT	Room Temperature
RTK	Receptor Tyrosine Kinase
rtTA	reverse tetracycline transactivator
SCP	Synaptonemal Complex Protein
SDS	Sodium dodecyl sulphate
SE	Status Epilepticus
sec	seconds
SV40	Simian Virus 40
TAMRA	Carboxytetramethyl rhodamine
TARP	Transmembrane AMPAR Regulatory Proteins
TBE	Tris Borate EDTA
TBS	Theta burst stimulation
TBST	Tris Buffered Saline with Tween 20
TCF	T-Cell Factor
TE	Tris EDTA

TEMED	Tetramethyl Ethylene Diamine
*tet*O	tetracycline Operator
*tet*R	tetracycline Response
TLE	Temporal Lobe Epilepsy
tPA	tissue Plasminogen Activator
Trk-B	Tyrosine-related kinase B
tRNA	transfer RNA
TSP	Tissue-Specific Promoter
tTA	tetracycline transactivator
U	Units
UTR	Un Translated Region
V	Volts
v/v	volume/volume
WB	Western Blotting
WT	Wild Type
w/v	weight/volume
ZBP	Zip code Binding Protein
Znf	Zinc finger

1 Introduction

1.1 Synaptic plasticity

The communication between an axon of one neuron and a dendrite of another neuron is mediated by so-called synapses whose strength can be either increased or decreased. This phenomenon is widely known as synaptic plasticity. Synaptic plasticity in the adult central nervous system (CNS) is best studied in the rodent hippocampus *in situ*. The hippocampus is essential for memory formation and its anatomy is suitable for electrophysiological investigations. A total of three pathways were proposed (Figure 1) for synaptic plasticity in the rodent hippocampus *in situ* (Kandel et al., 2000):

i) **Perforant pathway,** in which the axons from the cortex surrounding the hippocampus (entorhinal cortex) form synapses onto the dendrites of granule cells.

ii) **Mossy fibre pathway,** in which the synapses are formed onto the dendrites of CA3 pyramidal neurons by the axons of dentate granule cells.

iii) **Schaffer collateral pathway,** in which the synapses are formed onto the dendrites of CA1 neurons by the axons of CA3 neurons.

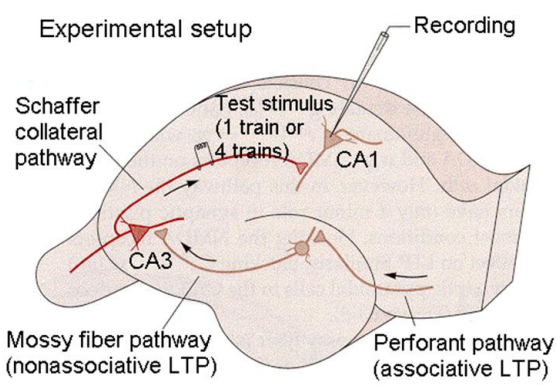

Figure 1: An experimental model to study activity-dependent synaptic plasticity in the rodent hippocampus. Three pathways, namely, perforant, mossy fibre and schaffer collateral pathways are described. The figure was adapted from Kandel et al., (2000).

Synaptic plasticity is thought to be the cellular basis for learning and memory. Changes in synaptic plasticity are described as long term potentiation (LTP) and long term depression (LTD) in vertebrates and long term facilitation (LTF) in invertebrates (Kandel, 2001; Malenka and Bear, 2004). LTP comprises two phases: i) an early phase (E-LTP, lasts for minutes to hours) which is protein-synthesis independent, and ii) a late phase (L-LTP, lasts for hours to

days) which is dependent on protein synthesis (Bramham and Wells, 2007). The synthesis of new proteins is important in order to convert the short term memory into long term memory. Both the long-lasting forms of synaptic plasticity and memory require protein synthesis (Kandel, 2001). Single high-frequency stimulation such as tetanus to any of the three pathways can increase the excitatory post synaptic potentials (EPSPs), this increase is termed LTP. Although the mechanism of LTP is not the same in all three pathways described, several experimental models exist to study LTP. It can be studied in acute hippocampal slices or in cell culture or in the intact animal where LTP can last for days to weeks (Kandel et al., 2000).
In a typical experiment to study synaptic plasticity *in situ*, LTP can be induced by stimulating hippocampal CA3 neurons by a single tetanic stimulation or repeated trains of stimuli while recording the postsynaptic responses from CA1 neurons. The communication at the synapse is mediated by neurotransmitter release. Action potentials generated at the axon hillock at the soma are propagated to the presynaptic release sites of the axon. At this site, depolarization opens voltage-gated Ca^{2+} channels which then lead to fusion of docked vesicles and to the release of neurotransmitters. These transmitters diffuse into the synaptic cleft and bind to the postsynaptic receptors present in the post synaptic density (PSD) which leads to de- or hyperpolarizations of the postsynaptic cell and activation of intracellular signalling pathways. The depolarization of membrane makes the synapse excitatory whereas the hyperpolarization makes the synapse inhibitory. A number of receptors are present at the postsynaptic site which includes two major classes: ionotropic and metabotropic. For the induction of LTP, especially two types of ionotropic glutamate receptors such as, NMDA (N-methyl D-aspartate) and AMPA (α-amino-3-hydroxy-5-methyl-4-isoxazolepropionic acid) receptors are important. In the early LTP (E-LTP), the stimulation caused by the high frequency depolarizes the membrane and detaches the Mg^{2+} ions that preoccupied and blocked NMDA receptors (Figure 2). This in turn allows the entry of Ca^{2+} into the cell which is necessary for the activation of various kinases such as Ca^{2+}/calmodulin dependent protein kinase (CaMKII), protein kinase C (PKC), and tyrosine kinase (Kandel et al., 2000). CaMKII is particularly important as it not only enhances the presynaptic release of transmitters by sending a retrograde signal (for example, nitric oxide, NO) but also phosphorylates AMPA receptors to increase the synaptic response. It also participates in the late phase of LTP, (L-LTP), in which the Ca^{2+} activates Ca^{2+}/calmodulin which is necessary to activate other kinases such as cyclic adenosine monophosphate (cAMP) kinase and adenylyl cyclase. The activated cAMP translocates to the nucleus of the cell and initiates transcription followed by protein synthesis (translation) which results in formation of new synapses.

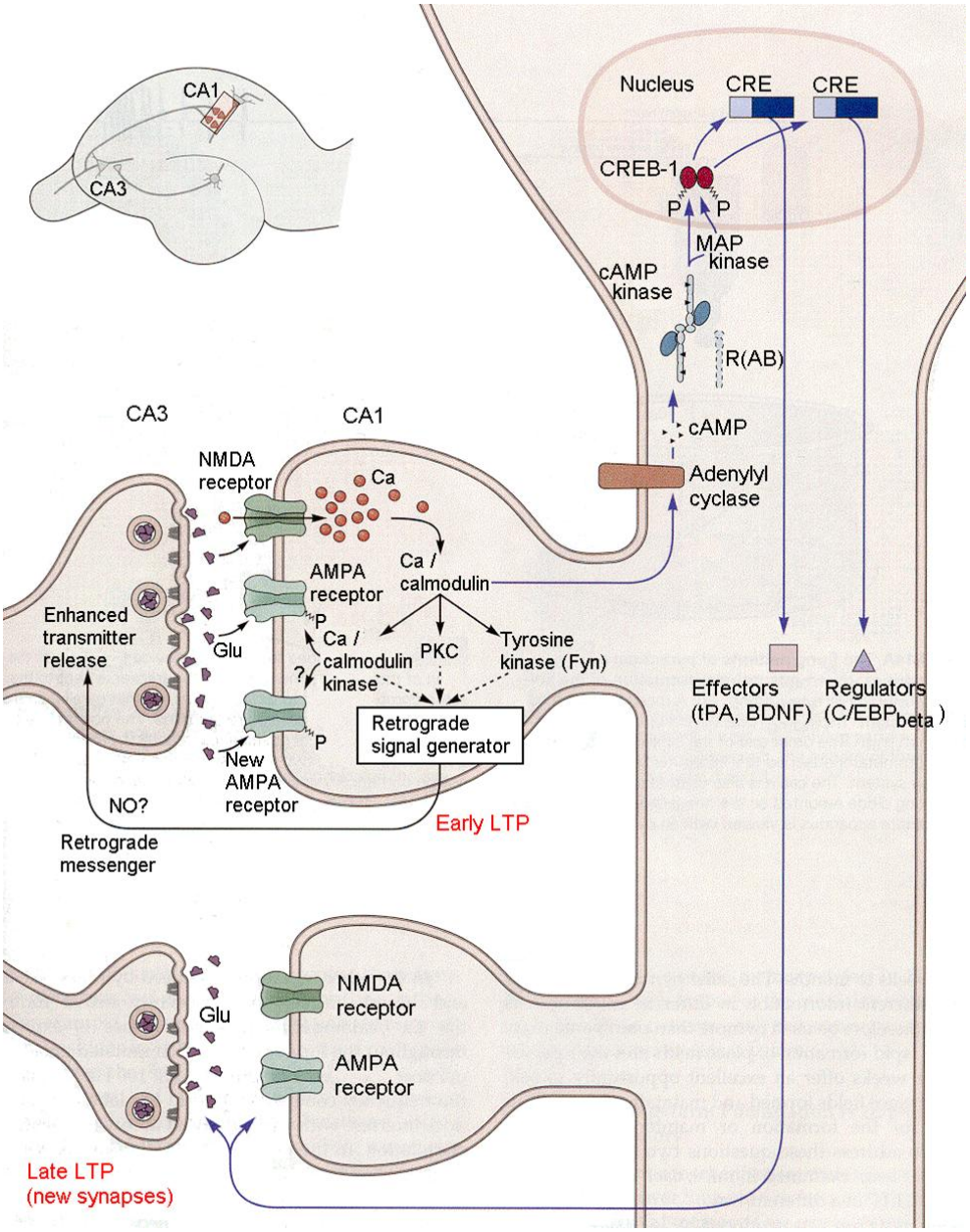

Figure 2: A schematic representing both early and late phases of LTP. Induction of LTP by single high frequency stimulation causes the activation of NMDA receptors thereby allowing Ca^{2+} to enter the cell. This entry of Ca^{2+} is necessary for the activation of several kinases shown in the schematic. LTP induction by repeated stimuli also leads to a persistent increase in intracellular Ca^{2+} which leads to the activation of adenylyl cyclase, which further activates cAMP-dependent protein kinase (cAMP kinase). This cAMP kinase translocates to the nucleus and phosphorylates cAMP response binding element (CREB) which in turn initiates the transcription of a set of genes. Effectors such as brain derived neurotrophic factor (BDNF), tissue plasminogen activator (tPA) and C/EBP beta transcription factor (regulators) are also involved. P = phosphate, PKA = protein kinase A, R (AB) = dominant negative PKA. The figure was adapted from Kandel et al., (2000).

1.2 Synapse-specific local protein synthesis

A number of synaptic proteins including receptors and several signalling molecules are present at synapses (Harris and Kater, 1994) whose transport and subsequent regulation is important for the synaptic strength (Tang and Schuman, 2002). According to an earlier view, proteins were thought to be synthesized in the cell body (soma) and then transported to dendrites. But, the modern view gave a clue about the dendritic protein synthesis with the discovery of a complete protein synthesis machinery (mRNAs, polyribosomes) in dendrites (Steward and Levy, 1982). This concept was further supported by the identification of several ribosomal proteins, initiation and elongation factors of translation as well as transfer RNAs (tRNAs) within the dendritic compartments (Tiedge and Brosius, 1996). Several mRNAs are transported and localized in dendrites which include activity-related cytoskeletal protein, Arc (Lyford et al., 1995), brain derived neurotrophic factor (BDNF; Tongiorgi et al., 1997), the α-subunit of CaMKII (Miyashiro et al., 1994), FMR1, the gene encoding FMRP (Antar et al., 2004), the NR1 subunit of the NMDA receptor (Pal et al., 2003), the α subunit of the glycine receptor (Racca et al., 1997), the microtubule associated protein (MAP2; Garner et al., 1988) and the tyrosine-related kinase B (TrkB) receptor (Martin and Zukin, 2006). The mRNAs are transported to the dendrites as RNA granules with the help of molecular motors such as members of the kinesin and dynein super families (Kanai et al., 2004), and RNA binding proteins such as Staufen (Kiebler et al., 1999), Zip code binding proteins (ZBP) 1 and 2 (Tiruchinapalli et al., 2003), cytoplasmic polyadenylation element binding (CPEB) protein (Huang et al., 2003), and fragile X mental retardation protein, FMRP (Eberhart et al., 1996).

1.3 Mechanisms of translational regulation

The functional expression of a gene can be regulated at different levels: transcription, mRNA splicing, nuclear mRNA export, mRNA transport and translation. The regulation of eukaryotic mRNAs can be modulated by elements present in either the 5’ or the 3’ untranslated region (UTR) of the mRNA. The 5’UTR has been reported to control the translation at the level of initiation (Pickering and Willis, 2005) whereas the 3’UTR contributes to several mechanisms such as mRNA transport, localization, stability and the efficiency of translation (Moore, 2005). The 3’UTRs of mRNAs were found to be extremely important for the transport of mRNAs to various subcellular compartments as well as in modulating their translation (Andreassi and Riccio, 2009). They harbor various *cis*-elements (those which can modulate the expression of its own mRNA), to which specific *trans*-acting

proteins bind and modulate the translation of bound mRNAs. The binding of these proteins depends either on sequence specificity or on the secondary structure of an mRNA. These *cis*-elements can be present either as a single copy or in multiple copies over the entire length of the 3'UTR and can range from few nucleotides to over 1 kb in length (Jambhekar and Derisi, 2007). In addition, translation can also be regulated by microRNAs (miRNAs), which are small non-coding RNAs of ~21 nucleotides in length and have binding sites in the 3'UTRs of several mRNAs (Kosik, 2006).

1.3.1 RNA binding proteins

There are several mechanisms proposed for the regulation of dendritic mRNAs. Increasing evidence suggests an important role for the RNA binding proteins in translational regulation. The regulation of these dendritic mRNAs by different RNA binding proteins was found to be crucial for synaptic plasticity (Kang and Schuman, 1996; Klann and Dever, 2004). Several RNA binding proteins were identified which regulate the translation of various proteins. Some of them include Staufen, FMRP, ZBP1, ZBP2, and CPEBs.

CPEBs are RNA binding proteins which regulate the translation of mRNAs depending on their phosphorylation status. Under basal conditions, CPEB *trans*-acting proteins bind to consensus cytoplasmic polyadenylation elements (CPE) present in the 3'UTR of many mRNAs (Mendez and Richter, 2001) and repress their translation. This repression is relieved upon phosphorylation of CPEBs which eventually stimulates the polyadenylation and protein synthesis of bound mRNAs (Richter, 2007).

1.4 The CPEB family

CPEB is a sequence-specific RNA binding protein which binds to the consensus CPE (UUUUUAU) present in the 3'UTR of many mRNAs (Mendez and Richter, 2001), usually in the vicinity of 100-300 bases from the polyadenylation sequence AAUAAA (McGrew and Richter, 1990). Although the classical (canonical) CPE is defined as UUUUUAU, variations from this sequence have been proposed (Du and Richter, 2005). Under basal conditions, CPEBs repress the translation of bound mRNA. Upon stimulation, CPEBs get phosphorylated and enhance the polyadenylation of the bound mRNA (Richter, 2007). CPEB1 regulates the translation of cyclin B1 mRNA (Kim et al., 2011). Based on a combinatorial code proposed in *Xenopus* oocytes (Pique et al., 2008), the timing and extent of translational regulation may

vary depending on i) the number of CPEs, ii) the distance between two CPEs, iii) the distance between CPE and poly(A), and iv) other regulatory elements surrounding the CPEs. The CPEB family includes four members: CPEB 1-4. Based on amino acid comparison and structural similarity, the CPEB family can be divided into two groups: CPEB1 and the CPEB 2-4 subfamily (Kurihara et al., 2003; Theis et al., 2003). The founding member CPEB1 was first described in *Xenopus* oocytes being involved in the maturation of oocytes (Hake and Richter, 1994) and later was also reported at the postsynaptic density of mouse brain (Wu et al., 1998). CPEB2 was described in germ cells (Kurihara et al., 2003) and in mouse brain (Theis et al., 2003; Turimella et al., in revision). CPEB3 and 4 were described in mouse hippocampus (Theis et al., 2003). They all share a similar structure with an N-terminal recognition motif and a C-terminal RNA binding motif which in turn includes two RNA recognition motifs (RRM) and a zinc finger (Znf). The N-terminal motif harbors a variable region which can be alternatively spliced to give rise to multiple splice isoforms for CPEB 2-4, while CPEB1 harbors a site for alternative splicing in the first RRM (Figure 3).

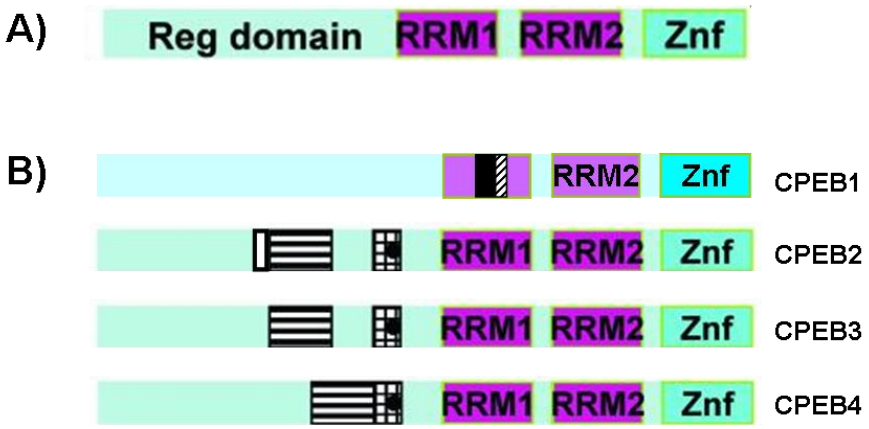

Figure 3: A) The general protein structure of all four CPEBs. The N-terminal regulatory domain and a C-terminal RNA binding domain with two RNA recognition motifs (RRM1 and RRM2) and a zinc finger (Znf) are shown. B) The protein structures of CPEB 1-4. CPEB1 contains a variable region in RRM1, the deletion of either one or both the regions (filled and striped boxes) marked give rise to different splice isoforms. In the CPEB 2-4 subfamily, the regulatory domain harbors a variable region: the B-region with a putative phosphorylation site (filled circle), and the C-region (striated box). CPEB2 possesses an extra region named the E-region (white box) which is not present in other CPEBs. Both 'B' and 'C' regions are separated in CPEB2 and CPEB3, whereas in the case of CPEB4, they are together. Adapted and modified from Theis et al., (2003) and Turimella et al., (in revision).

For CPEB1, three splice isoforms were described: A full length version (n) and a form with a small deletion in the RRM1 (Δ5) were reported (Wilczynska et al., 2005). Another isoform with a long deletion in the RRM1 (Δ17) was recently identified (Turimella et al., in revision). For CPEB2, four splice isoforms were identified in mouse brain (2a, 2a*, 2c and 2c*) (Turimella et al., in revision). For CPEB3 and CPEB4, four splice isoforms each were

identified. CPEB3 isoforms: 3a, 3b, 3c and 3d; CPEB4 isoforms: 4a, 4b, 4c and 4d. (Theis et al., 2003). Additional splice isoforms of CPEB3 have been described in mouse retina (Wang and Cooper, 2009). A summary of different splice isoforms described for each CPEB with their domain compositions can be found below in table 1.

CPEB	Isoform	Domain composition	Reference
CPEB1	full length (n)	full length isoform	Gebauer and Richter, 1996
	short (sm/Δ5)	deletion of 5 aa	Wilczynska et al., 2005
	long (lg/Δ17)	deletion of 17 aa	Turimella et al., in revision
CPEB2	2a	B+C+E-	Turimella et al., in revision
	2a*	B+C+E+	
	2c	B+C-E-	
	2c*	B+C-E+	
CPEB3	3a	B+C+	Theis et al., 2003
	3b	B-C+	
	3c	B+C-	
	3d	B-C-	
CPEB4	4a	B+C+	Theis et al., 2003
	4b	B-C+	
	4c	B+C-	
	4d	B-C-	

Table 1: A summary of multiple splice isoforms identified for each CPEB. Note that some isoforms of CPEB 2-4 contain a B-domain proposed to contain a putative phosphorylation site for different kinases. Some isoforms of CPEB2 differ from CPEB3 and 4 in having an extra E-domain of 3 aa. aa – amino acids, sm - small, lg - long.

The N-terminal region also possesses a putative phosphorylation site for different kinases. CPEB1 differs from the CPEB 2-4 subfamily in having a phosphorylation site for Aurora A kinase (Mendez et al., 2000) which is not found in the CPEB 2-4 subfamily. CPEB1 is known to be phosphorylated by CaMKIIα (Atkins et al., 2004), whereas for the other CPEBs (CPEB 2-4), putative phosphorylation sites were predicted for CaMKIIα, protein kinase-A (PKA) and S6 kinase (Theis et al., 2003). The zinc finger present in the C-terminal RNA binding domain is rich in cysteine and histidine amino acids and is shown to be essential for RNA binding (Hake et al., 1998; Theis et al., in revision; Turimella et al., in revision).

1.4.1 Mechanism of CPEB regulation

Among all CPEBs, much information is available about how CPEB1 regulates activity-induced polyadenylation and translation of bound mRNA. Figure 4 depicts the role of CPEB1 in neurons. CPEB1 binds to CPE containing mRNA and represses its translation (Richter, 2007). In this state, CPEB is being bound by maskin (a translational inhibitor) (Stebbins-Boaz et al., 1999) which also interacts with the eukaryotic initiation factor 4E (eIF4E). The interaction of maskin with eIF4E prevents its association with eIF4G which is necessary to recruit the 40S ribosomal subunit to the AUG start codon in the 5'end of mRNA, in this way maskin prevents the initiation of translation (Gingras et al., 1999). This repression is relieved by phosphorylating CPEB1 which induces polyadenylation of bound mRNA. Polyadenylation causes the dissociation of maskin from eIF4E (Cao and Richter, 2002), the eIF4E in turn interacts with eIF4G and initiates the translation along with the other protein complex (Stebbins-Boaz et al., 1999). Maskin is not present in the brain, where a related protein (neurogidin) exerts maskin's function (Richter, 2007).

CPEB1 can be phosphorylated by two kinases: by Aurora A kinase (a serine/threonine kinase) in *Xenopus* oocytes (Mendez et al., 2000) at the serine 174 residue (Sarkissian et al., 2004) and by CaMKIIα in rodent neurons at the threonine 171 residue (Atkins et al., 2004). Both progesterone (Mendez et al., 2000) and glutamate (Atkins et al., 2004) stimulate the phosphorylation of CPEB1 in oocytes and hippocampal neurons respectively. Phosphorylation induces CPEB1 to recruit cleavage and polyadenylation specificity factor (CPSF) and stabilizes it on the hexanucleotide sequence (AAUAAA) (Mendez et al., 2000) and recruits poly(A) binding protein (PABP) (Kahvejian et al., 2005) and poly(A) polymerase to elongate the poly(A) tail of bound mRNA.

CPEB1 localizes at the postsynaptic density in neurons (Wu et al., 1998) and modulates the translation of CaMKIIα mRNA. In neurons, glutamate released from the presynapse activates the NMDA receptor which further activates Aurora A kinase to phosphorylate CPEB1 (Figure 4) (Atkins et al., 2004). This phosphorylation breaks down the dormancy and relieves the maskin from eIF4E which in turn can interact with eIF4G and recruits a complex of proteins to initiate translation.

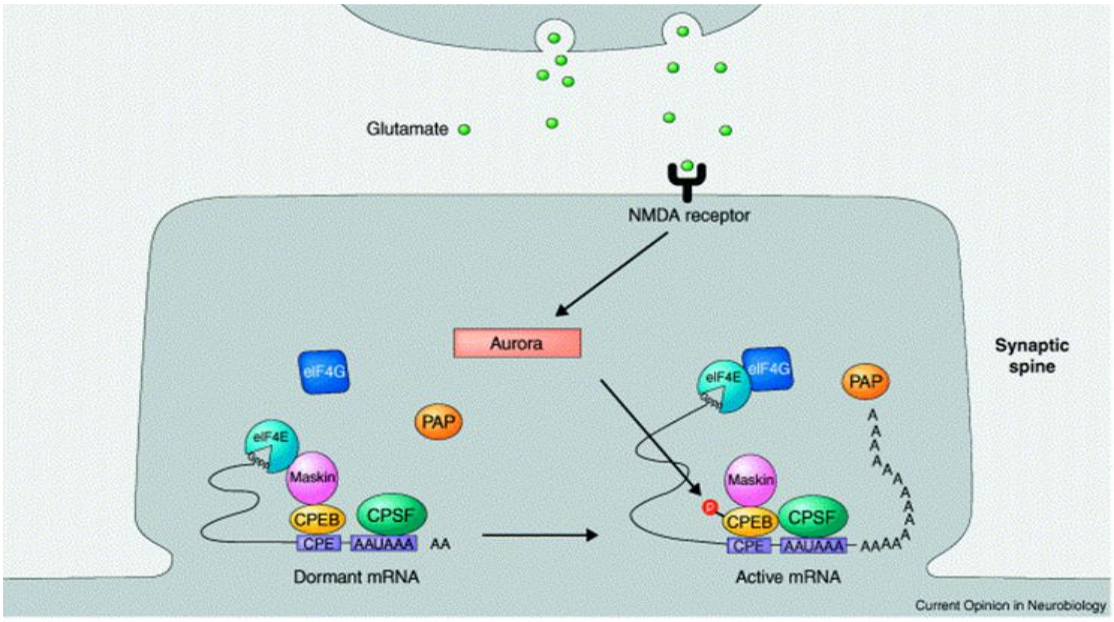

Figure 4: CPEB1-mediated translational regulation in neurons. Under basal conditions, CPEBs bind to CPEs and keep the mRNA in a dormant state. Following NMDA receptor activation, the aurora kinase gets activated and phosphorylates CPEB. CaMKII has also been shown to phosphorylate CPEB (Atkins et al., 2004). Phosphorylation stabilizes CPSF on the AAUAAA hexanucleotide, which attracts PAP to catalyze polyadenylation. Maskin dissociates from eIF4E (cap binding factor). The eIF4G then binds eIF4E and initiates translation. The figure was adapted and modified from Richter and Lorenz (2002).

1.4.2 Role of CPEBs in different cell types

CPEBs are important translational regulators which control several key processes both in invertebrates and vertebrates. Much of the work has been done in elucidating the function of CPEB1 in various cell types. CPEB1 was first described in *Xenopus* oocytes where it regulates the maturation of oocytes (Hake and Richter, 1994). CPEB1 was found to be essential for the germ-cell development as the ablation of this gene impaired the translation of two synaptonemal complex proteins 1 and 3 (SCP1 and SCP3) and further inhibiting the germ-cell development (Tay and Richter, 2001). In addition, CPEB1 is also important for cell division in *Xenopus* embryos. In mouse embryonic fibroblasts (MEFs), CPEB1 represses the translation of a transcription factor, *myc* which encodes a proto-oncogene, thereby driving the cells into senescence (Groisman et al., 2006).

In neurons, CPEB1 regulates a number of mRNAs such as β-catenin in growth cones (Kundel et al., 2009), CaMKIIα (Wu et al., 1998) at synapses, and tissue plasminogen activator (tPA), a protease important for synaptic plasticity (Shin et al., 2004). Among the CPEB 2-4 subfamily members, CPEB2 interacts with hypoxia inducible factor (Hif-1α) (Hagele et al., 2009). CPEB3 and CPEB4 regulate the translation of GluR2, an AMPA receptor subunit regulating calcium permeability of the receptors (Huang et al., 2006). The translation of a

number of target mRNAs is regulated by different CPEBs in different cell types. A list of proven CPEB targets is shown in table 2.

CPEB	Target mRNA	Function	Reference
	p53	Cell senescence	Groisman et al., 2006
	β-catenin	Neuronal morphogenesis	Kundel et al., 2009
	CaMKIIα	Synaptic plasticity	Wu et al., 1998
	Cyclin B1	Cell cycle	Hake and Richter, 1994 Kim et al., 2011
CPEB1	MAP2	Microtubule associated protein	Huang et al., 2003
	Myc	Proto oncogene	Groisman et al., 2006
	Synaptonemal complex proteins (SCP1 and SCP3)	Germ-cell development	Tay and Richter, 2001
	tPA	Serine protease	Shin et al., 2004
CPEB2	Hif-1α	Hypoxia	Hagele et al., 2009
	Eukaryotic elongation factor, eEF2	Elongation step of translation	Chen and Huang, 2011
	TWIST1	Breast cancer progression	Nairismaegi et al., 2012
CPEB3	GluR2	Ca^{2+} permeability	Huang et al., 2006
CPEB4	GluR2	Ca^{2+} permeability	Huang et al., 2006

Table 2: A list of proven CPEB targets in different cell types and their functions.

1.4.3 CPEBs in synaptic plasticity, learning and memory

Increasing evidence suggests that local protein synthesis is important for certain forms of synaptic plasticity (Kandel, 2001). CPEB1 is present in the postsynaptic density and regulates the translation of the α subunit of CaMKII (Wu et al., 1998), a key player involved in synaptic plasticity. To find out if ablation of CPEB1 impairs synaptic plasticity, LTP experiments were performed in CPEB1 knockout (CPEB1 KO) mice (Tay and Richter, 2001). In classical LTP experiments (induced by theta-burst stimulation), only a modest deficit was observed in CPEB1 KO mice compared to their wild type littermates (Alarcon et al., 2004). As the other CPEB family members (CPEB 2-4) were reportedly present in the postsynaptic density (Huang et al., 2006) and share similarity in their RNA binding domains (Theis et al., 2003), the authors speculated that the mild deficit in LTP observed might be due to a compensatory effect by the other CPEB family members (CPEB 2-4) for CPEB1 ablation. In addition, CPEB1 KO mice showed impairments in extinction of memory which is dependent on the hippocampus (Berger-Sweeney et al., 2006). Extinction is a type of behavioral response

where memory engrams gradually become extinct if not reinforced; this results in the formation of new memories (Abel and Lattal, 2001), but is not equal to forgetting. In addition, transgenic mice expressing dominant negative CPEB (DN-CPEB) in neurons which competes with endogenous CPEBs for binding to CPE containing mRNAs, showed impairments in L-LTP (which is dependent on protein synthesis) and memory (Theis et al., in revision). DN-CPEB is CPEB1 without the N-terminal regulatory domain containing the critical phosphorylation site for activation; hence it can't be activated by phosphorylation. Altogether, these findings suggest that CPEBs, and not only CPEB1, in neurons are required for synaptic plasticity, learning and memory.

1.4.4 CPEBs in Epilepsy

Epilepsy is a common neurological disorder affecting 1% of the world population (Binder and Steinhauser, 2006), and is characterized by gliosis and recurrent seizures (Seifert et al., 2006). The seizures might arise either from the temporal lobe (called mesial temporal lobe epilepsy, MTLE) or from hippocampus (called lateral TLE, LTLE). The spontaneous seizures arise due to the hyper-activation of neurons leading to excitotoxicity, neurodegeneration and mossy fibre sprouting, the hallmarks of epilepsy (Morimoto et al., 2004). The seizure activity also leads to reorganization of the brain which is contributed by several factors including protein synthesis. The application of kainic acid (KA) leads to hyperactivity of neurons in the hippocampus (recurrent seizures), to status epilepticus (SE) and neurodegeneration (Zagulska-Szymczak et al., 2001).

CPEB3 and CPEB4 transcripts levels were upregulated *in vivo* by the administration of KA, a glutamate receptor agonist (Theis et al., 2003). As some of the CPEB transcripts are upregulated following KA treatment which also causes seizures, and seizure activity results in protein synthesis, it can be speculated that CPEBs might play an important role in the development and progression of epilepsy.

1.5 CPEB2

CPEB2 is a 63 kDa molecular weight protein and together with CPEB3 (KIAA0940) and CPEB4 (KIAA1673) make the CPEB 2-4 subfamily. Though it was first described in germ cells (Kurihara et al., 2003), later reports claim the expression of CPEB2 in mouse brain (Theis et al., 2003; Hagele et al., 2009). But, it remained to be unexplored among the CPEB

family members in mouse CNS until the description of the multiple splice isoforms of CPEB2 as well as the protein distribution in mouse brain (Turimella et al., in revision). Only few reports show that CPEB2, similar to CPEB1 binds to the 3'UTRs of CaMKIIα (Turimella et al., in revision) and Hif-1α (Hagele et al., 2009) mRNAs. Because of its similarity with the other CPEB family members and potential expression in mouse CNS, CPEB2 could very well be a translational regulator, the role of which is yet to be explored.

1.5.1 Putative targets of CPEB2

The translation of several mRNAs in neurons is regulated by CPEB family members. CPEB3 and CPEB4 were thought to regulate translation not by binding to CPEs but depending on the secondary structure of the 3'UTR (Huang et al., 2006). CPEB2 interacts with Hif-1α (Hagele et al., 2009) and CamKIIα (Turimella et al., in revision). As several mRNAs contain CPEs in their 3'UTRs (Du and Richter, 2005), CPEB2 might likely regulate translation of any of the target mRNAs. A description of some of the putative targets of CPEB2 can be found below. Some of these mRNAs have been reportedly regulated by other CPEB family members.

1.5.1.1 β-catenin

The protein complexes that are present at cell-cell junctions and anchor the cells are called adherens junction (AJ) or zonula adherens which constitute the classical cadherins and their cytoplasmic partners, catenins. There are more than 80 members in the cadherin family, which constitute type I and II cadherins. They interact by their cytoplasmic domains with catenins. Catenins include three subgroups: two β-catenin like proteins (β-catenin and plakoglobin), three α-catenins and four p120catenin-related proteins (Arikkath and Reichardt, 2008). The cadherin/catenin complex is present early in development (Benson and Tanaka, 1998) at high levels in neuronal processes and colocalizes with synaptic proteins (Togashi et al., 2002). Cadherins are present at the synaptic junctions (Uchida et al., 1996). In neurons, they are present at the synapses as visualized by immunoelectron microscopy and participate in the induction of LTP (Huntley et al., 2002).

β-catenin is one of the AJ proteins which participate in both cell-cell signalling and in various stages of neuronal development. On one side, it interacts with α-catenin and on the other side, it interacts with actin cytoskeleton (Gumbiner, 1996) thereby participating in the intracellular signalling. It is an important component of the classical Wnt signalling pathway (Clevers,

2006). The Wnt signal inactivates glycogen synthase kinase 3β (GSK-3β) which otherwise phosphorylates β-catenin and subsequently degrades it by ubiquitinylation, thereby leading to the accumulation of β-catenin in the cytoplasm of the cell. This β-catenin then enters the nucleus to mediate the transcription of several genes together with lymphoid enhancer factor/T-cell factor (LEF/TCF) family of transcription factors (Cadigan and Nusse, 1997).

β-catenin functions at both pre- and postsynaptic sites (Arikkath and Reichardt, 2008). By binding to cadherin and recruiting PDZ domain-containing proteins with its C-terminal PDZ-binding motif, β-catenin participates in synaptic vesicle localization at presynaptic sites. This is supported by the reduction in the reserve pool of vesicles observed in the absence of β-catenin (Bamji et al., 2003). The PDZ domain is a ~ 90 amino acids long protein-protein interaction motif, which links several proteins. The PDZ domain occurs either as a single domain or in repeats in a particular protein. The name is derived from three proteins which contain this motif: PSD-95 (Cho et al., 1992), its homologue *Drosophila* discs-large tumour suppressor gene (Dlg-A) product (Woods and Bryant, 1991) and ZO-1, a tight junction protein (Itoh et al., 1993). At postsynaptic sites, β-catenin influences the structure of the synapse. β-catenin is critical for dendritic morphogenesis (Yu and Malenka, 2003) and the loss of β-catenin negatively affects the synaptogenesis as well as the morphology of spines (Okuda et al., 2007). The overexpression of GFP tagged β-catenin enhanced the dendritic arborization. On the other hand, the sequestration of endogenous β-catenin by the intracellular domain of N-cadherin prevented the arborization (Yu and Malenka, 2003).

Both synaptic activity (Takeichi and Abe, 2005) and post-translational modifications such as tyrosine phosphorylation (Murase et al., 2002) regulate β-catenin. As β-catenin possesses multiple roles in neuronal development and as the loss of β-catenin leads to abnormalities in dendritic spines, the regulation of the expression and function of β-catenin is of high importance. Indeed, Clapper et al (2004) suggested that targeting of β-catenin-mediated gene regulation could be a promising strategy for treating several cancers. RNA binding proteins such as CPEBs regulate β-catenin translation (Jones et al., 2008; Kundel et al., 2009). Recently, CPEB1 was shown to regulate the translation of β-catenin in neurons (Kundel et al., 2009). The authors have shown that β-catenin is present in the growth cones and upon treating the neurons with neurotrophin-3 (NT3), β-catenin protein synthesis was enhanced by CPEB1 (stimulated protein synthesis). A schematic of β-catenin 3'UTR with potential binding sites for CPEB can be found in figure 5.

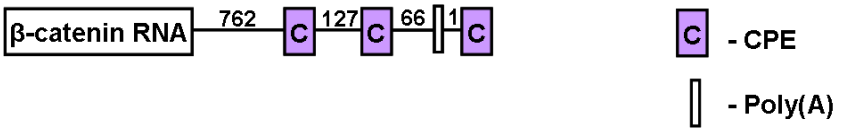

Figure 5: The 3'UTR of β-catenin with CPEs and poly(A) marked. The numbers indicate the distance in bases between two elements.

1.5.1.2 GluR2

GluR2 is an important subunit of the AMPA receptor complex. AMPA receptors (AMPAR) mediate fast synaptic transmission in the CNS. They are composed of up to four subunits: GluR1-4 (also called as GluR A-D) (Dingledine et al., 1999). All four subunits share a similar structure with an amino terminal domain, three membrane associated domains (M1-4) and a C-terminal domain (Isaac et al., 2007); out of which the membrane associated domain M2 forms a hairpin loop and is a site for RNA editing. The subunits are synthesized in the endoplasmic reticulum (ER), they first form dimers and later two dimers combine together to form tetramers (Cull-Candy et al., 2006) which are the functional AMPA receptors. Depending on their subunit assembly, AMPAR can be formed as homotetramers or various heterotetramers. Among the different combinations, the most favoured combination is a heteromeric complex of GluR1 and GluR2 (Cull-Candy et al., 2006). It is already known that AMPAR exist both in neurons and glia (Belachew and Gallo, 2004). In the CNS, most of the AMPAR exist as GluR2 containing heteromers (Greger et al., 2002). GluR1 and GluR2 were reported as the predominant subunits in forebrain especially in hippocampus whereas GluR3 and GluR4 are of rather low abundance (Tsuzuki et al., 2001; Sans et al., 2003). The subunit composition also varies based on the region of brain, cell type as well as developmental stage (Song and Huganir, 2002).

GluR2 is a subunit which has a strong influence on AMPAR function. GluR2 differs from the other subunits in having an edited arginine (R) in place of glutamine (G). This editing occurs due to the change of a single adenosine to inosine by the enzyme adenosine deaminase (ADAR2) (Higuchi et al., 1993a) and is specific for GluR2 (> 95% of GluR2 mRNA transcripts in postnatal brain are edited). In addition to RNA editing, alternative splicing also accounts for the diversity of different subunits (Liu and Zukin, 2007). The channels which lack edited GluR2 subunit allow more divalent cations such as Ca^{2+} and Zn^{2+} to permeate and exhibit an inwardly-rectifying current-voltage (I-V) relationship (Burnashev et al., 1992). Due to the extra positive charge introduced by the presence of arginine (Q/R editing) in GluR2, AMPAR which contain the edited GluR2 subunit are impermeable to Ca^{2+} and Zn^{2+}. They

exhibit a linear current-voltage relationship (Boulter et al., 1990) and can be blocked by intracellular polyamines. The presence of GluR2 not only changes the channel conductance (Swanson et al., 1997), but also influences AMPAR assembly and trafficking from ER and targeting to the postsynaptic density (Passafaro et al., 2001; Greger et al., 2002).

Ca^{2+} permeable AMPA receptors play a major role in synaptic plasticity. The entry of Ca^{2+} into the cell modulates synaptic plasticity by several mechanisms, for example Ca^{2+} activates the intracellular signalling cascades which in turn influences AMPA receptor trafficking. The Ca^{2+} entry can also change the subunit composition of AMPARs in the postsynaptic density which further leads to changes in the properties of synapses such as AMPAR kinetics and permeability (Liu and Zukin, 2007). In addition to a rise in Ca^{2+} levels, AMPAR with unedited GluR2 (or lacking edited GluR2) might lead to a later rise in toxic Zn^{2+} levels supporting excitotoxic death of neurons (Kwak and Weiss, 2006). Ca^{2+} permeable AMPA receptors not only alter the properties of a synapse but also contribute to various neurological disorders. A number of diseases including excitotoxicity, epilepsy, amyotrophic lateral sclerosis (ALS), ischemia (Liu et al., 2004) and pain were shown to be associated with altered GluR2 function (Cull-Candy et al., 2006). The excess flow of Ca^{2+} into the cell leads to spontaneous seizures thereby increasing the excitability of hippocampal neurons (Brusa et al., 1995). A summary of various neurological disorders associated with altered GluR2 expression or function can be found below in table 3.

Neurological disorders linked to altered GluR2 function	
Disease	**Reference**
Alzheimer's disease	Ikonomovic et al., 1997
Amyotrophic lateral sclerosis (ALS)	Kawahara et al., 2004
Antipsychotics	Fitzgerald et al., 1995
Corticosteroids	Nair et al., 1998
Drugs of abuse	Fitzgerald et al., 1996
Epilepsy	Brusa et al., 1995
Excitotoxicity	Carriedo et al., 1998
Ischemia	Noh et al., 2005
Pain	Hartmann et al., 2004
Spinal cord injury	Grossman et al., 1999
Stroke	Liu et al., 2004
White matter injury	Follett et al., 2004

Table 3: A summary of various neurological disorders associated with altered GluR2 expression/function.

It has been shown that GluR2 translation is regulated by CPEB3 in neurons based on its 3'UTRs secondary structure (Huang et al., 2006). Two transcripts for GluR2: 4 kb and 6 kb in length were described which differ in their 3'UTRs (Kohler et al., 1994). In addition, miRNA binding sites were found in rat GluR2 3'UTR, hence miRNAs might also participate in the regulation of GluR2 translation (Rocchi and Tkatch, A179, IBRO abstract, 2011). In the present study, the analysis of the 3'UTR revealed a number of potential CPEB binding sites and poly(A) sequences, but no information is available about which of them are functional. As GluR2 influences synaptic properties and is associated with several neurological disorders, it is important to regulate GluR2 function. Therefore, understanding the complex mechanisms that regulate the expression and localization at synapse as well as subunit composition of AMPA receptors are of high interest.

1.5.1.3 GluR2 interacting partners

As GluR2 plays a crucial role in determining the AMPA receptor function, the mechanisms that regulate the insertion of functional AMPARs at synapses are of great interest. The trafficking of AMPA receptors to and from synapses is the underlying mechanism for long-term changes in the synaptic efficiency (Liu and Zukin, 2007). In addition to trafficking, recent findings claim that activity-dependent local protein synthesis of AMPAR in dendrites also plays an important role in regulating the number and distribution of AMPAR (Grooms et al., 2006). The interaction of GluR2 with several proteins is important for the expression and trafficking of AMPAR as well as for post-translational modifications (Braithwaite et al., 2000). These proteins interact with the C-terminus of GluR2 at i) the N-ethylamide-sensitive factor /adaptor protein-2 (AP2) binding site and ii) at the PDZ binding site. NSF is an ATPase that regulates the membrane insertion and stabilization of GluR2 containing functional AMPAR at synapses (Lee et al., 2002), whereas AP2 is an adaptor protein which has a role in clathrin-dependent endocytosis.

The PDZ domain-containing proteins that interact with the C-terminus of GluR2 include the glutamate receptor interacting protein 1 (GRIP1), AMPAR binding protein (ABP) (also called GRIP2) (Osten et al., 1998; Srivastava et al., 1998), and the protein interacting with C-kinase 1 (PICK1) (Xia et al., 1999). GRIP1 contains seven PDZ domains and has been described as the first protein interacting with the C-terminus of GluR2 by yeast hybrid assay (Dong et al., 1997). ABP (also called GRIP2) shares 64-93% similarity with GRIP1, and only differs from

it by lacking the seventh PDZ domain. Both ABP/GRIP2 and GRIP1 are splice isoforms of the same gene with six and seven PDZ domains, respectively (Wyszynski et al., 1999) and are present in the PSD. Both ABP/GRIP2 and GRIP1 are important for clustering of AMPAR at synapses (Srivastava et al., 1998). PICK1 contains a single PDZ domain and is important for the clustering of AMPAR at synapses as well as for facilitating the expression of AMPAR at the cell surface (Braithwaite et al., 2000). The interaction of GluR2 with the PDZ domain containing proteins found to assist with the exit of assembled AMPAR from ER as well as trafficking to the synapse (Cull-Candy et al., 2006). Another class of proteins interacting with GluR2 are transmembrane AMPAR regulatory proteins (TARPs). These are auxiliary subunits of AMPAR which help in the trafficking of AMPAR and also affect their conductance (Rouach et al., 2005; Nicoll et al., 2006). A summary of different proteins that interact with the C-terminus of GluR2 and their functions can be found below in table 4.

Proteins interacting with GluR2	Function	Reference
Adaptor protein-2 (AP2)	Clathrin-dependent endocytosis	Lee et al., 2002
AMPA receptor binding protein (ABP/GRIP2)	Clustering of AMPAR at synapses	Srivastava et al., 1998
Glutamate receptor interacting protein 1 (GRIP1)	Clustering of AMPAR at synapses	Dong et al., 1997
N-ethylamide-sensitive factor	Expression of GluR2-containing AMPAR at synapse	Lee et al., 2002
Protein interacting with C-kinase 1 (PICK1)	Clustering of AMPAR at synapses	Xia et al., 1999
Transmembrane AMPAR regulatory proteins (TARP)	Trafficking and conductance of AMPAR	Nicoll et al., 2006 Rouach et al., 2005

Table 4: A summary of proteins shown to interact with the C-terminus of GluR2.

Bioinformatics indicated potential binding sites for CPEBs in the 3'UTR of some of the GluR2 interacting partners. Although there might be CPEs in several of the GluR2 interacting partners, ABP was shown to undergo stimulated polyadenylation (Du and Richter, 2005) and has been confirmed as a CPEB target (Theis et al., in revision). The authors found impaired protein synthesis of ABP after kainate injection (stimulated protein synthesis). Both ABP (GRIP2) and GRIP1 possess CPEs in their 3'UTRs (Figure 6).

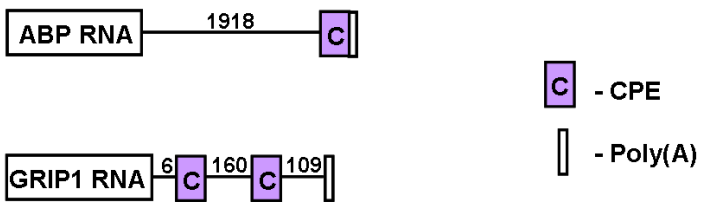

Figure 6: The 3'UTRs of ABP/GRIP2 and GRIP1 with CPEs and poly(A) marked. The numbers indicate the distance in bases between two elements.

1.5.1.4 EphA4

The Ephrin (Eph) receptors are the largest family of receptor tyrosine kinases (RTKs) (Zhou, 1998), present in both developing and mature tissues with predominant expression in neurons (Murai and Pasquale, 2003). The Eph receptors were first identified as tyrosine kinases involved in cancer and were named after their source of isolation, erythropoietin-producing hepatocellular carcinoma cell line (Hirai et al., 1987). Eph receptors are divided into two subclasses based on their affinity for the ligands: i) EphA receptors and ii) EphB receptors. The ligands that interact with Eph receptors were named as Eph family receptor interacting proteins or simply ephrins (Committee, 1997). In mammals, the Eph receptor family includes 14 members: nine EphA (EphA1-EphA8 and EphA10) receptors and five EphB (EphB1-EphB4 and EphB6) receptors. Their ligands, the ephrins, constitute a family of 8 members: five ephrin-A (ephrinA1-A5) ligands and three ephrin-B (ephrin B1-B3) ligands (Murai and Pasquale, 2003; Calo et al., 2006). Although both Eph receptor subtypes share a similar structure, they differ in their affinities to their ligands: the A-type receptors bind to glycosyl phosphatidyl inositol (GPI)-linked ephrin-A ligands, whereas the B-type receptors bind to transmembrane ephrin-B ligands. EphA4 is an exception, since it can interact with both ephrin-A and ephrin-B ligands (Pasquale, 2005).

The Eph receptors and their transmembrane ligands, the ephrins, are collectively named ‘‘Eph proteins’’. The binding of an ephrin ligand to its respective Eph receptor results in bidirectional signalling: it will affect both the receptor expressing cells (called forward signalling), as well as the ligand expressing cells (called reverse signalling) (Pasquale, 2005). Although the classical signalling of Eph proteins is bidirectional, ephrins and Eph receptors can function independently of each other or function in association with other cell signalling systems (Pasquale, 2008). The Eph proteins contribute to several mechanisms which include cell migration, axon guidance (Kullander and Klein, 2002), activity-dependent synaptic plasticity and subsequently learning and memory (Yamaguchi and Pasquale, 2004). They were also reported to be important in actin cytoskeleton remodelling (Noren and Pasquale, 2004) and in clustering of NMDA receptors (Murai and Pasquale, 2004). An important function of Eph proteins is the neuron-glia crosstalk in the hippocampus (Murai et al., 2003).

Among Eph receptors, EphA4 is very interesting and unique because of its interaction with both classes of ligands (ephrin-A and -B) as well as its role in neuron-glia crosstalk (Filosa et

al., 2009). EphA4 is highly expressed in the adult hippocampus, particularly in the dendritic spines of hippocampal neurons where it modulates the spine architecture (Murai et al., 2003). It is also present in the PSD where it co-localizes with PSD-95 (Carmona et al., 2009). EphA4 interacts with ephrin-A3 ligand present in astrocytes (Figure 7) thereby participating in the neuron-glia crosstalk (Murai et al., 2003; Carmona et al., 2009). It leads to bidirectional effects: EphA4 modulates the spine length by forward signalling and on the other hand, ephrin-A3 ligand negatively regulates the expression of astrocytic glutamate transporters by reverse signalling. The interaction between neuronal EphA4 and astrocytic ephrin-A3 is important for the regulation of glutamate transport which further regulates the synaptic glutamate concentration thereby modulating LTP at excitatory synapses (Filosa et al., 2009).

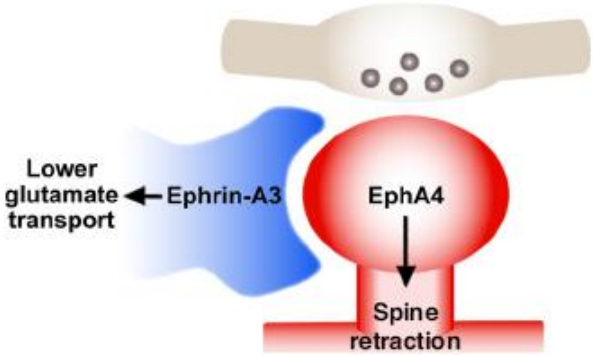

Figure 7: EphA4-ephrin-A3 bidirectional signalling at hippocampal synapses. The interaction of astrocytic ephrin-A3 with postsynaptic EphA4 leads to forward signalling in neurons, inducing the retraction of dendritic spine; and ephrin-A3 reverse signalling in astrocytes, downregulating glutamate transport. The presynaptic terminal is shown in gray, the postsynaptic dendritic spine in red and a glial process near synapse is shown in blue. The figure was adapted from Carmona et al., (2009).

In addition, enhanced protein levels of both the glutamate transporters: glutamate transporter-1 (GLT-1) and glutamate aspartate transporter (GLAST) were observed in knockout mice that lack either EphA4 or ephrin-A3, but their transcript levels remained unaltered which suggested that there might be a posttranscriptional form of regulation (Carmona et al., 2009). These results were further confirmed by the reduction in glutamate transporter levels observed with transgenic overexpression of ephrin-A3, and subsequent glutamate excitotoxicity which might further lead to dendritic swellings (Filosa et al., 2009). The dysfunction of Eph results in dendritic spine abnormalities which might eventually lead to several neurological disorders such as schizophrenia (Glantz and Lewis, 2000), autism and mental retardation (Kaufmann and Moser, 2000).

It was already shown that the 3'untranslated region of EphA4 contains binding sites for several regulatory proteins such as CPEs, AU-rich elements (AREs) and Hu antigen R (HuR) binding sites (Winter et al., 2008). Either of these binding sites is bound by the regulatory proteins which might control the translation of EphA4 thereby indirectly regulating glutamate transporter expression. A schematic of the EphA4 3'UTR with its CPEs and the polyadenylation signal is shown in figure 8.

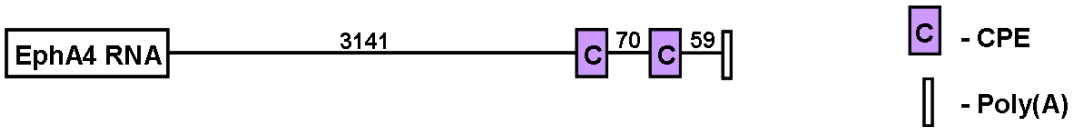

Figure 8: EphA4 3'UTR with CPEs and poly(A) marked. The numbers indicate the distance in bases between the two elements.

1.6 Conditional transgenic systems to study gene function *in vivo*

The function of a gene can be studied by developing animal models with either gain or loss of function of the particular gene. The development of these animal models which mimic a disease condition in humans will help in understanding the disease as well as in designing treatment approaches (Sun et al., 2007). To do so, the gene expression should be controlled in a precise way. A number of genetic manipulation techniques have been developed which comprise the use of conventional transgenic systems (overexpression of a protein or of a dominant negative protein) and knock-out approaches (gene deletion). As knock-out approaches are sometimes deleterious during development, the best approach to study gene function would be a "conditional transgenic system". The ideal system should meet the following criteria: i) it should be possible to switch on or off the transgene expression at any time point, ii) it should be possible to reverse the expression rapidly in the desired cell or tissue type (Sun et al., 2007).

Among the transgenic systems, the tetracycline-inducible system developed by Manfred Gossen and Hermann Bujard is most widely used (Gossen and Bujard, 1992) because of its spatial and temporal control of the transgene. The *tet*-inducible system is the preferred system for transgene overexpression due to several advantages (Gingrich and Roder, 1998): i) it is based on *cis* regulatory elements from bacteria (prokaryotes); these elements were known to cause no/minimal pleiotropic effects, ii) it shows a very low level of basal expression, iii) it is easily inducible and iv) transgene regulation (switching on or off) is easily achieved in desired cells or tissues. The system is easily inducible by tetracycline or its derivatives such as

doxycycline. This inducer is ideal for the generation of transgenic animals (Kistner et al., 1996) as it is cost effective, nontoxic, and can penetrate the placenta and blood/brain barrier which eventually can be taken up rapidly by the cells. There are two versions of the *tet* system, called ***tet*-OFF** (Gossen and Bujard, 1992) and ***tet*-ON** (Gossen et al., 1995) systems.

The *tet*-inducible systems consist of two major components (see also Figure 9):

a) Transcriptional transactivators [eg., tTA (tetracycline transactivator), rtTA (reverse tTA)]: they interact with bacterial *cis* regulatory elements called *tet* operator (*tet*O).
b) Antibiotics: they modulate the binding of transactivators at doses below toxic levels (Shockett and Schatz, 1996). eg., tetracycline, doxycycline.

The tTA is a fusion protein of *Escherichia coli* tetracycline-repressor protein (*Tet*R) and the C-terminus (activation domain) of the protein 16 of herpes simplex virus (VP16). The tTA can be controlled by either tetracycline or its derivatives such as doxycycline. Another important component of the system is a tissue specific promoter (TSP), which drives the transgene expression in a specific cell type. For example, the CaMKIIα promoter drives the expression specifically in forebrain neurons such as pyramidal neurons of the hippocampus and cortex (Mayford et al., 1997) whereas the human GFAP promoter is specific to astrocytes and radial glia (Fiacco et al., 2007). The promoter is composed of a minimal promoter containing the binding site for RNA polymerase II (TATA box) fused to *tet* operator sequences to which the tTA binds. The fusion with the VP16 activation domain transforms the *tet* repressor into a transcriptional transactivator in eukaryotic cells.

The original *tet* system developed was the *tet*-OFF system in which the transcription of a gene occurs in the absence of an inducer [tetracycline or doxycycline (Dox)] (Figure 9A; Lewandoski, 2001). In the absence of Dox, the tTA binds to *tet*O and the tTA-dependent promoter drives the transgene expression in the desired cell type. But, in the presence of Dox, the tTA undergoes a conformational change and can't bind to the *tet*O thereby not driving the transgene expression. As the antibiotics (*tet* or Dox) are not present endogenously in the animals, their exogenous application allows the temporal control of gene expression. Since the presence of Dox silences the transgene expression, it is termed *tet*-OFF system. A modified version, called *tet*-ON system (Gossen et al., 1995) was developed later in which the transcription occurs only in the presence of an inducer (Figure 9B; Lewandoski, 2001). In this system, a mutant form of tTA, called reverse tTA (rtTA) binds to recombinant *tet*O and drives

the transcription only when Dox is present. Since the presence of Dox allows the gene expression, it is termed *tet*-ON system (Gossen et al., 1995).

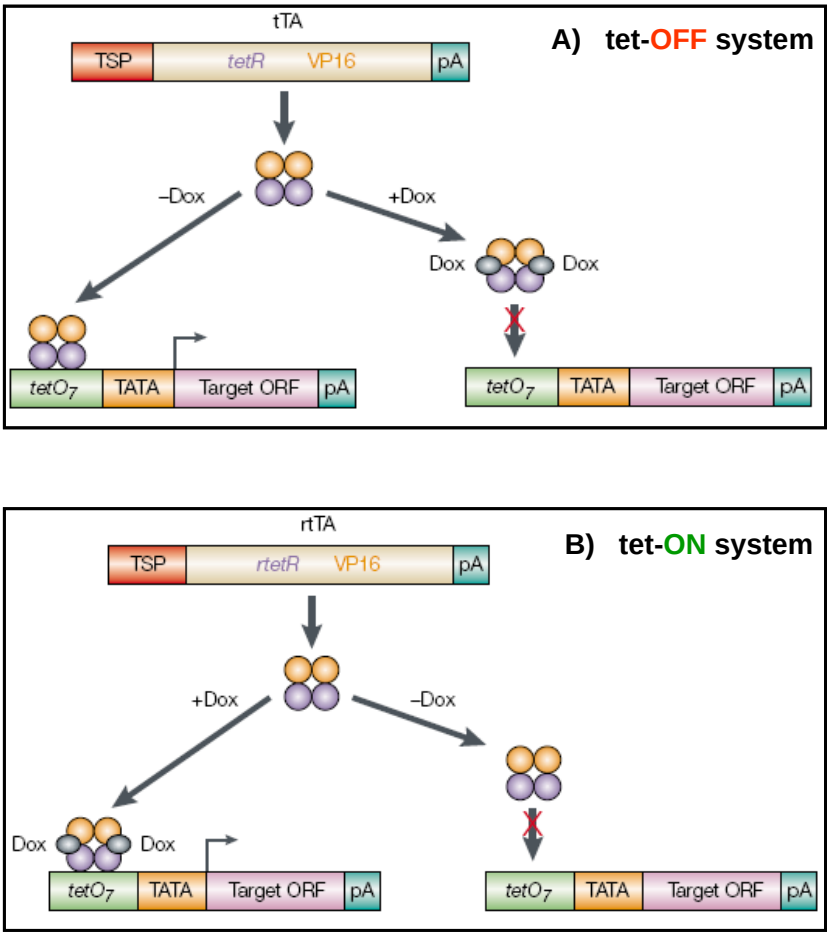

Figure 9: Two variants of *tet*-inducible conditional transgenic systems. A) *tet*-OFF system, in which tTA binds to *tet*O and drives the expression of a target open reading frame when the Dox is not present. B) *tet*-ON system, in which a variant of tTA, rtTA, binds to *tet*O and drives the expression of a target open reading frame only in the presence of Dox. TSP: tissue-specific promoter, *tet*R: tetracycline response, pA: polyadenylation, Dox: doxycycline, *tet*O: *tet* operator, ORF: open reading frame. The figure was adapted and modified from Lewandoski, (2001).

2 Aim of the thesis

The main aim of the thesis was to investigate the expression of CPEBs in neurons and glial cells of mouse hippocampus, particularly focussing on CPEB2 function in neurons. The following questions were addressed:

1) Investigating the expression pattern of CPEBs (1-4) in neurons and glia

Even though the expression of CPEBs (1-4) was reported in neurons, astrocytes and microglia, the expression of CPEBs in NG2 glia was not studied before. Only few reports indicated the presence of multiple splice isoforms for each CPEB. Until now, none of the reports have described the distribution of various splice isoforms of each CPEB in different cell types and across different species. Hence, the present study was aimed to investigate the expression of different splice isoforms of CPEBs (1-4) in detail in neurons and glial cells (astrocytes, NG2 glia and microglia) as well as in different species.

2) Investigating the role of CPEB2 in neurons

CPEB2 is not a well described member of the CPEB family. Even though the expression of CPEB2 was reported in mouse brain, the functional role of it in mouse brain is not known. Therefore, and to avoid compensatory effects by other CPEBs, a conditional *tet*-OFF approach was used to generate transgenic mice which overexpress CPEB2 in neurons of the mouse brain hippocampus and cortex. CPEB1 requires the zinc finger in order to bind to the target mRNAs. To find out whether CPEB2 requires the zinc finger for translational regulation, a zinc finger mutant (CPEB2ΔZn) was generated in the present study. Using this set of transgenic mice, the impact of CPEB2 on the translation of target mRNAs was studied.

3) Investigating the interaction of CPEB2 with target mRNAs *in vitro*

So far CPEB2 is known to interact with few mRNAs. Since the RNA binding domain is conserved across CPEB family members, more than one CPEB can regulate same target mRNA. Hence, the present study was aimed to find out if there is any overlap in the binding specificity of CPEB1 and CPEB2 to the target mRNAs.

3 Materials and Methods

3.1 Materials

3.1.1 Chemicals

The chemicals were purchased from Applichem (Darmstadt, Germany), Carl Roth (Karlsruhe, Germany), New England Biolabs (Frankfurt, Germany) Invitrogen (Darmstadt, Germany), Roche (Mannheim, Germany) and Sigma-Aldrich (Munich, Germany). All the cell culture media, antibiotics and serum were purchased from Gibco (Darmstadt, Germany). All the primers were purchased from MWG (Ebersberg, Germany). Restriction enzymes were purchased from New England Biolabs (Frankfurt, Germany).

3.1.2 Buffers for Western blotting

Buffer	Composition	Final concentration
Lysis buffer (modified RIPA buffer)	6.05 g Tris 8.76 g NaCl 5 ml NP40 5 g Sodium deoxycholate 10 ml Triton X-100 The contents (except NP40 and triton) were dissolved in 700 ml dH_2O, and the pH was adjusted to 7.5. Later, NP40 and triton were added and the volume was adjusted to 1l. The buffer was aliquoted 10 ml each and stored at -20^oC.	50 mM 150 mM 0.5% 0.5% 1%
1.5 M Tris (pH 8.8)	18.16 g Tris was dissolved in 100 ml dH_2O, the pH was adjusted to 8.8 and the solution was stored at +4^oC.	1.5 M
0.5 M Tris (pH 6.8)	6.05 g Tris was dissolved in 100 ml dH_2O, the pH was adjusted to 6.8 and stored at +4^oC.	0.5 M
APS	0.1 g APS was dissolved in 1 ml of dH_2O	10%

	(always prepared immediately before use)	
SDS	10 g SDS was dissolved in 100 ml of dH_2O and stored at RT.	10%
Resolving gel (10%)	6.15 ml	dH_2O
	3.75 ml	1.5 M Tris (pH 8.8)
	150 µl	
	4.95 ml	10% SDS
	75 µl	Acrylamide
	7.5 µl	10% APS
	The components were added in the same order as above and mixed gently before use.	TEMED
Stacking gel (4%)	6.1 ml	dH_2O
	2.5 ml	0.5 M Tris (pH 6.8)
	100 µl	
	1.3 ml	10% SDS
	50 µl	Acrylamide
	10 µl	10% APS
	The components were added in the same order as above and mixed gently before use.	TEMED
3x Sample buffer	0.77 g	50 mM Tris HCl (pH6.8)
	2 g	2% SDS (w/v)
	1.54 g	100 mM DTT
	10 ml	10% Glycerol (v/v)
	10 µl	
	The contents were dissolved in 100 ml dH_2O, aliquoted 1 ml each and stored at -20^oC.	0.01% Bromophenol blue (w/v)
10X Tris-Glycine-SDS buffer (gel running buffer)	30.3 g	25 mM Tris
	144 g	192 mM Glycine
	10 g	0.1% SDS
	The contents were dissolved in 1l dH_2O.	pH 8.3
1x gel running	50 ml of 10x Tris-Glycine-SDS buffer and	1x Tris-Glycine-

buffer	450 ml of distilled water.	SDS
10x Tris-Glycine	30.3 g	25 mM Tris
buffer	144 g	192 mM glycine
(Blotting buffer)	The contents were dissolved in 1l dH_2O.	pH 8.3
1x Blotting buffer	50 ml of 10x Tris-Glycine buffer	1x Tris-Glycine
	100 ml of methanol	20% methanol
	Volume was adjusted to 500 ml with distilled water.	
10x TBST	30.28 g	25 mM Tris
(pH 7.4)	87.66 g	150 mM NaCl
	0.5 ml	0.05% Tween-20
	Tris and NaCl were dissolved in 700 ml dH_2O, adjusted the pH to 7.4. Later, Tween was added and the volume was adjusted to 1l.	
1x TBST	100 ml of 10x TBST and 900 ml of distilled	1x
(pH 7.4)	water. Stored at $+4^oC$.	
1x TBST with	50 ml of 1x TBST with 0.05% tween-20 was	1x
0.1% Tween-20	taken and 250 µl Tween-20 was added. The	
(pH 7.4)	volume was adjusted to 500 ml.	
Blocking solution	0.5 g milk powder	5% milk powder
for all blots	10 ml 1x TBST (pH 7.4)	1x TBST (pH 7.4)
Blocking solution	0.3 g bovine serum albumin (BSA)	3% BSA
for EphA4 blot	10 ml 1x TBST with 0.1% Tween-20 (pH 7.4)	0.1% Tween-20
		1X TBST (pH 7.4)

3.1.3 Buffers for RNA Co-immunoprecipitation

Buffer (Stock)	**Composition**	**Final concentration**
0.5 M HEPES	11.92 g of HEPES was dissolved in 100 ml dH_2O	0.5M
1 M NaCl	5.84 g of NaCl was dissolved in 100 ml dH_2O	1 M
0.5 M EDTA	14.61 g of EDTA was dissolved in 100 ml dH_2O	0.5 M
20%	10 ml of TritonX-100 dissolved in 50 ml of	20%

Triton X-100	RNase-free water and stored at +4^{o}C.	
RNA-FLAG	HEPES (1 ml of 0.5 M)	10 mM
Lysis buffer	NaCl (10 ml of 1 M)	200 mM
	EDTA (3 ml of 0.5 M)	30 mM
	Triton X-100 (1.25 ml of 20%)	0.5%
	RNasin	200 U/ml
	The volume was adjusted to 50 ml with RNase-free water. Before use, one complete mini protease inhibitor cocktail tablet and 10 µg tRNA/10 ml of buffer was dissolved and the solution was sterile filtered.	
RNA-FLAG	HEPES (1 ml of 0.5 M)	10 mM
wash buffer	NaCl (25 ml of 1 M)	500 mM
	EDTA (3 ml of 0.5 M)	30 mM
	1.25 ml of 20%	0.5% Triton X-100
	The volume was adjusted to 50 ml with RNase-free water. Before use, 100 U RNasin and one complete mini protease inhibitor cocktail tablet/50 ml of buffer was dissolved and the solution was sterile filtered.	

3.1.4 Solutions for Genotyping

Solution	**Composition**
Laird buffer	100 mM Tris, pH 8.5 200 mM NaCl 5 mM EDTA 0.2% SDS 1l dH_2O Tris and NaCl were mixed, the pH adjusted to 8.5, and then EDTA and SDS were added. The volume was adjusted to 1l with dH_2O.
Proteinase-K (50 µg)	The working concentration was 20 mg/ml in dH_20.

70% Ethanol	70 ml of > 99% ethanol 30 ml of dH_2O
10x Tris Borate EDTA buffer (10x TBE)	1 M Tris 0.83 M boric acid 10 mM EDTA 1l dH_2O
1x TBE	100 ml of 10x TBE 900 ml of dH_2O
Ethidium Bromide (10 mg/ml)	The solution was diluted 1:10 with 1x TBE.

3.1.5 Solutions for Immunocytochemistry (ICC)

Solution	Composition
Fixative	4% PFA, 5% sucrose in 1x PBS
Permeabilizing Solution	0.5% Triton in 1x PBS
Blocking Solution	1% BSA, 3% NGS in 1x PBS
Primary antibody solution	Appropriate primary antibodies were diluted in blocking solution.
Secondary antibody solution	Appropriate secondary antibodies were diluted in 1x PBS with 0.1% Tween-20.
Hoechst	1:10,000 Hoechst, 0.1% Tween-20 in 1x PBS

3.1.6 Solutions for Immunohistochemistry (IHC)

Solution	Composition
4% PFA	4 g of PFA was dissolved in 90 ml dH_2O, heated to 60^oC and 1M NaOH was added to clear the solution. Later ~10 ml of 10x PBS (pH 7.4) was added, mixed and the pH was adjusted to 7.4. The solution was filtered and stored at -20^oC.
10x PBS (pH 7.4)	2.04 g NaH_2PO_4 (17 mM) and 14.77 g $Na_2HPO_4.2H_2O$ (3 mM), 87.6g NaCl (1.5 mM) were dissolved in 1l

	dH_2O and the pH was adjusted to 7.4.
1x PBS	100 ml of 10x PBS (pH 7.4) was taken and the volume adjusted to 1l.
1x PBS with 0.01% sodium azide	0.1 g of sodium azide was dissolved in 100 ml of 10x PBS, adjusted the volume to 800 ml. The pH was adjusted to 7.4 and the volume was adjusted to 1l with dH_2O.
30% sucrose in 1x PBS	30 g of sucrose was dissolved in 100 ml of 1x PBS, pH 7.4.
Blocking solution	10% Normal Goat Serum (NGS), 0.4% Triton X-100 in 1x PBS pH 7.4.
Primary antibody solution	Appropriate dilutions of primary antibodies were prepared in 5% NGS, 0.1% Triton X-100 in 1x PBS.
Secondary antibody solution	Appropriate dilutions of secondary antibodies were prepared in 1x PBS.
Hoechst (Nuclei staining solution)	1:50 dilution of Hoechst was prepared in distilled water.

3.1.7 Ready-to-use solutions

Chemical	**Company**
Acrylamide-Bis ready-to-use solution (30%)	Merck
Ethanol	Carl Roth
Glycerol	Carl Roth
Hoechst	Molecular probes
Methanol	Applichem
Normal Goat Serum (NGS)	Millipore
Nonidet P-40 (NP-40)	Carl Roth
Permafluor	Thermo Scientific
2-Propanol (Isopropanol)	Carl Roth
Qiazol	Qiagen
Restore Western Blot Stripping Buffer	Thermo Scientific
RNase Away	Molecular Bioproducts

RNase Zap	Ambion
Stripping Buffer	Thermo Scientific
SuperSignal West Dura Extended Duration Substrate	Thermo Scientific
TEMED	Carl Roth
Tissue-Tek	Sakura Finetek
Triton X-100	Carl Roth
Tween-20	Carl Roth

3.1.8 Antibiotics

Antibiotic	Concentration	Supplier
Ampicillin	100 µg/ml	Carl Roth
Kanamycin	50 µg/ml	Carl Roth
Penicillin/Streptomycin	100 u/ml	Gibco

3.1.9 Restriction Enzymes

Enzyme	Restriction site	Incubation	Heat inactivation	Company
*EcoR*I	5´- GAATTC –3´	37°C	65°C/20 min	NEB
*EcoR*V	5’- GATATC -3’	37°C	80°C/20 min	NEB
*Not*I	5’- GCGGCCGC -3’	37°C	65°C/20 min	NEB
*Sal*I	5’- GTCGAC -3’	37°C	65°C/20 min	NEB
*Sfi*I	5’- GGCCNNNNNGGCC -3’	50°C	No	NEB
*Xba*I	5’- TCTAGA -3’	37°C	65°C/20 min	NEB

3.1.10 DNA Polymerases

Enzyme	Purpose	Supplier
Advantage2 polymerase	3’ RACE	Clontech
Advantage HD polymerase	In-fusion cloning	Clontech
Advantage HF2 polymerase	Cloning	Clontech

GoT*aq* Flexi DNA polymerase	Genotyping	Promega
Platinum T*aq* DNA polymerase	Nested PCR	Invitrogen
Superscript III reverse transcriptase	Reverse transcription	Invitrogen
T*aq* DNA polymerase	First round of PCR	Invitrogen

3.1.11 Antibodies

3.1.11.1 Primary Antibodies

Antibody	Species	Type	Dilution (WB)	Dilution (ICC/IHC)	Catalogue no.	Company
β-actin	Ms	M	1:5000	-----	A3853	Sigma-Aldrich
β-catenin	Ms	M	1:1000	1:500	MAB2081	Millipore
ABP/GRIP2	Rb	P	1:1000	-----	AB5569	Millipore
CPEB1	Rb	P	-----	1:100	#65	Custom made
CPEB2	Rb	P	-----	1:250/1:500	#68	Custom made
CPEB3	Rb	P	-----	1:100	ab10883	Abcam
CPEB4	Rb	P	-----	1:100	#71	Custom made
EphA4	Ms	M	1:500	-----	37-1600	Invitrogen
GFP	Rb	P	-----	1:1000	132002/12	Synaptic Systems
GFP	Ch	P	-----	1:500	Ab13970	Abcam
GluR1	Rb	P	1:1000	-----	AB1504	Millipore
GluR2	Rb	P	1:1000	-----	AB1768	Millipore
GLT-1	Gp	P	1:1000	-----	AB1783	Millipore
GRIP1	Ms	M	1:1000	-----	611318	BD Biosciences
M2 FLAG	Ms	M	1:1000 (IP)	-----	F3165	Sigma-Aldrich
MAP2	Ms	M	-----	1:200 (IHC)	188 011	Synaptic Systems
MAP2	Ms	M	-----	1:100(ICC)	M4403	Sigma-Aldrich
NeuN	Ms	M	-----	1:500	MAB377	Millipore
Synaptophysin	Ms		-----	-----	MAB5258	Millipore
Tubulin	Ms	M	1:10,000	-----	T9026	Sigma-Aldrich

Ms: mouse, Rb: rabbit, Ch: chicken, GP: guinea pig, M: monoclonal, P: polyclonal, WB: Western blotting, IP: immunoprecipitation, ICC: immunocytochemistry, IHC: immunohistochemistry.

3.1.11.2 Secondary Antibodies

Antibody	Dilution	Company
Sheep anti-mouse-HRP	1:10,000 (WB)	Amersham
Donkey anti-rabbit-HRP	1:10,000 (WB)	Amersham
Goat anti-guinea pig-HRP	1:5,000 (WB)	Abcam
Alexa 488 Goat anti mouse IgG	1:500 (IHC)	Molecular Probes
Alexa 488 Goat anti rabbit IgG	1:500 (IHC)	Molecular Probes
Alexa 594 Goat anti mouse IgG	1:500 (IHC)	Molecular Probes
Alexa 594 Goat anti rabbit IgG	1:500 (IHC)	Molecular Probes
Alexa 488 Goat anti chicken IgG	1:500 (IHC)	Molecular Probes

WB: Western blotting, IHC: immunohistochemistry.

3.1.12 Kits used

Name of the kit	Company
Advantage2 PCR kit	Clontech
Advantage HD polymerase	Clontech
BCA Protein Assay kit	Pierce
Endofree plasmid maxi kit	Qiagen
Expand High Fidelity PCR System	Roche
In-fusion Dry down PCR cloning kit	Clontech
Marathon Ready cDNA amplification kit	Clontech
PeqGold Gel Extraction kit (C-Line)	Peqlab
PeqGold Plasmid Miniprep kit I (C-Line)	Peqlab
PureLink HiPure Plasmid Filter Midiprep kit	Invitrogen
QIAprep Spin Miniprep kit	Qiagen
QIAquick Gel extraction kit	Qiagen
RNeasy Mini kit	Qiagen
TOPO XL PCR Cloning kit	Invitrogen
Wizard SV Gel and PCR Clean-up system	Promega
Wizard Plus SV Miniprep DNA Purification system	Promega

3.1.13 Competent E. *coli*

Competent cells	Source
Fusion Blue Competent E. *coli*	Clontech
TOP10 chemically competent E. *coli*	Invitrogen
TOP10 chemically competent E. *coli*	Made in the lab (Appendix A9.1)

3.1.14 Molecular weight markers

Marker	Company
1 kb DNA Extension Ladder (1 µg/µl)	Invitrogen
100 bp DNA Ladder (1 µg/µl)	Invitrogen
DNA Molecular Weight Marker VIII	Roche
Novex Sharp Protein Standard	Invitrogen

3.1.15 General lab materials

Material	Company
Agarose	Invitrogen
Blotting paper	Whatman
Cell culture equipment	Gibco/Invitrogen
Sterile Filters	Whatman
Sterile filters	Millipore
LB Agar	Carl Roth
LB broth	Carl Roth
SuperFrost Ultra Plus microscope slides	Thermo Scientific
Proteinase-K	Carl Roth
Pipette tips, plastic ware	Sarstedt
Polyvinylidene fluoride (PVDF) membrane	Millipore
27G needles	B. Braun

3.1.16 Laboratory Equipment

Equipment	Company
ABI 7900HT Fast Real-Time PCR system	Applied Biosystems
Axiophot microscope	Carl Zeiss
Biophotometer	Eppendorf
Centrifuge 5424	Eppendorf
Cooled centrifuge	Thermo Scientific
Cryo-star 560 Cryostat	Microm
DynaMag magnet	Invitrogen
Gel documentation system	Syngene
Gene Gnome Imaging system	Syngene
Heat block	VWR
Heildolph Rotamax120	Heidolph
Heraeus Labofuge 400 centrifuge	Thermo Scientific
Microwave	Severin 700
Mycycler Thermal Cycler	Bio-rad
Nanodrop	Eppendorf
Pearl Nanophotometer	Implen
Owl Agarose gel electrophoresis systems	Thermo Scientific
pH meter	Mettler Toledo
PTC-200 Peltier Thermal Gradient Cycler	Bio-Rad
Rotator PTR-30	Grant Bio
SDS gel Electrophoresis power supply	Bio-Rad
Shaker	Grant Bio
Vortexer	VWR
Water bath	P-D Industriegesellschaft GmbH
Weighing balance	Acculab
Western blot module	Invitrogen
37^{o}C incubator	Binder
37^{o}C shaking incubator	G.F.L
55^{o}C shaking water bath	Memmert
+4^{o}C Refrigerator	Liebherr
-20^{o}C Freezer	Liebherr

-80^{o}C Freezer	Thermo Scientific

3.1.17 Softwares used

Software	Purpose	Source
Gene Tools	Quantification of Western blots	Syngene
In-fusion primer designer	Designing primers for in-fusion cloning	Clontech
Multalin	Alignment of DNA sequences	(Corpet, 1988)
Primer3	Designing PCR primers	(Rozen and Skaletsky, 2000)
Primer Express 3.0	Designing primers/probe set for Real Time PCR	Applied Biosystems
SDS 5.0 qPCR	Quantitative Real Time PCR	Applied Biosystems

3.2 Methods

3.2.1 RT-PCR of rat/human hippocampus

Human brain hippocampal cDNA was purchased from Clontech (France) where as rat brain hippocampal cDNA was isolated in the lab. Hippocampus was isolated from rat brain, homogenized in trizol and then chloroform was added and mixed vigorously for 30 sec. The tubes were centrifuged at 10,000g for 10 min at 4^{o}C and the upper aqueous layer was collected into new eppendorf tubes. The RNA was precipitated with isopropanol, incubated on ice for 10 min and centrifuged at 10,000g for 10 min at 4^{o}C. The supernatant was removed, washed with 70% ethanol and centrifuged at 7,500g for 5 min at 4^{o}C. Ethanol was removed, the RNA pellets were air dried for 5 min and dissolved in DEPC-water and the RNA samples were stored at -20^{o}C until use. The first strand cDNA was synthesized from the RNA samples using Omniscript RT kit (Qiagen, Hilden, Germany), protocol followed according to manufacturer's instructions.

The hippocampal cDNAs from rat and human brains was PCR amplified with the corresponding species specific primers. Accuprime kit (Invitrogen, Darmstadt, Germany) with the following PCR program was used: initial denaturation at 94^{o}C/2 min, followed by 35 cycles of denaturation at 94^{o}C/30 sec, annealing at 54^{o}C (rCPEB2) or 55^{o}C (rCPEB2/hCPEB2/hCPEB3) or 58^{o}C (rCPEB4) or 53^{o}C (hCPEB4) for 30 sec, 68^{o}C/1 min and a final elongation at 68^{o}C/20 min. The primers used were, rCPEB3: 5'- GGA TAT GAT CAG GAC TGA TCA TGA GCC TCT GAA AG -3' (forward) and 5'- CCA TGG CTG TCA TCC AAG AAG GCG TC -3' (reverse); rCPEB4: 5'- CCC AGG ACA TTT GAC ATG CAC TCA TTG -3' (forward) and 5'- CAG ACC ACT GTG AAG AGG CTG GTC CCC ACG G -3' (reverse). hCPEB2: 5´- AAC TCC ATC ACT GAC TCC AAA ATC T -3´ (forward) and 5´- CAA GCC ATC ATC TAT TGG AAA GAG GGA AGA -3´ (reverse); hCPEB3: 5´- CAA AAA GCC CTT CTC CAG CAA C -3´ (forward) and 5´- TTC AGC TTT GTG AGG CCA GTC TA -3´ (reverse); hCPEB4: 5´- CAG CTC TGC CTT TGC ACC TAA AT -3´ (forward) and 5´- GGC CAT CAT CCA AGA ATC CAT C -3´ (reverse). For rCPEB2, primers #177 and #179 listed in table 8 were used.

The PCR products were run on a 1.5% agarose gel, the bands excised and cloned into PCR-XL-TOPO vector (Invitrogen) with manufacturer's instructions. TOP10 E. *coli* were

transformed with the resulting clones and the DNA was plated onto Luria Bertani (LB) plates containing 50 µg/ml kanamycin (Carl Roth, Karlsruhe, Germany) and incubated overnight at 37^{o}C. Single colonies were inoculated each in 2 ml of LB with kanamycin and grown overnight at 37^{o}C with 250 rpm rotation. After 12-16 h of incubation, DNA was isolated from overnight cultures using Qiagen miniprep kit (Qiagen) with manufacturer's instructions. The concentration of minipreps was checked and the DNA was sent for sequencing (Sequencing service, Qiagen). For sequencing, two primers which bind in the TOPO vector region (M13f-20 and M13r-24) were used. The Multalin program (Corpet, 1988) was used to align the sequencing reads with reference sequences of different CPEBs and the different splice isoforms for each CPEB were analyzed.

3.2.2 Immunocytochemistry

The expression of all CPEBs (1-4) was investigated in primary hippocampal cultures (PHCs). The cultures were provided by Dr. Georg Zoidl, Ruhr University, Bochum (Zoidl et al., 2002). Experiments were done on 7 day old cultures (7 days *in vitro*, DIV). The cells were plated on cover slips, washed twice with 1x PBS (5 min each) and fixed with 4% PFA and 5% sucrose in 1x PBS for 20 min at room temperature. After fixing, they were washed two times with 1x PBS (each time 5 min) and permeabilized using 0.5% triton in 1x PBS for 5 min at room temperature. After washing twice quickly with 1x PBS, blocking was done with 1% BSA, 3% normal goat serum (NGS) for 1h at room temperature. Then, they were incubated in respective primary antibodies diluted in blocking solution overnight at 4^{o}C. The antibodies used were custom made affinity purified rabbit polyclonal antibodies raised against CPEB1 (#65; 1:100), CPEB2 (#68; 1:250) and CPEB4 (#71; 1:100) (Eurogentec, Cologne, Germany). For CPEB3, a 1:100 dilution of rabbit polyclonal antibody from Abcam (ab10883) was used (Abcam, Cambridge, UK). Double stainings were performed together with neuron-specific MAP2 antibody for specificity (cat. No. 4403; 1:100, mouse monoclonal, Sigma-Aldrich, Munich, Germany). After 24h incubation, the cells were washed three times with 1x PBS (5 min each) and incubated with secondary antibodies (1:500, Alexa 488 goat anti-rabbit and 1:500 Alexa 594 goat anti-mouse) for 1h at room temperature. They were washed again with 1x PBS (3 times, 5 min each), followed by counterstaining with Hoechst (1:10,000 in 0.1% tween-20 in dH_2O) for 5 min. After washing with 1x PBS (3 times, 5 min each), the cover slips were mounted in Prolong Gold (Invitrogen).

3.2.3 Single cell RT-PCR

3.2.3.1 Harvesting cytoplasm from neurons, astrocytes, NG2 glia and microglia

The cell type specific expression of different CPEBs (1-4) was investigated using single cell (sc) RT-PCR. A two round multiplex PCR was done from harvested cytoplasm of different cell types (neurons, astrocytes, NG2 glia and microglia) after electrophysiological characterization of the cell type. For harvesting CA1 pyramidal neurons and astrocytes, hGFAP/EGFP transgenic mice (Nolte et al., 2001) were used. For harvesting NG2 cells, NG2ki-EYFP mice (Karram et al., 2008) were used. For harvesting microglia, Cx3cr1ki-EGFP mice were used. The different cell types were identified based on their current pattern and morphology. The harvesting was done by Dr. Peter Bedner and Mr. Vamshidhar Vangoor in the institute. The mice were anesthetized and the brain was isolated. Hippocampal coronal sections of 200 μm thickness were made with a vibratome (Leica Microsystems, Wetzlar, Germany) and incubated in artificial cerebrospinal fluid (ACSF) with continuous carbogen supply. There are two types of glial cells which co-exist in the mouse hippocampus (Matthias et al., 2003) which include astrocytes and NG2 glia. These two cell types differ in their current patterns, antigen profiles as well as in their functional properties (Wallraff et al., 2004). As various reporter mice were used for harvesting, the different cell types were identified because of their fluorescence. Astrocytes can be identified by their time and voltage independent passive current pattern whereas NG2 glia shows a time and voltage dependent complex current pattern (Matthias et al., 2003). Membrane currents were measured in the whole cell configuration *in situ* with an upright microscope Nikon Eclipse FN1 equipped with infra red differential interference contrast (IR/DIC) optics (Nikon, Dusseldorf, Germany). Current signals were amplified (EPC-8, HEKA, Lambrecht, Germany), filtered at 3 and 10 kHz and sampled at 10 and 100 kHz by an interface connected to a computer system. After electrophysiological characterization of different cell types, the cytoplasm of the respective cell was harvested under careful supervision with an CCD camera (VX45, Optronics, Kehl, Germany) in a tube filled with DEPC-water (~3 μl). The tubes were frozen immediately in liquid nitrogen, and then stored at -80^{o}C until use. The authenticity of the harvested cytoplasm was tested by amplifying with cell-type specific markers (synaptophysin for neurons, S100β for astrocytes, NG2 for NG2 glia and Iba-I for microglia). The procedure of patch clamping and harvesting cytoplasm from a typical pyramidal neuron is depicted schematically in figure 10A. The typical current patterns of all the cell types analyzed are shown in figure 10 B-D.

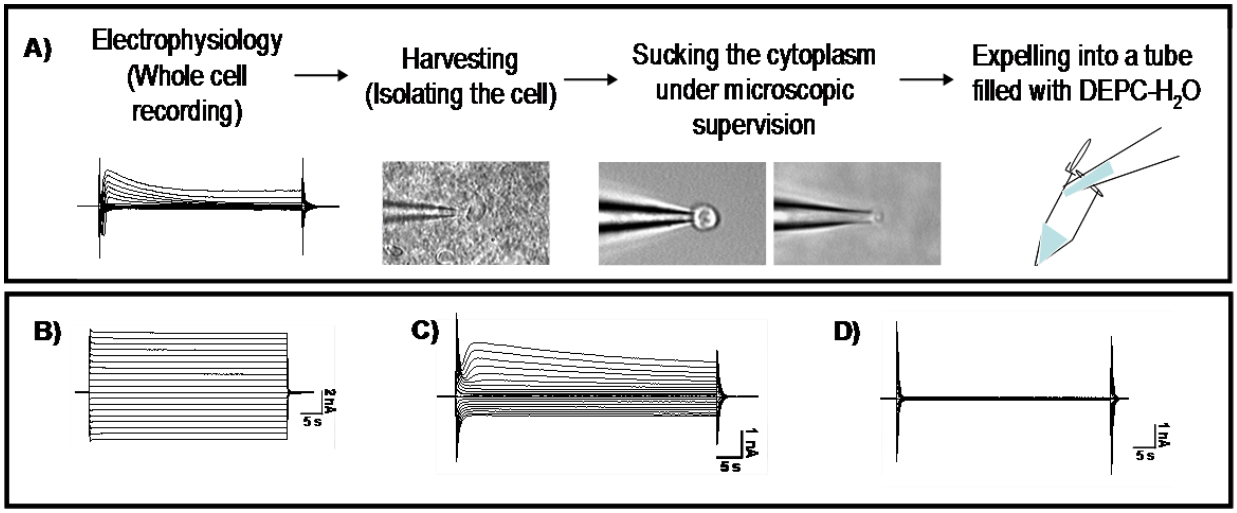

Figure 10: A) Procedure for patch clamp analysis and subsequent harvesting of cytoplasm from a typical pyramidal neuron. The figure was adopted and modified from Seifert and Steinhaeuser, (2007). B-D: Typical current patterns of different neural cells analyzed: B) Astrocytes C) NG2 glia and D) Microglia. na – nano amperes, s – seconds.

3.2.3.2 Reverse transcription of RNA to first strand cDNA

RNA present in the cytoplasm of harvested cells was reverse transcribed to synthesize first strand cDNA. Superscript III reverse transcriptase (Invitrogen) was used and the reaction mix is shown in table 5. The reaction mixture was added to the cytoplasm harvested and incubated at 37^{o}C for 1h.

5x RT buffer (Invitrogen)	2 µl
10 mM Dithiothreitol (DTT) (Invitrogen)	1 µl
dNTPs (2.5 mM each) (Applied Biosystems)	1 µl
Recombinant RNasin ribonuclease Inhibitor (40 U/µl; Promega)	0.5 µl
Random hexamer (50 U/ml; Roche)	0.5 µl
100 U/µl Superscript III reverse transcriptase (Invitrogen)	0.5 µl
Total volume	**5.5 µl**

Table 5: Reaction mix for Reverse transcription reaction.

3.2.3.3 Two round multiplex PCR

A two round multiplex PCR was done in parallel to identify both the CPEB expression as well as expression of a cell-type specific gene to confirm the origin of cytoplasm. The schematic showing the two round PCR can be found in figure 11.

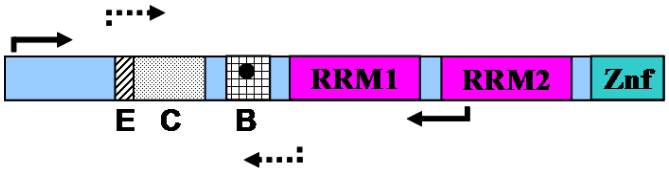

Figure 11: The procedure of two round multiplex PCR. As an example, primers designed for CPEB2 were shown in the figure; similar strategy was followed for other CPEBs as well. The splicing region of CPEB2 contains an 'E' region (striped box), 'C' region (dotted box) and a 'B' region (squared box) harboring a putative phosphorylation site (filled circle). Both sets of primers were marked in the CPEB2 coding region. The arrows represent the outer primer set where as the dotted arrows indicate the nested primer set. The nested primers flank the alternatively spliced region there by making it possible to detect multiple isoforms by PCR. RRM – RNA recognition motif, Zn^{2+} - zinc finger.

In the first round of PCR, two sets of primers were added to the reaction mix (one for a housekeeping gene and another one for CPEB). The PCR mix was prepared as shown in table 6. This mix was added directly to the cDNA samples and PCR amplification was applied.

10x reaction buffer	5 µl
2.5 mM $MgCl_2$	2.5 µl
Upstream primer (for CPEB1/2/3/4) (10 pmol/µl)	1 µl
Downstream primer (for CPEB1/2/3/4) (10 pmol/µl)	1 µl
Upstream primer (for a housekeeping gene)	1 µl
Downstream primer (for a housekeeping gene)	1 µl
dH_2O	27.5 µl
Total volume	**39 µl**

Table 6: Master mix used for the first round of PCR. This master mix was added directly to the cDNA which is ~10 µl. Whenever NG2 primers were used, 0.5 µl each of dimethyl sulfoxide (DMSO) and betaine were added to the master mix.

The typical PCR program used for the first round of PCR can be found below in table 7. The annealing temperature used for CPEB1 was 51°C and for CPEBs (2-4), 54°C.

95°C	3 min	
85°C	hold (during this time, 1 µl of T*aq* DNA polymerase was added)	
95°C	25 sec	5x
54°C	2 min	
95°C	25 sec	40x
54°C	45 sec	
72°C	25 sec	
72°C	7 min	

Table 7: PCR program used for the first round of PCR.

All the primers were designed using Primer 3.0 software (Rozen and Skaletsky, 2000) and synthesized from MWG. The annealing temperatures were calculated depending on the melting temperatures of the primers used in that particular master mix. A list of primers used can be found below in table 8.

Primer	Sequence	Gene
C1 outer left	5´- AGGCTGCAGCTGTGAATGAAGCTA -3´	
C1 outer right	5´- CAAGACCCAAGGGATTACCTGTACC -3´	
# 31	5´- AGGCCATCTGGGCTCAGCGGG -3´	CPEB1
# 52	5´- GGATTGGTTAACACCTTCCGTGTTTTTGGC -3´	
Primers C1 outer left and C1 outer right (outer set), primers 31 and 52 (nested set)		
# 194	5´ - TAC TCC ATC ACT GAC TCC AAA ATC T – 3´	
# 195	5´ - AAA TAG GAT TTA CTT TCT GCT TTG TGG – 3´	
# 177	5´ - ATG TGT TCA GGA CAG ACA ACA ATA GTA ACA – 3´	CPEB2
# 179	5´ - CAA GCT ATC ATC TAT TGG AAA TAG GGA AGA –3´	
Primers 194 and 195 (outer set), primers 177 and 179 (nested set)		
# 34	5´ - GGT CGG CGT GGG CGT GGG TGT AGG TGT G – 3´	
# 60	5´ - GTC CAC CAC AAG GGG TCC AAA CCT GCG AAA GC – 3´	
# 81	5´ - GGA TAT GAT AAG GAC TGA CCA TGA GCC TCT GAA AG –3´	CPEB3
# 82	5´ - CCA TGG CTG TCA TCC AAG AAG GCG TC – 3´	
Primers 34 and 60 (outer set), primers 81 and 82 (nested set)		
# 209	5´ - AGC AGC TAC CAG AGT CCT TCT CCA – 3´	
# 210	5´ - TCA TCA ATA TCA GGA GGC AAT CCA – 3´	
# 55	5´ - CCC AGG ACG TTT GAC ATG CAC TCA CTG – 3´	CPEB4
# 54	5´ - CAG ACC ACT ATG AAG AGG TTG ATC CCC ACG –3´	
Primers 209 and 210 (outer set), primers 55 and 54 (nested set)		
Syn us	5'-AGG TGC TGC AGT GGG TCT TT -3'	
Syn ds	5'- GTC TGG CGG CAC ATA GGC ATC T -3'	
Syn ne us	5'- CGG CTG AGC GTG GAG TGT GC -3'	Synaptophysin
Syn ne ds	5'- AGG GCC CCC ATGGAG TAG AGG AA -3'	
Primers Syn us and ds(outer set), primers Syn ne us and ne ds (nested set)		
S100β us	5'- AGG CCA TGG TTG CCC TCA TTG AT -3'	
S100β ds	5'- ACT CAT GGC AGG CCG TGG TCA -3'	S100β
S100β ne us	5'- TAC TCC GGG CGA GAG GGT GAC AA -3'	
S100β ne ds	5'- GGC GAC GAA GGC CAT GAA CTC C -3'	
Primers S100β us and ds (outer set), primers S100β ne us and ne ds (nested set)		
NG2 us	5'- CACACTTCTCCTGGACATTTCTTC- 3'	
NG2 ds	5'- TGGCAGGTGGTGAGGACAGT- 3'	
NG2 ne us	5'- GGAGGGCACCCGGAAGTTGA- 3'	NG2
NG2 ne ds	5'- GCTGGGCATGGAGGAGTCG- 3'	
Primers NG2 us and ds (outer set), primers NG2 ne us and ne ds (nested set)		
Iba-I us	5'-TTCCTCGATGATCCCAAATAC-3'	
Iba-I ds	5'-CTGTAGGTGGAGGTTAGT-3'	
Iba-I ne us	5'-GGATCTGCCGTCCAAACTTGAA-3'	Iba-I
Iba-I ne ds	5'-GAGAACGGGTCGTAGTAAGACTC-3'	
Primers IbaI us and ds (outer set), primers IbaI ne us and ne ds (nested set)		

Table 8: List of primers used for single cell RT-PCR.

The second PCR (nested) was performed using nested primers and 2 µl of first PCR product as a template. The master mix and PCR program used for nested PCR were as in tables 9 and 10 respectively.

10x reaction buffer	5 µl
2.5 mM $MgCl_2$	2.5 µl
dNTPs (2.5 mM each)	1 µl
Nested upstream primer (for CPEB1/2/3/4) (10 pmol/µl)	1 µl
Nested downstream primer (for CPEB1/2/3/4) (10 pmol/µl)	1 µl
Platinum T*aq* DNA polymerase	0.5 µl
dH_2O	37 µl
Total volume	**48 µl**

Table 9: Master mix used for nested PCR. This table shows a typical master mix prepared for nested PCR. Two PCRs were performed with a similar mix as above in parallel, one for CPEB (1/2/3/4) and another one for a house keeping gene (synaptophysin/s100β/NG2/Iba-I). Respective nested primers (table 11) were used. 0.5 µl of each of DMSO and betaine were added to the master mix when NG2 primers were used.

95°C	25 sec	
95°C	25 sec	5x
54°C	2 min	
95°C	25 sec	30x
54°C	25 sec	
72°C	25 sec	
72°C	7 min	

Table 10: PCR program used for nested PCR.

3.2.3.4 Analysis of the PCR products

The PCR products were run on 1.5% agarose gel at 90 V for 1.5 h. A DNA ladder was run along with the samples to estimate the size of the PCR product. The bands corresponding to different PCR products were excised and the DNA was purified using Peqlab gel extraction kit (Peqlab) according to the manufacturer's instructions. The purified PCR products were cloned into PCR-XL-TOPO vector. TOP10 competent E. *coli* (Invitrogen) were transformed with the TOPO cloned gel products and the DNA was plated on to LB plates with 50 µg/ml kanamycin (Carl Roth), incubated overnight at 37°C overnight. The procedure was done according to the manufacturer's instructions.

Single colonies were placed in 2 ml of LB medium with kanamycin (50 µg/ml) (Carl Roth) and incubated at 37°C overnight with 250 rpm rotation. After 12-16 h of incubation, DNA was isolated from overnight cultures using the Peqlab miniprep kit (Peqlab, Erlangen, Germany) or Promega miniprep kit (Promega, Mannheim, Germany). The procedure was followed as per the manufacturer's instructions. The concentration of minipreps was checked

after which the DNA was sent for sequencing (Qiagen). For sequencing, two primers which bind in the TOPO vector region (M13f-20 and M13r-24) were used. The Multalin program (Corpet, 1988) was used to align the sequencing reads with reference sequences of different CPEBs and the different splice isoforms for each CPEB were analyzed.

3.2.4 Generation of vectors for generation of transgenic mice

In order to study CPEB2 function in neurons, transgenic mice which overexpress CPEB2 protein specifically in pyramidal neurons of the mouse hippocampus were generated using the *tet*-OFF system. The CamKIIα promoter was used to drive the expression of transgene; tTA in turn binds to *tet*O and drives transgene expression (Gossen and Bujard, 1992; Mayford et al., 1996) specifically in pyramidal neurons. Both CPEB2-EGFP and CPEB2ΔZn-EGFP proteins were cloned separately into the pMM403-400 vector, which has *tet*O and a simian virus polyadenylation signal (SV40 pA), using in-fusion technology (Clontech).

3.2.4.1 Restriction digestion of pMM403-400 vector

Five micrograms of pMM403-400 vector was digested with *EcoR*V (New England Biolabs, Frankfurt, Germany) for 2 h at 37^{o}C. The enzyme mix used for restriction digestion is shown in table 11. After restriction digestion, the DNA was run on a 1% agarose gel, run for 2 h at 90 V. The band corresponding to linearized pMM403-400 was excised and the DNA was purified using Qiagen Gel extraction kit according to manufacturer's instructions (Qiagen).

pMM403-400 midiprep DNA (339 ng/µl)	14.7 µl
NEB buffer '3'	3 µl
10x BSA	3 µl
*EcoR*V	2 µl
dH_2O	7.3 µl
Total volume	**30 µl**

Table 11: Restriction digestion of pMM403-400 vector.

3.2.4.2 Amplification of insert (CPEB2-EGFP/CPEB2ΔZn-EGFP)

CPEB2 or CPEB2ΔZn-EGFP was amplified using Advantage HD Polymerase (Clontech). In-fusion primers were designed using the in-fusion primer design tool (Clontech) and synthesized from MWG. Primers: INF1 (forward): 5'- GCG GAT CCT GCG GAT CCG

CCA TGA ATT TAC CTC AA- 3' and INF2 (reverse): 5'- ACG TGA TGG ATG GAT TTA CTT GTA CAG CTC GTC CA- 3'. A two step-PCR method was employed: initial denaturation at 98°C for 30 sec followed by 30 cycles of 98°C/10 sec, 68°C/2.5 min and a final extension at 68°C for 20 min. The master mix used for the PCR was as in table 12; a total of 100 ng of each DNA sample was used as a template.

5x Advantage HD buffer with Mg^{2+}	5µl
dNTP mixture	2 µl
Left primer (10 pmol/µl)	1 µl
Right primer (10 pmol/µl)	1 µl
Advantage HD polymerase	0.25 µl
Template DNA (20 ng/µl)	5 µl
dH_2O	10.75 µl
Total reaction volume	**25 µl**

Table 12: PCR reaction mix for amplification of CPEB2/CPEB2ΔZn-EGFP.

3.2.4.3 Infusion cloning

As the PCR amplified products seemed to be specific without any smear, they were treated with cloning enhancer as per the manufacturer's recommendations (Clontech). A 2 µl of cloning enhancer was added to 5 µl of PCR product and incubated at 37°C for 15 min followed by 80°C for 20 min; this mix was subsequently used in ligation reaction. Cloning enhancer treated PCR products (either CPEB2-EGFP or CPEB2ΔZn-EGFP) were separately cloned into pMM403-400 vector; the volumes of both the insert and vector were taken as in table 13. This mix (10 µl) was added to infusion dry-down mix and incubated at 37°C for 15 min followed by 50°C for 15 min and then kept on ice. This infusion mix was diluted further with 40 µl of TE buffer (pH 8.0), and Fusion Blue competent cells (Clontech) were transformed with the plasmid according to the manufacturer's recommendations (Clontech).

Cloning enhancer treated PCR product (CPEB2/2ΔZn-EGFP)	2 µl
Linearized pMM403-400 vector	2.2 µl
dH_2O	5.6 µl
Total volume	**10 µl**

Table 13: Infusion cloning of CPEB2/CPEB2ΔZn-EGFP into pMM403-400 vector.

3.2.4.4 Analysis of clones

Single colonies from each cloning (CPEB2-pMM and CPEB2ΔZn-pMM) were inoculated each into 2 ml of LB with 100 µg/ml ampicillin (Carl Roth), incubated at 37^{o}C overnight with 250 rpm rotation. DNA was isolated from the clones using Qiagen miniprep kit with manufacturer's instructions (Qiagen). The clones obtained were analyzed by restriction digestion of minipreps as well as by sequencing. DNA from minipreps was digested with *Not*I (NEB) at 37^{o}C for 1.5 h, run on 1% agarose gel, for 2 h at 90 V. The reaction mix used for restriction digestion was as in table 14. The positive clones which gave expected band sizes in the restriction digestion were selected and sequenced at Qiagen Sequencing Service (Qiagen). The primers used for sequencing are primer 207: 5'- GTG ACA ATG ACA TCC ACT TTG CC- 3' and primer 208: 5'- GAT CCT CTA GCA TTT AGG TGA CAC TAT AGA ATA GG- 3'.

Miniprep DNA	3 µl
NEB buffer '3'	2 µl
10x BSA	2 µl
*Not*I	0.5 µl
dH_2O	12.5 µl
Total volume	**20 µl**

Table 14: Restriction digestion of CPEB/CPEB2ΔZn-pMM minis with *Not*I.

3.2.5 Generation of transgenic mice with overexpression of CPEB2/CPEB2ΔZn in pyramidal neurons of mouse hippocampus

One clone each for CPEB2 and CPEB2ΔZn with the correct reading frame was selected and retransformed using chemically competent E. *coli* made in the lab (Appendix A9.1). To each vial, 2 µl of DNA was added and the transformation was done as above. Single colony each from CPEB2-pMM and CPEB2ΔZn-pMM clonings were inoculated in 100 ml of Luria Bertani (LB) broth with 100 µg/ml ampicillin, incubated at 37^{o}C overnight with 250 rpm rotation. Maxiprep kit (Qiagen) was used to prepare pure and endotoxin free DNA and the procedure was followed as in the manual.

The maxipreps were digested with *Sfi*I (NEB) for 2 h and run on 1% agarose gel. The respective bands (4.1 kb band for CPEB2-pMM and 3.9 kb band for CPEB2ΔZn-pMM) were excised and the DNA was purified using Peqlab gel extraction kit with manufacturer's instructions. Purified DNA was eluted in an injection buffer (centrifuged at 4^{o}C for 20 min

before use), and the concentration was checked using a Pearl nanophotometer (Implen, Munich, Germany). The DNA was diluted with injection buffer to a concentration of 4 ng/µl and given to the house for experimental therapy for injection into the male pronucleus of the zygotes.

3.2.6 Screening of newborn mice for transgene expression

3.2.6.1 Lysis of tail tips from mice and isolation of DNA

The mice tails were lysed in 250 µl of Laird buffer (100 mM Tris, pH 8.5, 200 mM NaCl, 5 mM EDTA, 0.2% SDS) with proteinase-K (20 U/ml) overnight at 55^{o}C. The samples were centrifuged at 13,500 rpm for 10 min and the supernatant was mixed with 250 µl of ispropanol to precipitate the DNA, centrifuged at 13,500 rpm for 10 min. The supernatant from this step was discarded and the DNA pellet was washed with 250 µl of 70% ethanol, centrifuged at 13,500 rpm for 10 min at +4^{o}C. The DNA pellet was air dried for 10 min and later dissolved in an appropriate volume (50-100 µl) of tris EDTA (TE) buffer (pH 8.0) or in distilled water.

3.2.6.2 Genotyping (tTA and *tet*O PCRs)

The newborn pups were genotyped at three weeks of age with two different sets of primers (*tet*O PCR, table 15) to confirm the presence of transgene (*tet*O-CPEB2/CPEB2ΔZn). The reaction mix used was as in table 16. The PCR program used was initial denaturation at 94^{o}C/3 min followed by 30 cycles of 94^{o}C/30 sec, 62^{o}C/1 min and a final extension at 72^{o}C/2 min. A 5 sec additional time was performed with each cycle to increase the amplification efficiency.

Primer	Sequence	PCR product size
tTA-A1	5´- GCG CTG TGG GGC ATT TTA CTT TAG -3´	318 bp.
tTA-A2	5´- CCG CCA GCC CCG CCT CTT C -3´	
tTA-B1	5´- TAG AAG GGG AAA GCT GGC AAG ATT -3´	539 bp.
tTA-B2	5´- CCG CGG GGA GAA AGG AC -3´	
Primer combinations: tTA A1+A2; B1+B2		
tetO-A/B	5´- GCG GCC GCC AAC TCT CG -3´	419 bp. (A+A/B)
tetO-A	5´- TCA AAA CAG CGT GGA TGG CGT CTC -3´	445 bp. (B+A/B)
tetO-B	5´- GAT CGG TCC CGG TGT CTT CTA TG -3´	
Primer combinations: tetO A+A/B; B+A/B		

Table 15: Primers used for tTA and tetO PCRs, bp: base pairs.

5x Promega PCR-buffer	5 µl
25 mM $MgCl_2$	1 µl
2.5 mM each dNTPs	1 µl
Primer up (10 µM)	1 µl
Primer down (10 µM)	1 µl
GoT*aq* Flexi DNA polymerase	0.2 µl
Template DNA	1 µl
dH_2O	14.8 µl
Total Volume	**25 µl**

Table 16: The PCR reaction mix used to genotype the newborn mice.

3.2.6.3 Breeding of *tet*O-CPEB2/*tet*O-CPEB2ΔZn mice with CamKII-tTA mice

The founder animals which were positive for either *tet*O-CPEB2/*tet*O-CPEB2ΔZn transgene were bred with CamKII-tTA mice. The tTA binds to *tet*O and the CamKII promoter drives the transgene expression specifically in pyramidal neurons of mouse hippocampus. The newborn pups from the *tet*O-CPEB2/*tet*O-CPEB2ΔZn X CamKII-tTA breedings were analyzed for the presence of both CamKII-tTA and *tet*O-CPEB2/*tet*O-CPEB2ΔZn transgenes. For both PCRs, two sets of primers were used (Table 15). Both positive and negative controls were included in the PCR. The PCR products were run on a 1% agarose gel. Based on the amplicon size, double transgenic (DT) animals (with both *tet*O and tTA) were identified.

3.2.7 Analysis of transgenic mice

3.2.7.1 Perfusion and cryosectioning

After genotyping, DT mice (tTA+tetO+) were selected for further screening. The mice were anaesthetized with 10% ketamine and cepetor and transcardially perfused with 4% PFA. The brains were fixed in 4% PFA overnight, then transferred to 30% sucrose in 1x PBS, left for 24-48 h. Later, the brains were cryoprotected in tissue-tek (Sakura Finetek, Staufen, Germany) and stored at -80^{o}C until further use. A total of five different lines were screened for CPEB2 (10 mice in total; lines 63, 104, 58, 94 and 27) and two different lines (6 mice in total; lines 35 and 6) for CPEB2ΔZn transgene expression. Coronal sections of 40 µm thickness were made using a Cryo-star HM560 cryostat (Microm, Walldorf, Germany) and stored at 4^{o}C in 1x PBS with 0.01% sodium azide.

3.2.7.2 Immunohistochemistry

The transgene (either CPEB2 or CPEB2ΔZn) expression was confirmed with GFP fluorescence since both proteins are tagged with EGFP protein at the C-terminus. The coronal sections from both DT animals and their control littermates were stained with rabbit GFP antibodies (Synaptic Systems, Goettingen, Germany). The sections were washed 3 times, 10 min each with 1x PBS, blocked with 10% NGS (Millipore, Germany), 0.4% Triton (Carl Roth) in 1x PBS, pH 7.4 for 2h at RT and then incubated at 4^{o}C overnight with the primary antibody in 5% NGS, 0.1% Triton in 1x PBS. After washing 3 times, 10 min each with 1x PBS, the sections were incubated in Alexa 488 goat anti-rabbit (1:500; Invitrogen) secondary antibody for 1.5h at room temperature. Then, the sections were washed three times 10 min each with 1x PBS, counterstained with Hoechst (1:50 in dH_2O; Invitrogen), again washed 3 times 10 min each and then mounted in permafluor (Thermo Scientific, Bonn, Germany).

As CPEB2/CPEB2ΔZn expression is confined to pyramidal neurons of hippocampus, double stainings with GFP and either MAP2 (which localizes to dendrites) or NeuN (which localizes to neuronal cell bodies) were done. CPEB2 and GFP double stainings were also performed to study if there is any colocalization of endogenous and overexpressed CPEB2. The staining protocol was the same as above, the antibodies used were: rabbit CPEB2 purified antibody (custom made #68, 1:500; Eurogentec), mouse NeuN (1:500; Millipore), mouse MAP2 (1:200; Synaptic Systems). Since β-catenin is a putative target of CPEB2, the sections were also stained with mouse β-catenin (1:500; Millipore) and rabbit GFP (1:1000; Synaptic Systems). The secondary antibodies used were Alexa 488 goat anti-rabbit (1:500; Invitrogen) and Alexa 594 goat anti-mouse (1:500; Invitrogen). Images were obtained using an Axiophot microscope (Carl Zeiss, Goettingen, Germany). Similar exposure times were set for both control and DT sections. The images were processed with Image J software (NIH).

3.2.8 Analysis of target protein levels in CPEB2/CPEB2ΔZn transgenic mice

3.2.8.1 Isolation of mouse hippocampus

The mice were sacrificed by cervical dislocation; brain was isolated and divided into two parts. One half of the brain was used for preparing protein lysates and the other half for immunohistochemistry to verify the transgene expression (this half of the brain was immediately fixed in 4% PFA overnight at 4^{o}C, then cryoprotected in 30% sucrose in 1x PBS

for 24-48 h and stored in tissue-tek at -80^{o}C). Only the hippocampus was used for Western blot. If not used immediately, the tissues were frozen in liquid nitrogen and stored at -80^{o}C.

3.2.8.2 Preparation of hippocampal protein lysates

To each tissue sample, 350 µl of prechilled modified RNA Immuno Precipitation Assay (RIPA) lysis buffer (50 mM Tris, 150 mM NaCl, 0.5% NP40, 0.5% sodium deoxycholate, 1% triton X-100, pH 7.5) containing complete mini protease inhibitor tablet (1 tablet/10 ml buffer; Roche, Mannheim, Germany) was added and homogenized using a plastic pistil until no further tissue chunks were visible. The lysate was passed through a 27G needle (prechilled) approximately 5-6 times to shear the genomic DNA, incubated on ice for 30 min and centrifuged at 13,000 g, 4^{o}C for 30 min. After centrifugation, the protein containing supernatant was transferred to a fresh tube. When the samples were not clear, they were briefly sonicated (10 sec) and then centrifuged. Five microlitres of each supernatant was used for measuring the protein concentration using BCA protein assay kit and the assay was done as per the manufacturer's instructions (Thermo Scientific).

3.2.8.3 Western blotting

Western blotting of the hippocampal lysates from DT animals (either *tet*O-CPEB2-EGFP or *tet*O-CPEB2ΔZn-EGFP) and their control littermates was done. Thirty µg of each protein sample was used for analysis. The samples were denatured at 65^{o}C for 10 min in 3x sample buffer (50 mM Tris HCl (pH 6.8), 2% SDS, 100 mM DTT, 10% glycerol and 0.01% bromophenol blue). The denatured protein samples were run on 10% SDS-PAGE gel and blotted onto polyvinylidene fluoride (PVDF) membrane (Millipore) as per the manufacturer's instructions (Invitrogen). The membranes were blocked for 1 h with 5% milk in 1x tris buffered saline containing 0.05% tween-20 (TBST) buffer and incubated with primary antibodies diluted in the same blocking solution with 0.01% sodium azide overnight at 4^{o}C. For EphA4, the membrane was blocked with 1X TBST with 0.1% tween-20 and 3% BSA and incubated with EphA4 primary antibody in the same blocking solution with 0.01% sodium azide overnight at 4^{o}C. Primary antibodies used were ABP (1:1000; AB5569, Millipore), β-actin (1:5000; Sigma-Aldrich), β-catenin (1:1000; MAB2081, Millipore), GluR1 (1:1000; AB1504, Millipore), GluR2 (1:1000; AB1768, Millipore), EphA4 (1:500; cat. no. 37-1600, Invitrogen), GLT-1 (1:500; AB1783, Millipore), GRIP1 (1:1000; cat. No. 611318, BD Biosciences, Heidelberg, Germany) and Tubulin (1:10,000; T9026, Sigma-Aldrich). Next

day, the membrane was washed 3 times with 1x TBST, incubated with respective secondary antibodies (diluted in 2.5% milk) for 1 h at RT. For EphA4, the secondary antibody was diluted in 1X TBST with 0.1% tween-20 and 3% BSA. Secondary antibodies used were sheep-anti-mouse IgG HRP (1:10,000; GE Healthcare, Munich, Germany), donkey-anti-rabbit IgG HRP (1:10000, GE Healthcare) and goat anti guinea pig HRP (1:5000, Abcam). After washing with 1x TBST (3 times, 5 min each time), Supersignal WestDura extended duration substrate (Thermo scientific) was added and the chemiluminiscence was detected using the Gene Gnome Imaging system (Syngene, Cambridge, UK). For loading control, membranes were stripped using restore western blot stripping buffer (Thermo scientific) for 15 min, washed with 1x TBST (3 times, 10 min each). The blots were blocked with 5% milk for 1 h at RT and then incubated with α-tubulin (1:10,000) or β-actin (1:5000) primary antibody overnight a 4^{o}C. After washing with 1x TBST (3 times, 10 min each), membranes were incubated with respective secondary antibodies for 1 h at RT and the blots were developed as above.

3.2.8.4 Quantification of blots

The images were quantified by densitometric analysis using Gene tools software (Syngene). The values of control animals were set to 100% basing on which the values of DT animals were calculated. The results were normalized to loading control used (tubulin or actin). Statistical analysis was carried out using student's t-test and the value $p<0.05$ was considered as significant.

3.2.9 Analysis of transcript levels of different targets in CPEB2/CPEB2ΔZn transgenic mice

3.2.9.1 Isolation of RNA from mouse hippocampus

The mice were sacrificed by cervical dislocation; brain was isolated and divided into two parts. One half of the brain was used for isolating RNA and the other half for immunohistochemistry to verify the transgene expression (this half of the brain was immediately fixed in 4% PFA overnight at 4^{o}C, cryoprotected in 30% sucrose in 1x PBS for 24-48 h and stored in tissue-tek at -80^{o}C). Hippocampus was isolated and used for RNA analysis. If not used immediately, the tissues were frozen in liquid nitrogen and stored at -80^{o}C.

RNA was isolated using the RNeasy mini kit (Qiagen). The entire protocol was performed in an RNase-free environment. The hippocampus was homogenized in 1ml of qiazol each using a plastic pistil until no visible chunks were observed. The whole reaction mixture was incubated at room temperature for 5 min, 200 µl of chloroform was added and vortexed vigorously. It was incubated again for 3 min and centrifuged at 12,000 g for 15 min at 4^{o}C. After centrifugation, the upper aqueous phase containing RNA was precipitated with 70% ethanol (600 µl each). The complete reaction mixture was then applied onto an RNeasy column, centrifuged at 10,000 g for 1 min. The supernatant was discarded and the columns were washed with 350 µl of RW buffer at 10,000 g for 1 min and the flow through was discarded. During this time, RNase-free DNase working solution was prepared by mixing 70 µl of RDD buffer with 10 µl DNase. The DNase working solution was added to each column and incubated at room temperature for 30 min. After DNase digestion, the columns were washed with 350 µl of RW1 buffer and centrifuged at 10,000 g for 1 min. The columns were washed two times each with 500 µl of RPE buffer and centrifuged at 10,000 g for 1 min. The flow through was discarded and the columns were placed in a new clean 2 ml tube and centrifuged at 14,000 g for 5 min to remove any residual ethanol left in the column. The columns were transferred to a clean RNase-free tube, and the RNA was eluted with 30 µl of RNase-free water at 10,000 g for 1 min.

3.2.9.2 Reverse transcription of RNA into cDNA

The concentrations of all the RNA samples were checked using a Pearl nanophotometer (Implen) and equal amounts were taken for reverse transcription reaction. One µg of each RNA sample was used and the reaction mix was as in table 17. The reaction was setup in a thermal cycler: 50^{o}C for 1 h followed by 70^{o}C for 15 min (Invitrogen).

5x First strand buffer	4 µl
Dithiothreitol (DTT)	1 µl
dNTPs	1 µl
Random hexamers	1 µl
Superscript III reverse transcriptase	1 µl
RNasin	1 µl
Template RNA	5 µl (250 ng/µl)
dH2O	6 µl
Total volume	**20 µl**

Table 17: Reverse transcription master mix for mouse brain hippocampal RNA samples.

3.2.9.3 Estimating the efficiencies of real time PCR primers

The efficiencies of the different t*aq*man primers used were calculated using the standard C_T slope method (Liu and Saint, 2002). The rate of amplification for each primer set was calculated from the linear regression slope obtained from dilution series. Mouse brain cDNA was serially diluted in a 10-fold dilution series (100 ng, 10 ng, 1 ng, 0.1 ng, 0.01 ng, and 0.001 ng) and amplified with the respective primers using an ABI 7900 HT real time PCR system. The t*aq*man primers and probe for each transcript were designed using primer express 3.0 software (Applied Biosystems). The C_T values were plotted versus the concentration of cDNA samples. The slopes (R^2 values) for a 10-fold dilution series of the cDNA sample were calculated. The efficiencies of the amplification were calculated from the slope of the graph obtained for each primer set. The following equation was used for estimating the efficiency (E) (Higuchi et al., 1993b).

$$E = 10^{(-1/slope)}$$

3.2.9.4 Quantitative real time PCR

Quantitative real time PCR was performed to analyze the transcript levels of β-catenin, GluR2 and EphA4 in DT animals compared to their control littermates. For β-catenin and GluR2, t*aq*man primers and probe were designed using Primer express 3.0 software (Applied Biosytems). The probes are labelled at the 5' end with fluorescein amidite (FAM) and at the 3' end with carboxytetramethylrhodamine (TAMRA). The β-actin primers/probe set (mouse ACTB, 4352933E, 5'FAM-probe-MGB3') was provided by Dr. Gerald Seifert in the institute (Seifert et al., 2004). EphA4 primers and probe were ordered from Applied Biosystems (T*aq*Man Gene Expression Assays #4331182, Mm00433056_m1). The reaction mix contained 6.25 µl gene expression master mix (Applied Biosystems), 0.5 µl of primers/probe mix and 5.75 µl of diluted cDNA sample. A primers/probe mix was prepared using 10 µM of each primer and 5 µM probe. The cDNA dilutions were prepared using 0.5 µl of each cDNA and 5.25 µl of water. The amplification was performed in a 384-well plate in the ABI 7900HT Real Time PCR instrument (Applied Biosystems). PCR conditions used were: 50°C/2 min, 95°C/10 min, 95°C/15 sec, 60°C/1 min. The PCR program was run for 40 cycles. Both an RNA control (RNA as a template without reverse transcription) and a non template control (NTC) were included in the reaction. The samples were analyzed in triplicates for each gene. Two house keeping genes: β-actin and GAPDH were used, to which the results were

normalized. A student's t-test was done to analyze the statistical significance. The primers/probe sequences were as in table 18.

Primer	Sequence	Gene
Forward primer	5'- ACA CCT CCC AAG TCC TTT ATG AAT -3'	
Reverse primer	5'- CCC GTC AAT ATC AGC TAC TTG CT -3'	β-catenin
Probe	5'- AGG CTT TTC CCA GTC CTT CAC GCA A -3'	
Forward primer	5'- GAC TGA CAC CCC ATA TCG ACA A -3'	
Reverse primer	5'- TCG CAT AGA CGC CTC TTG AA -3'	GluR2
Probe	5'- CAG TCA CCA ATG CTT TCT GCT CCC AGT -3'	
Forward primer	5'- CGA CAG TCA GCC GCA TCT T -3'	
Reverse primer	5'- CCG TTG ACT CCG ACC TTC AC -3'	GAPDH
Probe	5'- CGT CGC CAG CCG AGC CAC A -3'	

Table 18: List of T*aq*man primers and probes used for real time PCR.

3.2.10 RNA Co-immunoprecipitation

3.2.10.1 Generation of CPEB2-FLAG construct

The CPEB2 coding region was PCR amplified with Advantage HD polymerase (Clontech) using in-fusion primers which have *Not*I and *EcoR*I restriction overhangs (underlined), 5'- GAC AAG CTT GCG GCC GCC ATG AAT TTA CCT CAA CAG CAG CCG CC -3' (forward) and 5'- ATC TAT CGA TGA ATT CGC TTA GTT CCA GCG GAA GTG GAT CTG ACG T -3' (reverse). The PCR product was treated with cloning enhancer and further cloned into p3xFLAG-CMV-7.1 vector (Sigma-Aldrich) which was pre-digested with the same set of enzymes. TOP10 E. *coli* (Invitrogen) were transformed with the resulting plasmid and the positive clones were selected by ampicillin resistance as well as by sequencing the minipreps (Qiagen).

3.2.10.2 Generation of EphA4 3'UTR-PGL construct

The 3'UTR region of EphA4 which contains two CPEs was PCR amplified using Advantage HF 2 Polymerase and primers which have *Xba*I and *Sal*I restriction overhangs (underlined), 5'- TCT AGA GAA CAT CTC TTG GTT CAT ACA TGT TCC -3' (forward) and 5'- GTC GAC CAG GTT TGT ATA CGG CAA CTA C -3' (reverse). The obtained PCR product was run on a 1.2% agarose gel, the band excised and cloned into PCR-XL-TOPO vector. It was digested with *Xba*I and *Sal*I and ligated into pGL4.75 luciferase vector (Promega) which was pre-digested with the same set of enzymes. TOP10 E. *coli* were transformed with the resulting plasmid and the positive clones were selected by ampicillin resistance as well as by sequencing the minipreps.

3.2.10.3 Transfection of HeLa cells

HeLa cells were cultured regularly in Dulbecco's Modified Eagle's Medium (DMEM) (Invitrogen) with 10% heat inactivated foetal calf serum (FCS) (Gibco/Invitrogen) and penicillin-streptomycin (100 U/ml). The cells were trypsinized and 1.5 x 10^6 cells were plated in each 10 cm dish and grown to 90% confluence for transfection. The cells were transfected with Lipofectamine as per the manufacturer's recommendations (Invitrogen). The cells were transfected with either CPEB2-FLAG or FLAG-GFP (a control vector) and the CPEB2 that was bound to the endogenous β-catenin mRNA was co-immunoprecipitated using mouse monoclonal M2 FLAG antibodies (Sigma-Aldrich). In another experiment, cells were transfected with either full length (CPEB2-EGFP) or truncated CPEB2 constructs (CPEB2ΔZn-EGFP) and the CPEB2 that was bound to endogenous β-catenin mRNA was co-immunoprecipitated using CPEB2 serum (custom made, designated as # 94). Similarly, the cells were transfected with either CPEB2-FLAG or FLAG-GFP and EphA4 3'UTR-PGL constructs, and the CPEB2 that was bound to EphA4 mRNA was co-immunoprecipitated using mouse monoclonal M2 FLAG antibodies.

For CPEB1/2-CamKIIα co-immunoprecipitation, HeLa cells were transfected either with FLAG tagged CPEB1/CPEB2 or FLAG-GFP (a control vector) and CamKIIα 3'UTR-PGL constructs and CPEB1/2 that was bound to the CamKIIα mRNA was co-immunoprecipitated using mouse monoclonal FLAG antibodies (Sigma-Aldrich). Similarly the cells were transfected either with FLAG tagged CPEB1/CPEB1Δ5/CPEB1Δ17 and CamKIIα 3'UTR-PGL constructs and CPEB1/CPEB1Δ5/CPEB1Δ17 isoforms that were bound to the CamKIIα mRNA was co-immunoprecipitated using mouse monoclonal M2 FLAG antibodies (Sigma-Aldrich).

3.2.10.4 Co-immunoprecipitation

The co-immunoprecipitation of β-catenin or EphA4/CamKIIα mRNAs was done using either CPEB2 serum or M2 FLAG antibodies respectively. The cells were washed briefly with 8 ml of prechilled 1x PBS and lysed in 1 ml of lysis buffer (10 mM HEPES, 200 mM NaCl, 30 mM EDTA, 0.5% triton X-100) with additives (200 U/ml RNasin, one protease inhibitor mini cocktail tablet/10 ml buffer, 1 µg tRNA/1 ml buffer). The cells were scraped using an ice cold cell scrapper for 1 min into a prechilled eppendorf tube. The cell lysates were passed through a 27 G prechilled needle to completely lyse the cells. The cells were centrifuged at 16,000 g

for 20 min and 1 ml of the supernatant was added to equilibrated Protein-A Sepharose (PAS) beads. The remaining material was used for Western blotting to confirm the expression of transfected construct. The equilibration of PAS beads was done as below: approximately 60 µl of slurry was taken; 1 ml of lysis buffer with out additives was added and centrifuged at 6000 g for a few minutes. The buffer was removed and fresh buffer was added. This was incubated at 4^{o}C for 1 h on a POS-300 rotator (Grant-Bio, Cambridgeshire, GB) with 10-12 rpm speed. After this incubation, the beads were pelleted down by centrifuging at 8000 g for 2 min. The preadsorbed lysates were transferred to equilibrated protein G Dynabeads (PGDB) (30 µl each). The equilibration of PGDB beads was done as below: 30 µl of beads were aliquoted in each tube, 1 ml of lysis buffer without additives was added and later removed using Dynamagnet (Invitrogen). The equilibrated PGDB beads were blocked each with 500 µl of lysis buffer (containing 1 µg tRNA per 30 µl of beads /500 µl lysis buffer with 3% BSA) for 1 h. To these beads, the preadsorbed lysates were added, and either 50 µl of CPEB2 serum or 10 µl of M2 FLAG (mouse monoclonal, Sigma-Aldrich) was added and incubated for 2-3 h at 4^{o}C on a rotator with 10-12 rpm speed. After this incubation, 30 µl of sample was taken out as input, 350 µl of RLT buffer (RNeasy kit, Qiagen) was added and freezed the tubes. The beads were washed 5-10 times, each time for 5 min with 1 ml of wash buffer (10 mM HEPES (pH 7.4), 500 mM NaCl, 30 mM EDTA, 0.5% triton X-100) with additives (100 U RNasin and one complete mini protease inhibitor cocktail table/50 ml of buffer). After washes, 350 µl of RLT buffer from RNeasy kit (Qiagen) was added to each tube and freezed the tubes.

3.2.10.5 Isolation of RNA from co-immunoprecipitated samples

RNA was isolated from both inputs and co-immunoprecipitated (pull downs) samples using RNeasy mini kit (Qiagen); the experiment was done in an RNase-free environment. To each tube, 245 µl of 100% ethanol (0.7 volume of the sample) was added and mixed by inverting the tubes several times. This mixture was applied onto the columns (provided in the kit) and centrifuged at 10,000 g for 1 min. After this step, isolation of RNA was performed as in methods part 3.2.9.1. The RNA samples were stored at -20^{o}C until further use.

3.2.10.6 Quantitative real time PCR

The eluted RNA samples were subjected to reverse transcription as in methods part 3.2.9.2. The concentrations of RNA samples from inputs were checked and equal amounts RNA samples were taken for reverse transcription reaction. For pulldowns, 10 µl of each RNA

sample was used. The conditions used were: 50^{o}C for 2 h followed by 70^{o}C for 15 min) (Invitrogen). To analyze β-catenin or EphA4 transcript levels, quantitative real time PCR was done from the cDNA samples using luciferase primers. Porphobilinogen Deaminase (PBGD) was used as a housekeeping gene to which the results were normalized. The reaction mix contained gene expression master mix, luciferase primers/probe mix and diluted cDNA samples. The PCR conditions and the master mixes were as above in methods part 3.2.9.4 with following modifications: 60 repeats were done instead of 40. The primers/probe sequences used for firefly luciferase were 5'- GGC TCC CGC TGA ATT GG -3' (forward), 5'- GCG ACA CCT GCG TCG AA -3' (reverse) and 5'- ATC CAT CTT GCT CCA ACA CCC CAA CA -3' (5'FAM-probe-TAMRA-3'); and for human PBGD were 5'-GCT ATG AAG GAT GGG CAA CT-3' (forward), 5'-GTG ATG CCT ACC AAC TGT GG-3' (reverse) and 5'-TGC CCA GCA TGA AGA TGG CC-3' (5'FAM-probe-non fluroscent-3').

3.2.11 Dual luciferase reporter assay

The 3'UTR region of Connexin36 (Cx36) which contains two CPEs was PCR amplified using Advantage HF PCR kit (Clontech) and primers which contain *Xba*I and *Sal*I restriction overhangs (underlined), 5'- CTC TAG AGG GCA GGT TTG GGG -3' (forward) and 5'- GTC GAC CCA GTT TAC AAA AAA AGG C -3' (reverse). The PCR program was 94^{o}C/15 sec, 30 cycles of 94^{o}C/15 sec, 52^{o}C/1.5 min, 68^{o}C/1.5 min with a final extension of 68^{o}C/3 min. The obtained PCR product was cloned into pGL4.75 vector (Promega) which was pre-digested with the same set of enzymes. TOP10 E. *coli* (Invitrogen) were transformed the ligated product and the positive clones were selected by ampicillin resistance as well as by sequencing the minipreps.

Approximately 150,000 HeLa cells/well were plated in 24-well plate and were grown to 90% confluence. Next day, the cells were transfected with CPEB2-EGFP (200 ng per well) and Cx36 3'UTR-PGL (200 ng per well) constructs using Lipofectamine 2000 (Invitrogen) following manufacturer's instructions. For knockdown, 40 pmol of siRNA against CPEB2 or a negative control siRNA was used per well. The siRNAs used were, AUA UCU GAU UCA UAG UCC CCC (CPEB2), UAA GCA CGA AGC UCA GAG UCC CCC (negative control), purchased from Riboxx GmbH (Radebeul, Germany). 24 h post transfection, the cells were washed 3 times with 1x PBS, lysed in passive lysis buffer (1 ml/well) with 1000U of RNasin (Promega) and then incubated at room temperature for 10 min with rotation. Twenty

microlitres of each lysate was used for assay using Dual luciferase system (Promega) in a 96-well polypropylene plate. Each assay was done in triplicates and the luminescence of both firefly and renilla luciferases were measured. FLAG-GFP was used as a non specific control to which the results were normalized. The ratio of firefly to renilla luciferase was calculated and the values were plotted in a graph.

3.2.12 Rapid Amplification of cDNA Ends (3' RACE) of CPEB2

To analyze the 3'UTR of CPEB2, 3'RACE of mouse brain cDNA was performed using the Marathon cDNA Amplification kit (Clontech) and Advantage 2 polymerase. The master mix used for the PCR is shown below in table 19.

Marathon-Ready cDNA	5 µl
Gene specific primer (3R 1.1) (10 pmol/µl)	1 µl
Adapter primer (AP1)	1 µl
10x Advantage 2 buffer	5 µl
10 mM dNTP	1 µl
50x Advantage polymerase mix	1 µl
dH_2O	36 µl
Total volume	**50 µl**

Table 19: PCR master mix for 3'RACE of CPEB2.

The PCR was performed using a gene specific primer that binds with in the CPEB2 coding region (primer 3R 1.1: 5'- GAC CAG ATG TGT GAC GAG TGC CAG GGT G -3') and an adapter primer (AP1) that was provided in the kit. A touchdown PCR program was used as in table 20.

94°C	30 sec	
94°C	5 sec	5x
72°C	4 sec	
94°C	5 sec	5x
70°C	4 sec	
94°C	5 sec	25x
68°C	4 sec	

Table 20: Touchdown PCR program used for 3'RACE of CPEB2.

The PCR product was run on a 1.2% agarose gel. In parallel, a nested PCR was set up according to manufacturer's recommendations using a nested adapter primer (AP2) and

primer 3R1.2 (5'- GCC AAC TGG CCT CGG TCT AGG AAG GAA GGA AA -3'). The above PCR product was diluted 1:10 with TE buffer and 5 µl was used as template for the nested PCR. The PCR program used is shown in table 21.

94°C	30 sec	
94°C	5 sec	5x
72°C	4 sec	
94°C	5 sec	5x
70°C	4 sec	
94°C	5 sec	10x
68°C	4 sec	

Table 21: Nested PCR program used for 3' RACE of CPEB2.

This nested PCR product was run on a 1.2% agarose gel, the band was excised and the DNA was purified using Peqlab gel extraction kit (Peqlab,) according to manufacturer's instructions. It was further cloned into the PCR-XL-TOPO vector (Invitrogen). TOP10 competent E. *coli* were transformed with this plasmid and plated onto Luria Bertani (LB) plates with 50 µg/ml kanamycin (Carl Roth) as per the manufacturer's recommendations. DNA was isolated from the clones (minipreps) and digested with *EcoR*I (New England Biolabs) since there are *EcoR*I restriction sites in the TOPO vector flanking the cloned product. The concentration of the minipreps was checked and the harvested plasmid DNA was sent for sequencing (Qiagen) with primers M13f-20 and M13r-24 which bind within the TOPO vector (Invitrogen). The sequencing reads were aligned using the Multalin program (Corpet, 1988) with the CPEB2 3'UTR reference sequence obtained from the Ensembl database (www.ensembl.org).

4 Results

4.1 CPEBs in rat and human brain hippocampus

Among CPEB family members, CPEB1 is well described in different species, whereas other CPEBs (CPEB2, 3 and 4) were studied only in mouse (Wilczynska et al., 2005; Theis et al., 2003; Turimella et al., in revision). Hence the present study was aimed to investigate the expression and distribution of splice isoforms across species; particularly in rat and human. RT-PCR of rat and human hippocampus cDNA was performed with the corresponding species-specific primers used in Theis et al (2003) and Turimella et al., (in revision) for mouse CPEBs. The present study identified that CPEB2, 3 and 4 are expressed in rat and human hippocampus (Figures 12 A, B; Turimella et al., unpublished). Multiple splice isoforms were observed for each CPEB (Figure 12C). The isoforms were named according to the nomenclature used for mouse CPEBs. Among rat and human, the 'a' isoform was found to be the major isoform, similar to mouse CPEBs (except for rat CPEB3, which expressed the 'c' isoform instead). All of them were found to contain the B-region which harbors a putative phosphorylation site for different kinases; in addition, 'd' isoform was also observed which lacks the B-region. This is in contrast to mouse CPEBs, where only B-region containing isoforms were observed in brain.

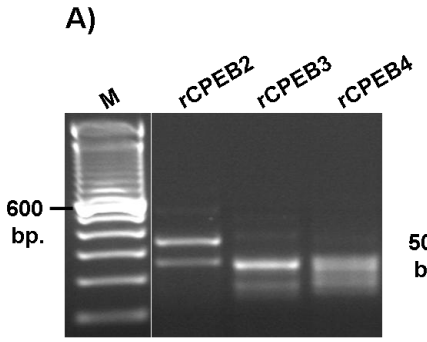

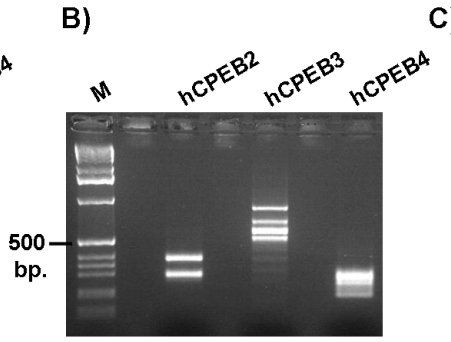

C)

CPEB	Isoforms observed
Rat CPEBs	
rCPEB2	a > c > d
rCPEB3	c > d = a > b
rCPEB4	a > b
Human CPEBs	
hCPEB2	a > c = c* > a* > d
hCPEB3	a > b = c
hCPEB4	a > d > b > c

Figure 12: Expression of CPEB2, 3 and 4 in rat (A) and human (B) brain hippocampus respectively. C) Multiple splice isoforms observed for each CPEB in the order of their distribution. M: marker, r: rat, h: human, and bp: base pairs.

4.2 CPEBs in PHCs

The expression of CPEBs (1-4) in PHCs was studied with immunofluorescence. The cultures were stained with both CPEB antibodies and MAP2 antibodies. The expression pattern appeared to be heterogeneous among CPEBs. The immunoreactivity (IR) for CPEB2 and CPEB3 was high (Figures 13 B, C), whereas the IR was weak for CPEB1 and CPEB4 (Figures 13 A, D). For CPEB2 and CPEB3, a typical punctate distribution was observed which was often dendritically localized, it is similar to the pattern of expression already described for CPEB3 (Huang et al., 2006). The nuclear exclusion was confirming its cytoplasmic localization as the name indicates.

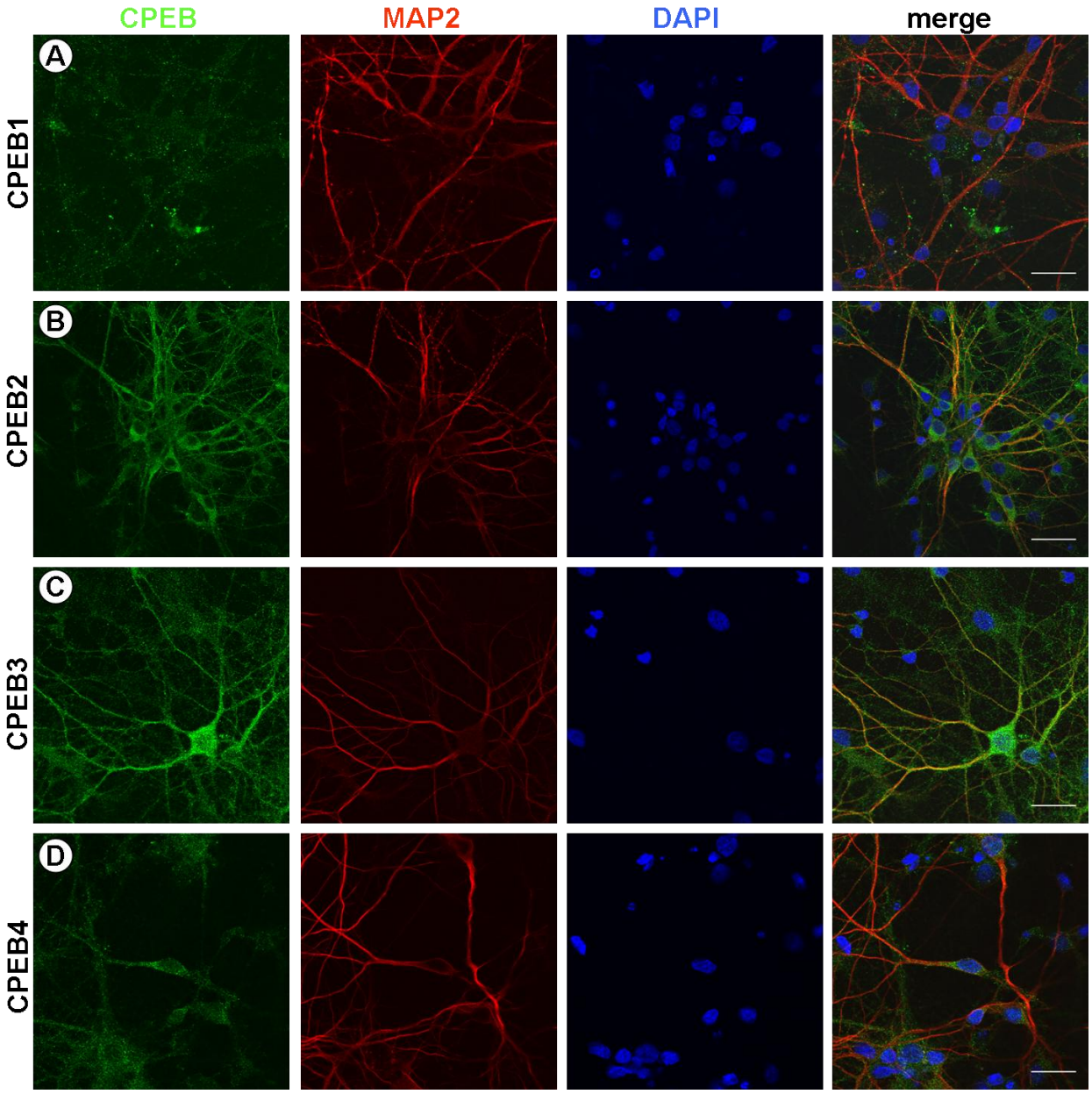

Figures 13: Expression of CPEBs (1-4) in PHCs. The cultures were stained with CPEB antibodies (CPEB 1/2/3/4) as well as with MAP2 antibodies. A) CPEB1, B) CPEB2, C) CPEB3 and D) CPEB4. DAPI was used as counter stain. The IR was higher for CPEB2 and 3 when compared to CPEB1 and 4. Scale bar: 25 µm.

4.3 Single-cell RT-PCR: Expression of CPEBs in neurons and glia

The expression of all four CPEBs (1-4) in different cells was studied in order to determine expression at the transcript level. Single-cell RT-PCR was done from the cytoplasm of harvested cells (neurons, astrocytes, NG2 glia and microglia) after whole cell patch clamp recording. The cell type specificity was confirmed using the following cell type specific markers in the PCR master mix: Synaptophysin for neurons, S100β for astrocytes, NG2 for NG2 glia and Iba-I for microglia. The expression pattern of CPEBs (1-4) was more frequent in neurons compared to glial cells. CPEB4 was the most abundant (> 50% incidence) among

all CPEBs (Figure 14A) whereas CPEB3 had the lowest abundance consistent with published results (Theis et al., 2003). The expression of CPEBs in astrocytes was rather infrequent (Figure 14B). Within glial populations, the expression of CPEBs was more frequent in NG2 glia (Figure 14C) compared to astrocytes. The heterogeneous expression of the CPEBs might be related to the various roles played by each CPEB in different cell types. The data for CPEB1 expression in NG2 glia (Figure 14C) and microglia (Figure 14D) was not included as the number of cells analyzed was insufficient.

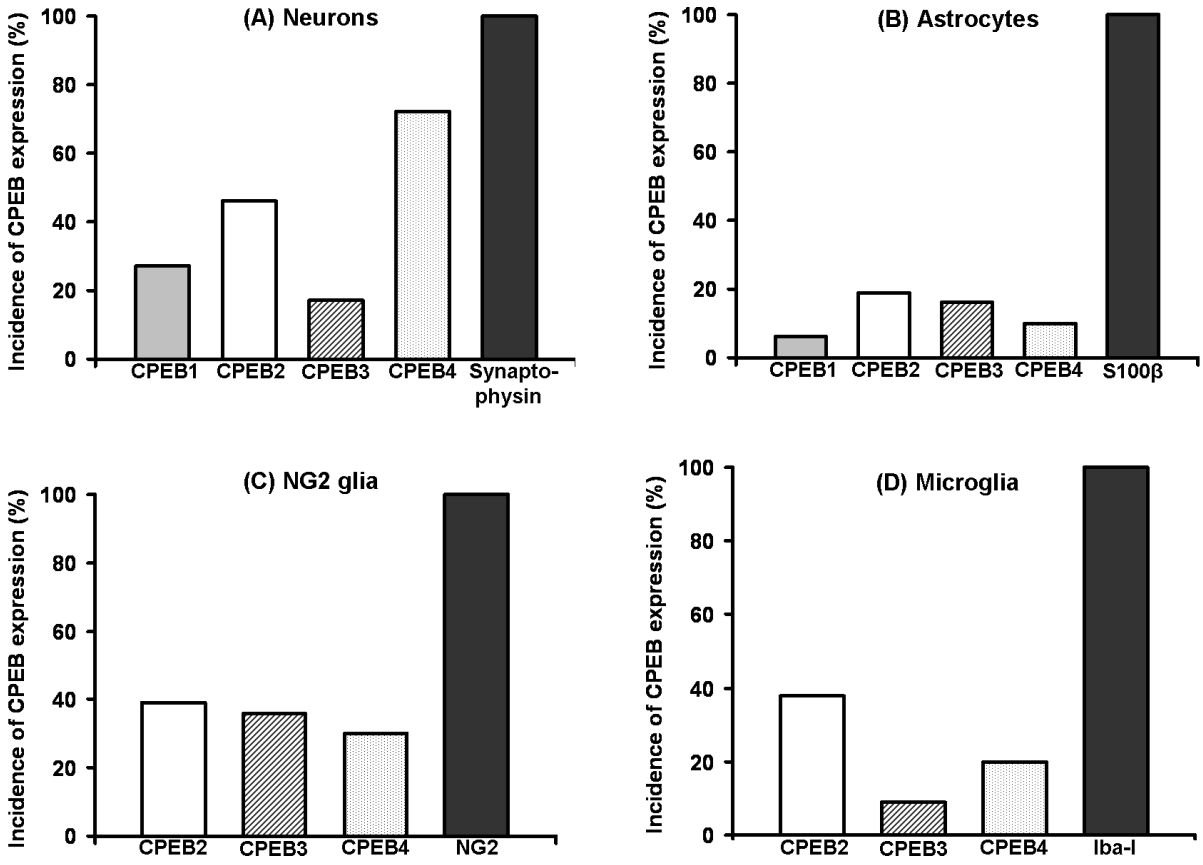

Figure 14: Single-cell RT-PCR. A summary of cell type specific expression of different CPEBs (1-4) in neurons (A), astrocytes (B), NG2 glia (C) and microglia (D). The data of CPEB1 expression in NG2 glia and microglia was excluded due to insufficient numbers of analyzed cells.

As an example, the expression of CPEB2 is shown across different cell types analyzed (Figure 15 A-D). Gel pictures showing the expression of other CPEBs (CPEB1, 3 and 4) can be found in appendix (A 9.2.1 - 9.2.3).

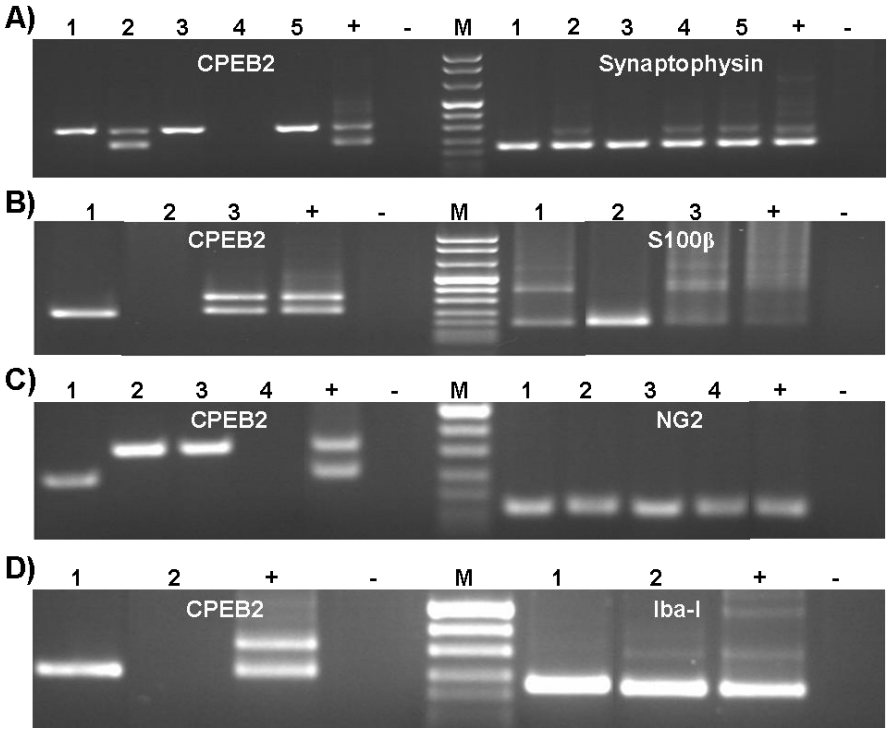

Figure 15: Representative gel pictures showing expression of CPEB2 in neurons (A), astrocytes (B), NG2 glia (C) and microglia (D). Numbers (1, 2, 3 etc.,) indicate the individual cells, '+' is a positive control (total RNA from mouse brain) and '-' is a negative control (dH_2O). The double bands represent multiple splice isoforms of each CPEB (see table 22), M: marker.

Individual PCR products were separated on 1.5% agarose gels, bands excised and the DNA was purified. These products were later cloned into PCR-XL-TOPO vector, and the minipreps were sequenced with both M13f-20 and M13r-24 primers. The resulting sequencing reads were aligned with the respective CPEB reference sequence using multalin program (Corpet, 1988). Different isoforms were observed for each CPEB. A summary of the different isoforms observed for each CPEB in different cell types can be found in table 22.

CPEB	Incidence of expression	Isoforms observed
	Neurons	
CPEB1	6 of 22	5x – sm 1x - lg 4x – a 1x – c > a 1x – c* > c
CPEB2	10 0f 22	1x – a* 1x - c > a > c* 1x – c 1x - f 1x - a
CPEB3	3 of 18	1x – a > b 1x – c 7x – d 2x – a 1x – d > a > c
CPEB4	13 of 18	1x – b > a

		1x – a, b
		1x – a > c
	Astrocytes	
CPEB1	1 of 17	1x - n
		2x - a
CPEB2	4 of 21	1x – d > c
		1x – a = c
		1x – a
CPEB3	3 of 19	1x – d > c
		1x – a = c = d
		1x – a
CPEB4	2 of 20	1x – d
	NG2 glia	
		2x – a
CPEB2	5 of 13	1x – c
		1x – c* > c
		1x - d
		4x – a
CPEB3	5 of 14	1x – d
		2x – d
CPEB4	3 of 10	1x – d > b
	Microglia	
		2x – c
CPEB2	3 of 10	1x - d
CPEB3	1 of 15	1x – a
CPEB4	2 of 10	2x - d

Table 22: Summary of different isoforms observed for each CPEB in different cells analyzed (neurons, astrocytes, NG2 glia and microglia). The data of CPEB1 in both NG2 glia and microglia was excluded as the 'n' was insufficient. Multiple splice isoforms were observed for CPEB2, 3 and 4. This heterogeneity was more frequent for CPEB2 and CPEB4 in neurons.

In neurons, the 'sm' isoform was the most abundant isoform for CPEB1. For CPEB2, the 'a' isoform was the most abundant isoform, similar to CPEB3 and CPEB4 in mouse brain (Theis et al., 2003). Although the majority of isoforms observed contain the B-region encoding a putative phosphorylation site for different kinases, CPEB4 is an exception with the 'd' isoform lacking the B-region as the major isoform in neurons. For CPEB 2-4, multiple isoforms were found within single neurons which might be due to different activity states of the corresponding neurons at the time of isolation. This heterogeneity could also be found in other cell types. The expression of CPEBs was rather infrequent in astrocytes compared to NG2 glia. Various isoforms were observed for CPEBs in glial cells. Until now, only the B-region containing isoforms were reported for CPEB2 in the principal cell layers of the hippocampus (Theis et al., 2003) whereas the B-region lacking isoforms were described in germ cells (Kurihara et al., 2003). But, in the present study, the 'd' isoform was observed in all the glial types analyzed (Table 22).

4.4 In-fusion cloning of CPEB2/CPEB2ΔZn into pMM403-400

Transgenic mice which overexpress either CPEB2 or CPEB2ΔZn particularly in CA1 pyramidal neurons of hippocampus were generated. The *Tet*-OFF system (Gossen and Bujard, 1992) was used to generate this set of mice. Either CPEB2-EGFP or CPEB2ΔZn-EGFP was cloned individually into the pMM403-400 vector which has *tet*O and a SV40 poly(A).

4.4.1 Cloning

The pMM403-400 vector was linearized with *EcoR*V (Figure 16A). The digested product was run on a 1% agarose gel, the corresponding band excised and the DNA was purified. Both CPEB2-EGFP and CPEB2ΔZn-EGFP were PCR amplified, run on a 1% agarose gel and the DNA was purified from gel (Figure 16B). Ligation of either CPEB2-EGFP or CPEB2ΔZn-EGFP into pMM403-400 vector was done using in-fusion technology (Clontech) and Fusion Blue competent cells (Clontech) were transformed with the resulting plasmids. The positive colonies were selected by ampicillin resistance.

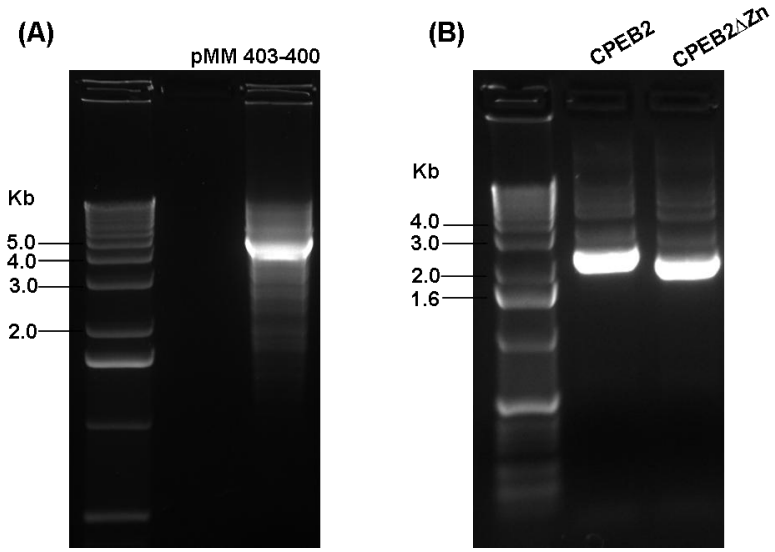

Figure 16: In-fusion cloning of CPEB2/CPEB2ΔZn into pMM403-400. A) Digestion of pMM403-400 vector with *EcoR*V. The digested product was run on a 1% agarose gel along with a DNA ladder. B) PCR products of CPEB2-EGFP and CPEB2ΔZn-EGFP. Kb: kilobases.

4.4.2 Verification of clones

Single colonies were selected from the ampicillin plates and DNA was isolated using a miniprep kit (Qiagen). The clones were named as CPEB2-pMM and CPEB2ΔZn-pMM. The clones were verified both by restriction digestion (Figures 17 A, B) as well as by sequencing. Restriction digestion of minipreps was performed using *Not*I, which gave the following

bands. They were also sequenced and aligned with the template sequence using multalin program (Corpet, 1988).

CPEB2-pMM:

4.3 kb band - 2.4 kb CPEB2-EGFP + 1.9 kb *tet*O + SV40 poly (A)

3.4 kb band - pMM403-400 (Figure 17A)

CPEB2ΔZn-pMM:

4.1 kb band - 2.2 kb CPEB2ΔZn-EGFP + 1.9 kb *tet*O + SV40 poly (A)

3.4 kb band - pMM403-400 (Figure 17B)

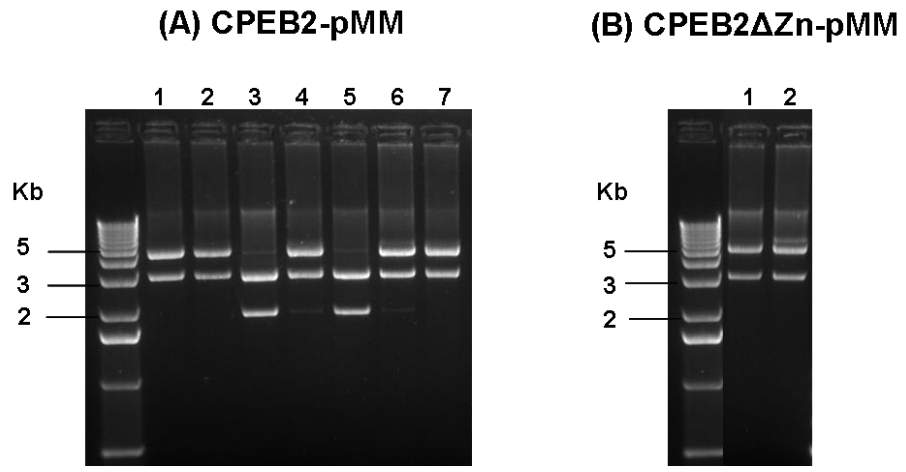

Figure 17: Restriction digestion of CPEB2-pMM and CPEB2ΔZn-pMM minipreps with *Not*I. A) CPEB2-pMM minis (lanes 1, 2, 4, 6 and 7) gave the expected bands of 4.3 kb and 3.4 kb in size. B) CPEB2ΔZn-pMM minis (lanes 1 and 2) gave the expected bands of 4.1 kb and 3.4 kb in size.

4.5 Generation of CPEB2/CPEB2ΔZn transgenic mice

One clone each for CPEB2 and CPEB2ΔZn cloning was selected and maxipreps (Qiagen) were done to obtain endotoxin free pure DNA. The DNA was digested and purified from the gel as described in methods part 3.2.5. The purified constructs (either CPEB2 or CPEB2ΔZn) were injected into the male pronucleus of zygotes for generating transgenic mice. The schematics of different constructs used for generating transgenic mice can be found in figure 18.

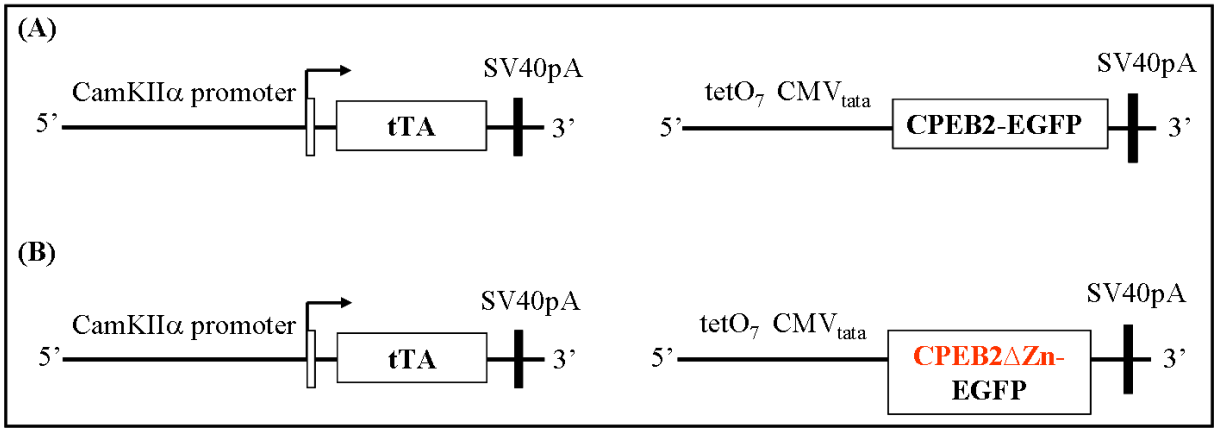

Figure 18: Constructs of CPEB2/CPEB2ΔZn-pMM for generating transgenic mice. A) The schematic used for generating CPEB2 transgenic mice. B) The schematic used for generating CPEB2ΔZn transgenic mice. The tTA binds to *tet*O sequences thereby driving the transgene expression specifically in pyramidal neurons of mouse hippocampus. The CamKIIα promoter was used to drive neuronal specific expression.

Genotyping of the newborn pups was done with two sets of *tet*O primers for *tet*O-CPEB2/CPEB2ΔZn transgene. The founder mice which were positive for *tet*O-CPEB2 / *tet*O-CPEB2ΔZn expression were bred with CamKII-tTA mice to achieve transgene expression specifically in pyramidal neurons of mouse hippocampus. The tTA binds to *tet*O thereby driving the transgene (either CPEB2 or CPEB2ΔZn) expression specifically in neurons.

4.6 Screening of newborn mice for the presence of the transgene

The newborn mice were tested for the presence of transgene: either CPEB2/CPEB2ΔZn. Genotyping was done with two different PCRs – *tet*O and tTA. The PCR products were run on a 1% agarose gel, and the positive samples were identified. The DT animals which were positive for both *tet*O-CPEB2/CPEB2ΔZn and CamKII-tTA were chosen for further analysis (Figure 19).

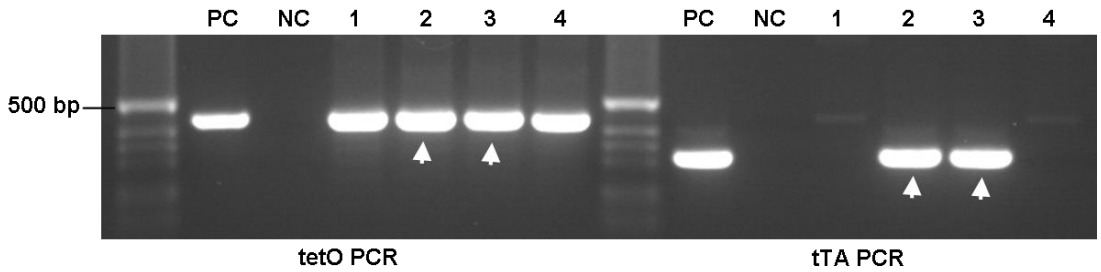

Figure 19: Genotyping of new born mice: tTA and *tet*O PCRs. PC – positive control, NC – negative control. Numbers 1, 2, 3 and 4 indicate individual mice tested, arrows represent the DT animals which are positive for both *tet*O and tTA PCRs, bp: base pairs.

4.7 Screening of lines for transgene expression

4.7.1 Screening different lines for CPEB2 transgene expression

The DT animals from different lines were screened for the neuronal expression of CPEB2 transgene by GFP staining. Among the five different lines screened, three lines (lines 27, 94 and 11) were positive for CPEB2 transgene expression (Table 23). Mice from lines 94 and 11 showed expression. Mice from line 27 showed moderate expression in hippocampus and cortex; some neurons expressed high amounts of CPEB2-EGFP whereas most neurons were weakly expressing (Figure 20), and hence were classified as moderate expressers.

Line	Name of mice	Sex	Genotype	Age of mice	Total no. of mice tested	Comments
63	149	F	tTA+*tet*O+	5 weeks	1	No expression
104	140	F	tTA+*tet*O+	5 weeks	2	No expression
	141	M	tTA+*tet*O+	5 weeks		
58	127	F	tTA+*tet*O+	5 weeks	1	No expression
27	187	F	tTA+*tet*O+	5 weeks	2	Moderate
	191	M	tTA+*tet*O+	5 weeks		expression
94	206	M	tTA+*tet*O+	5 weeks	3	
	210	F	tTA+*tet*O+	9 weeks		Expression
	215	M	tTA+*tet*O+	9 weeks		
11	294	F	tTA+*tet*O+	5 weeks	3	
	295	F	tTA+*tet*O+	5 weeks		Expression
	311	F	tTA+*tet*O+	7 weeks		

Table 23: Analysis of *tet*O-CPEB2-EGFP mice lines.

4.7.2 Screening different lines for CPEB2ΔZn transgene expression

Two different lines (6 mice in total; lines 35 and 6) were screened for CPEB2ΔZn-GFP expression, out of which line 6 showed expression (Table 24).

Line	Name of mice	Sex	Genotype	Age of mice	Total no. of mice tested	Comments
35	105	M	tTA+*tet*O+	5 weeks	3	No expression
	111	M	tTA+*tet*O+	4 weeks		
	128	F	tTA+*tet*O+	6 weeks		
6	246	F	tTA+*tet*O+	8 weeks	3	No expression
	251	M	tTA+*tet*O+	8 weeks		Moderate
	256	M	tTA+*tet*O+	8 weeks		expression

Table 24: Analysis of *tet*O- CPEB2ΔZn-EGFP mice lines.

4.8 Analysis of transgenic mice

4.8.1 Immunofluorescence of CPEB2-EGFP

The expression of CPEB2 transgene was confirmed with GFP fluorescence. To select the best age group for functional studies, CPEB2 expression was analyzed at three different ages of mouse development: 7, 13 and 20 weeks. After birth, CPEB2 expression can be seen in all the groups (Figure 20 A-L) analyzed, but mice aged 13 weeks were chosen for further experiments. The CaMKII promoter driven expression of CPEB2 transgene was found in the DG (Figures 20 A-F) and in cortex (Figures 20 G-L). The sections were also counterstained with Hoechst for nuclei.

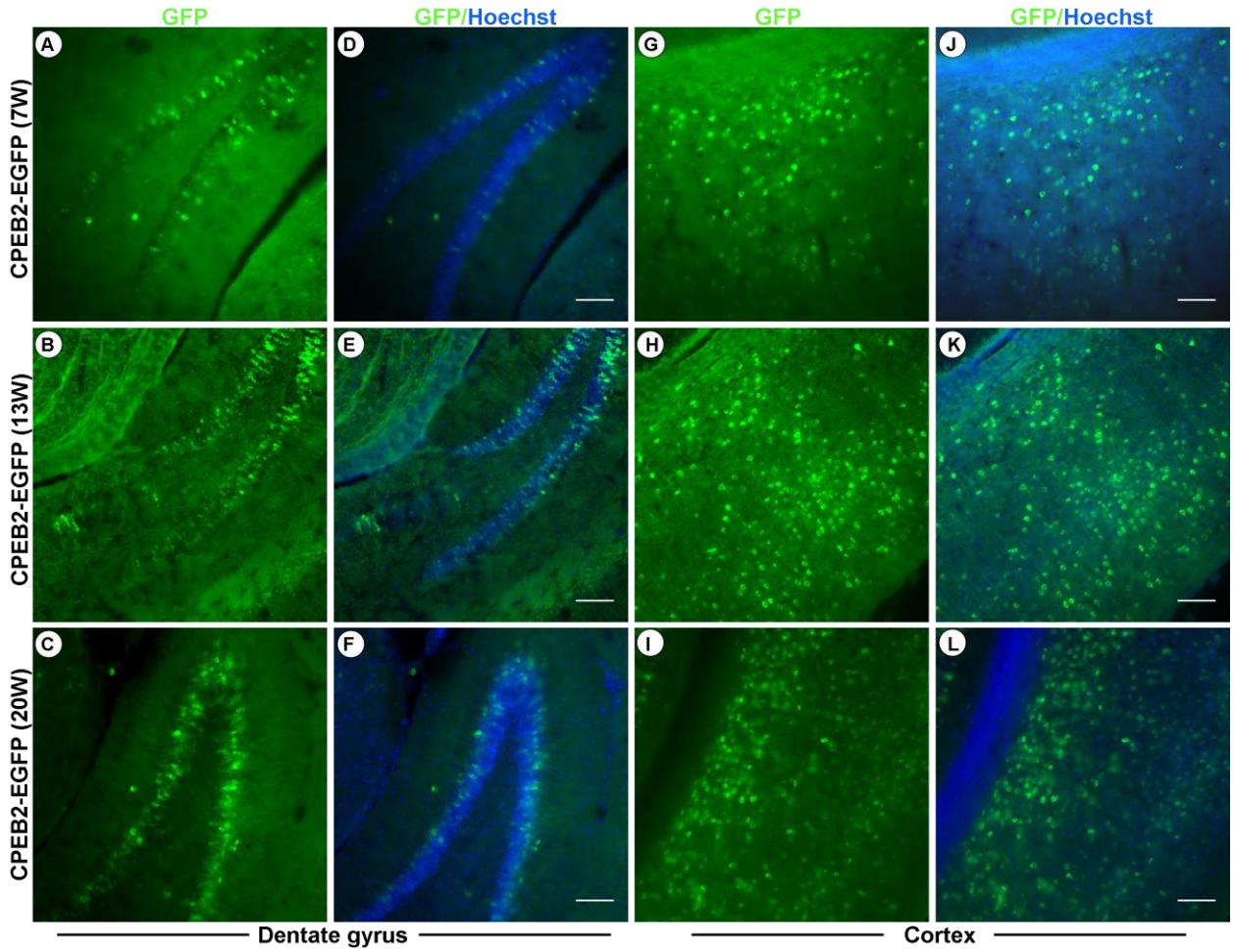

Figure 20: Expression pattern of CPEB2-EGFP in mouse hippocampus. Immunofluorescence of CPEB2-EGFP at three different age groups analyzed (7, 13 and 20 weeks) across brain regions: DG (Fig A-F) and cortex (G-L). Scale bar: 25 µm.

The expression of CPEB2 can be seen in the CA1 region where CPEB2 is often dendritically localized (Figure 21 A-C). Similar dendritic localization has been described for other CPEB family members such as CPEB3 in neurons (Huang et al., 2006).

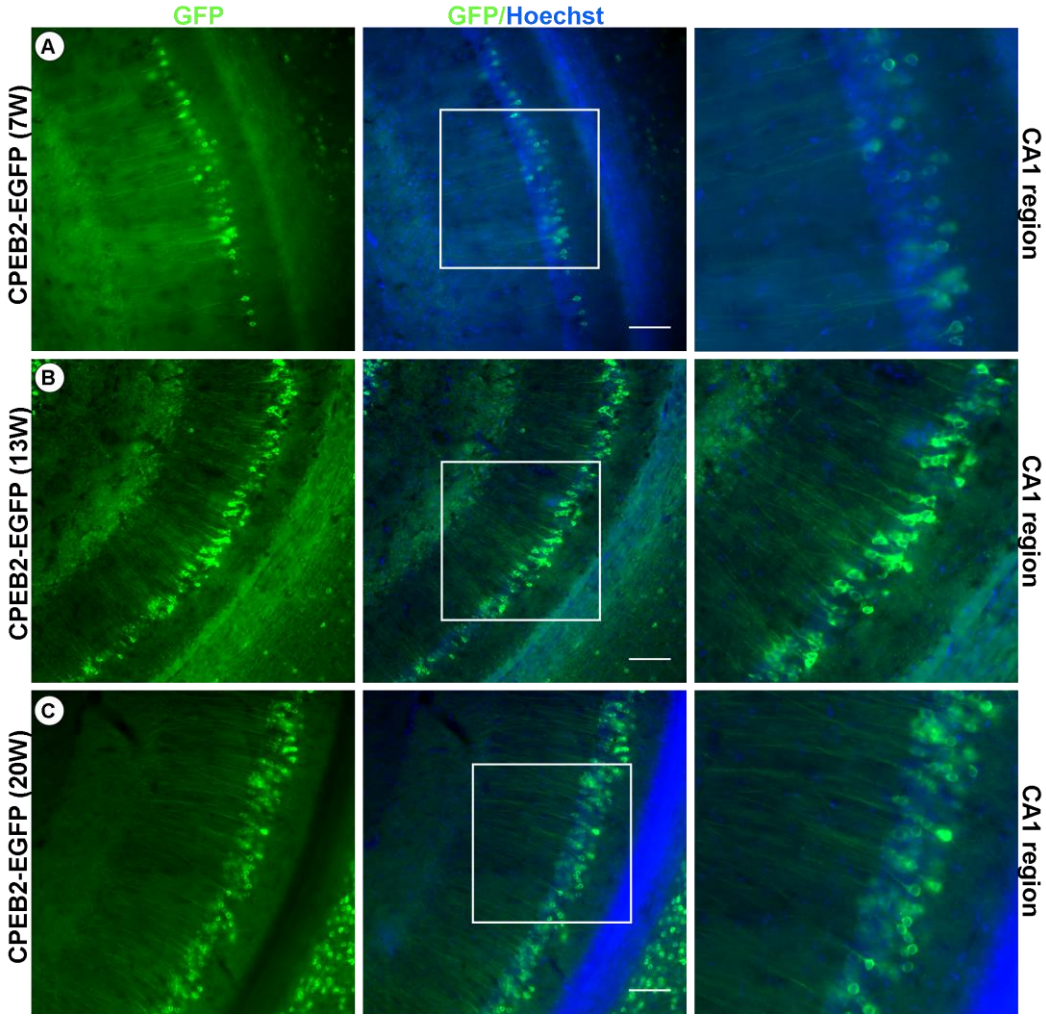

Figure 21: Expression pattern of CPEB2-EGFP in mouse hippocampus. Immunofluorescence of CPEB2-EGFP at three different age groups analyzed (7, 13 and 20 weeks) in CA1 region. Scale bar: 25 µm.

As all CPEB family members are expressed endogenously in brain (Wu et al., 1998; Theis et al., 2003), double immunostainings were performed with both CPEB2 antibodies (to detect endogenous CPEB2) and GFP antibodies (to detect overexpressed CPEB2). Both the endogenous and overexpressed CPEB2 are found to be colocalized (Figures 22 A, B).

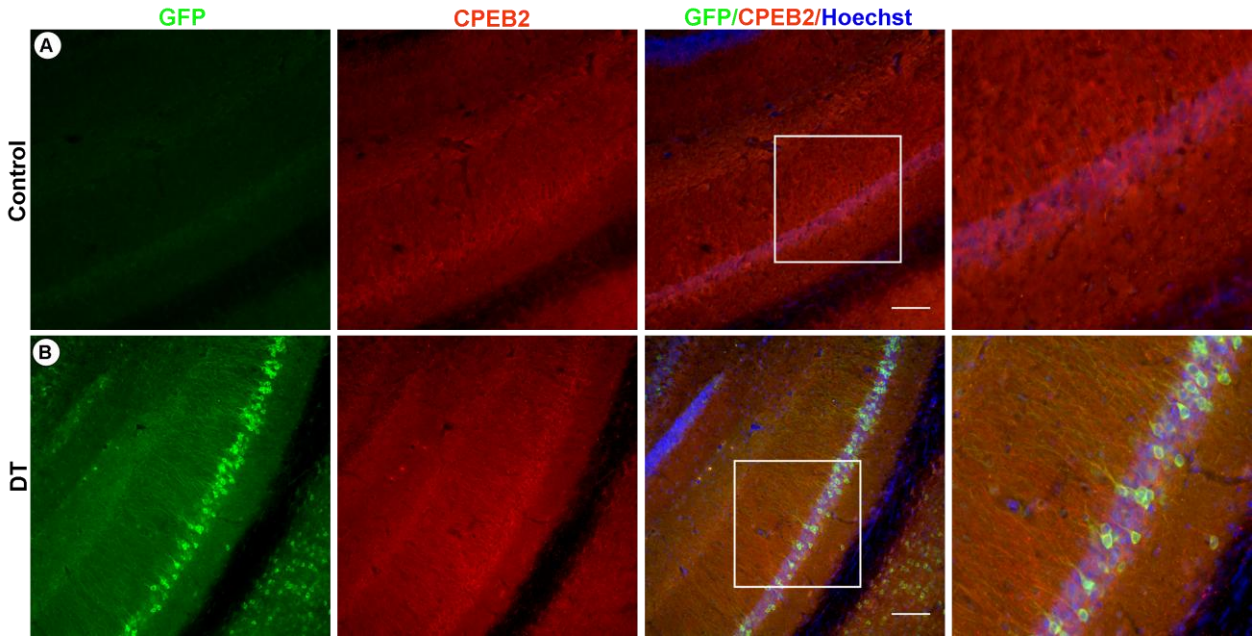

Figure 22: Analysis of CPEB2 transgene expression. A) Expression of endogenous CPEB2 in CA1 pyramidal neurons of mouse hippocampus of control animals. B) Double labelling with GFP and CPEB2 shows colocalization of the endogenous and overexpressed CPEB2 in CA1 pyramidal neurons of DT animals. Scale bar: 25 µm.

To analyze the extent of neuronal overexpression, double stainings with the neuronal marker, NeuN and GFP were performed. Using Image J software (http://rsbweb.nih.gov/ij/), the number of GFP positive cells that are co-localizing with NeuN were quantified. It was found that 38% of neurons showed overexpression of the transgene and were GFP positive (Figure 23). A total of 85% GFP positive cells were found to colocalize with the neuronal marker, NeuN.

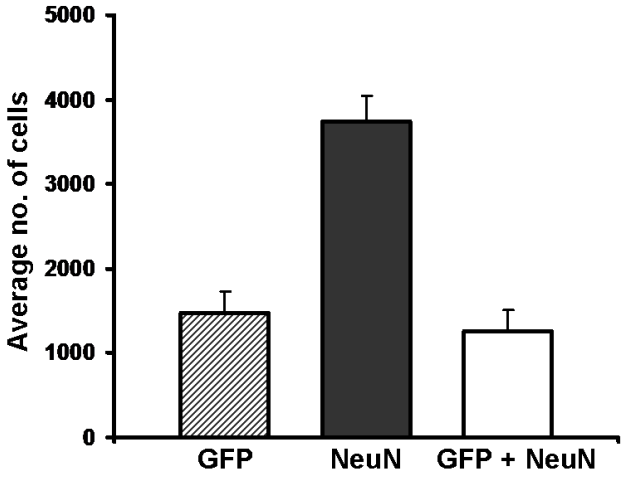

Figure 23: Histogram showing the extent of CPEB2 transgene expression. Approximately 38% of neurons overexpress CPEB2 transgene and 85% GFP positive neurons colocalize with NeuN. Error bars represent standard error of mean, n = 4 animals.

As CPEB2 was often dendritically localized (Figure 21), double stainings were performed with MAP2, a marker for dendrites. Double labelling with MAP2 and GFP revealed dendritic localization of CPEB2 where it might regulate the translation of different target mRNAs (Figures 24 A, B).

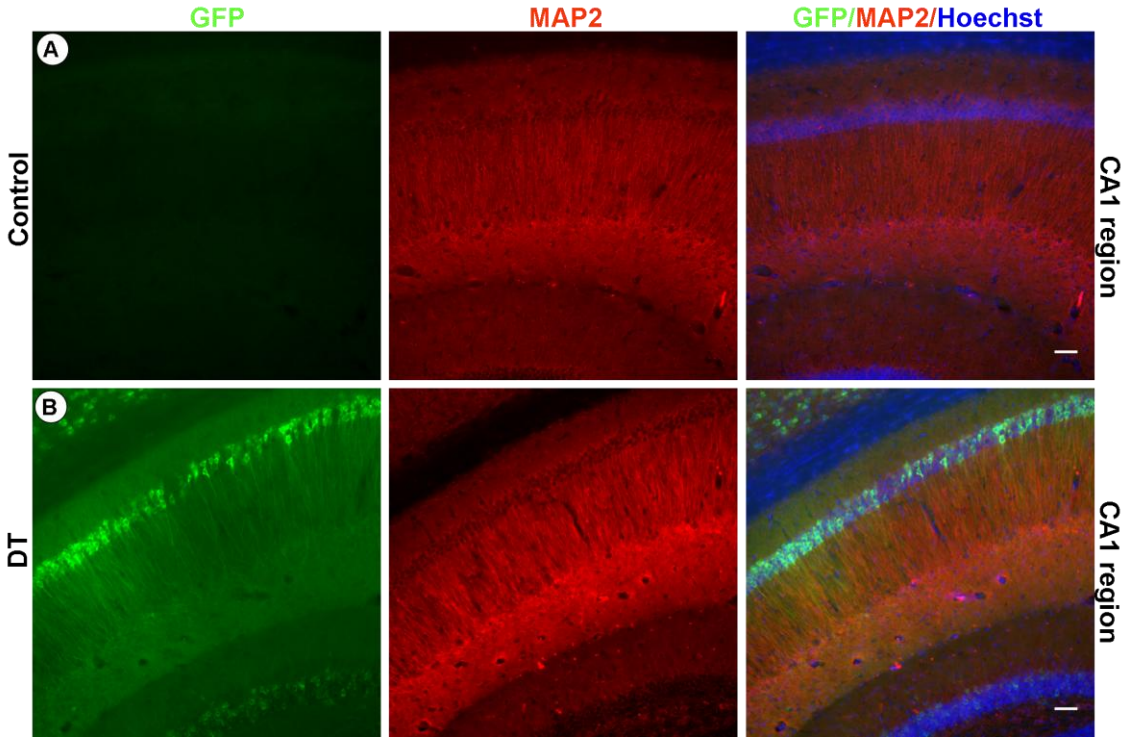

Figure 24: Double labelling with GFP and MAP2, which labels dendritic processes. A) Control, B) DT animals. Scale bar: 25 µm.

4.8.2 Immunofluorescence of CPEB2ΔZn-EGFP

The CPEB2ΔZn transgene expression was confirmed with GFP immunofluorescence (Figure 25). The expression of CPEB2ΔZn was observed in DG (Figures 25A, D), CA1 region of hippocampus (Figures 25B, E) as well as in cortex (Figures 25C, F). It also showed dendritic localization in CA1 pyramidal neurons similar to CPEB2 full length overexpression (Figure 21).

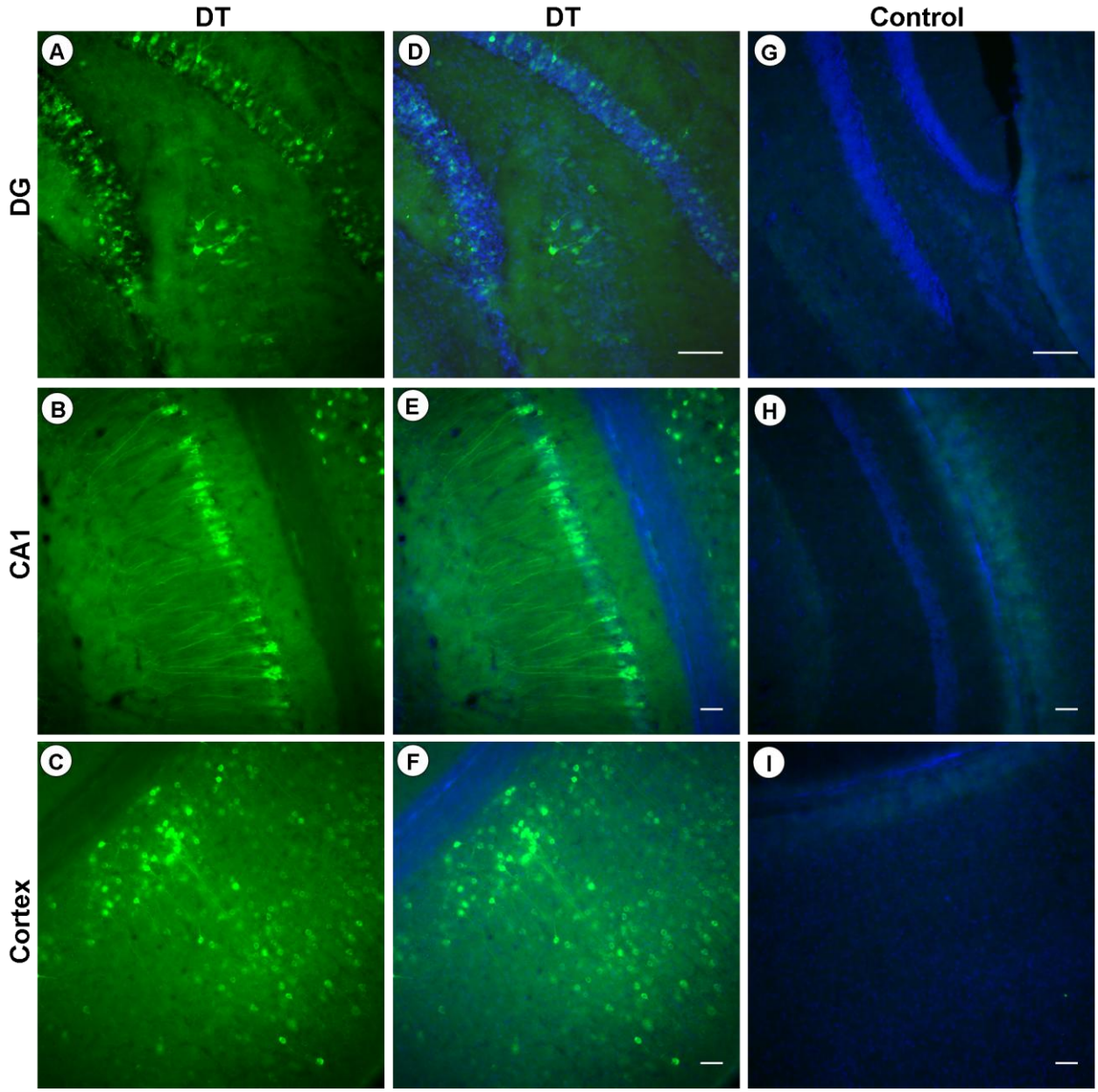

Figure 25: Immunofluorescence of CPEB2ΔZn-EGFP in mouse hippocampus. Expression of CPEB2ΔZn-EGFP can be seen in DG (A, D), CA1 region (B, E) and cortex (C, F). Control sections were also stained in parallel (G, H and I). Scale bar: 25 µm. A-C were stained with GFP, D-L were stained with GFP and Hoechst.

4.9 Analysis of protein levels of putative targets in CPEB2/CPEB2ΔZn mice

A number of mRNAs were proposed as putative CPEB targets (Du and Richter, 2005). Some of the CPEB targets with potential CPEB binding sites and polyadenylation sequences in their 3'UTRs can be found below in table 25. The protein levels of all the targets mentioned in the following table were analyzed in *tet*O-CPEB2-EGFP mice in comparison with their control littermates.

Target mRNA	No. of CPEs in its 3'UTR	CPEs	Poly(A)
β-catenin (Kundel et al., 2009)	3	UUUUUAAU UUUUAU UUUUAAUU	AUUAAA
EphA4 (Winter et al., 2008)	2	UUUUAU UUUUAU UUUUAU	AAUAAA
GluR1 (Bioinformatics analysis)	3	UUUUAAU UUUUAU UUUUAU	AUUAAA
GluR2 (Bioinformatics analysis)	14	UUUUAU UUUUAAAU UUUUAU UUUUAU UUUUAAU UUUUUAU UUUUUUUUUUAAU UUUUAU UUUUUAAAU UUUUUAU UUUUUUAAUUU UUUUUAU UUUUAAU UUUUAAAU	AUUAAA
ABP/GRIP2 (Du and Richter, 2005)	1	UUUUUUUUAAAU	AAUAAA
GRIP1 (Bioinformatics analysis)	2	UUUUAU UUUUAAAU	AAUAAA

Table 25: CPEB2 targets analyzed in the present study with potential CPEB binding sites and polyadenylation sequences in their 3'UTRs.

4.9.1 CPEB2 represses the basal translation of β-catenin in neurons

4.9.1.1 β-catenin downregulation *in situ*

A putative target of CPEB2 is β-catenin, which has binding sites for CPEBs in its 3'UTR (Figure 5) and is regulated by CPEB1 (Kundel et al., 2009) in neurons. Since all four CPEBs (1-4) share strong similarity in their RNA binding domains (Theis et al., 2003), CPEB2 might be also regulating β-catenin translation. To check this possibility, the expression of β-catenin in CPEB2 mice was analyzed. In those neurons which overexpress CPEB2-EGFP, no signal (or very weak signal) for β-catenin was observed and vice versa (Figure 26). This negative correlation of β-catenin with CPEB2 was observed at the single cell level *in situ*. From these immunohistochemistry results, it could be speculated that CPEB2 might negatively regulate β-catenin translation.

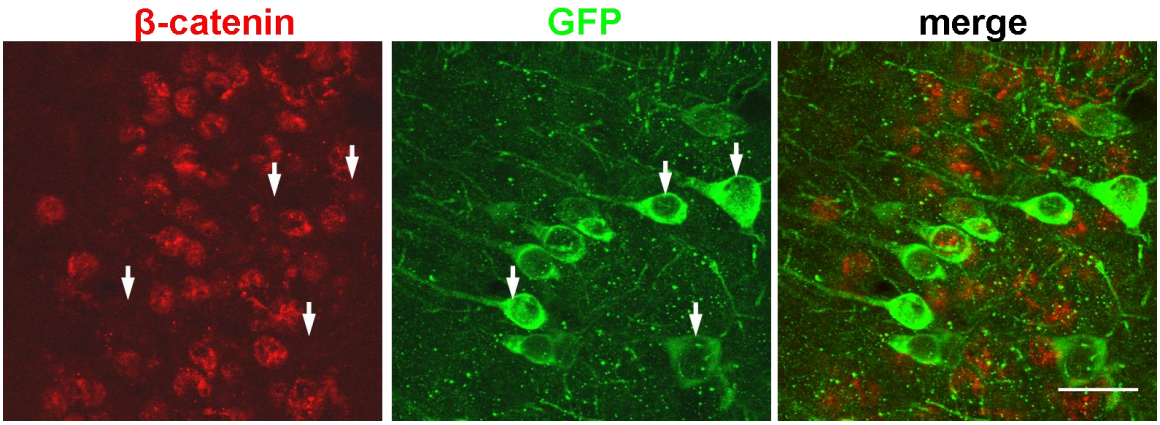

Figure 26: β-catenin downregulation *in situ* in CPEB2 overexpressing mice. Coronal sections of CPEB2 mice were stained with β-catenin and EGFP antibodies. Neurons with CPEB2-EGFP overexpression (labelled in green) showed no signal (or very weak signal) for β-catenin (labelled in red) and vice versa. As an example, some of the neurons are marked with arrows in both channels to show the downregulation. Scale bar: 25 µm.

4.9.1.2 Decreased β-catenin protein levels in CPEB2 overexpressing mice

Since a negative correlation was observed between β-catenin and CPEB2 immunoreactivity *in situ* (Figure 26), immunoblotting of protein lysates was done to study the impact of CPEB2 on β-catenin translation. The immunohistochemistry data confirmed the genotypes of different mice (whether it was a control or a DT mouse). Immunoblotting of hippocampal protein lysates from both DT animals and their control littermates was performed and the intensity of the bands from both the genotypes was quantified using gene tools software (Syngene). The protein values of control animals were set to 100%. With immunoblotting, it was found that β-catenin protein levels were significantly decreased by 50% in CPEB2 overexpressing mice (Figures 27 A, B) compared to their control littermates (**$p < 0.01$, student's t-test). Hence, from the immunohistochemistry and immunoblotting data, it can be concluded that overexpression of CPEB2 in pyramidal neurons repressed the basal translation of β-catenin in neurons.

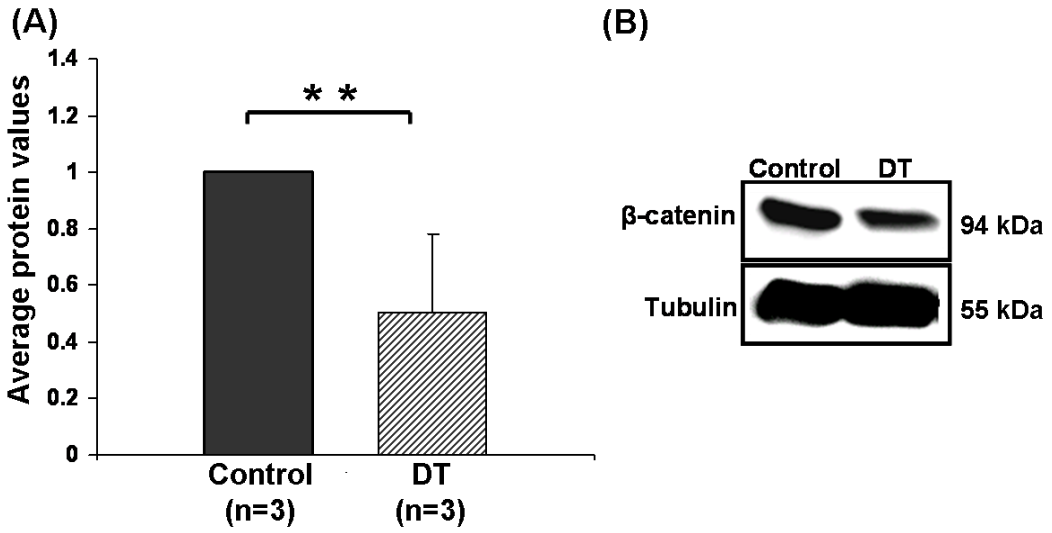

Figure 27: Western blot analysis of β-catenin protein levels in CPEB2 mice. A) Histogram showing decreased protein levels in DT animals compared to their control littermates (**p < 0.01, student's t-test). B) Representative Western blot image. n=3 animals/genotype. Error bars represent standard deviation. kDa: kilo Dalton.

4.9.1.3 CPEB2- β-catenin co-immunoprecipitation

As both immunohistochemistry (Figure 26) and immunoblotting (Figure 27) results confirmed that CPEB2 represses the basal translation of β-catenin, the physical interaction of CPEB2 with β-catenin was investigated *in vitro*. HeLa cells were transiently transfected with CPEB2-FLAG or FLAG-GFP (a non-CPE containing control) and the CPEB2 protein that was interacting with endogenous β-catenin mRNA was co-immunoprecipitated using FLAG antibodies. It was found that CPEB2 specifically interacts with β-catenin mRNA (Figures 28 A, B) and this interaction was specific as shown by comparing the retention of β-catenin mRNA over PBGD mRNA which is a non specific control (Figure 28B). In another experiment, the cells were transfected with either CPEB2-EGFP or CPEB2ΔZn-EGFP and the bound β-catenin mRNA was co-immunoprecipitated using CPEB2 serum (custom made, designated as #94). The binding was significantly reduced when the cells were transfected with CPEB2ΔZn-EGFP which could not bind to β-catenin as it lacks the zinc finger essential for binding (Figures 28A). Real time PCR of transcripts from both the transfections was done and the results were normalized to the levels of PBGD, a housekeeping gene, which was used to test the specificity of binding.

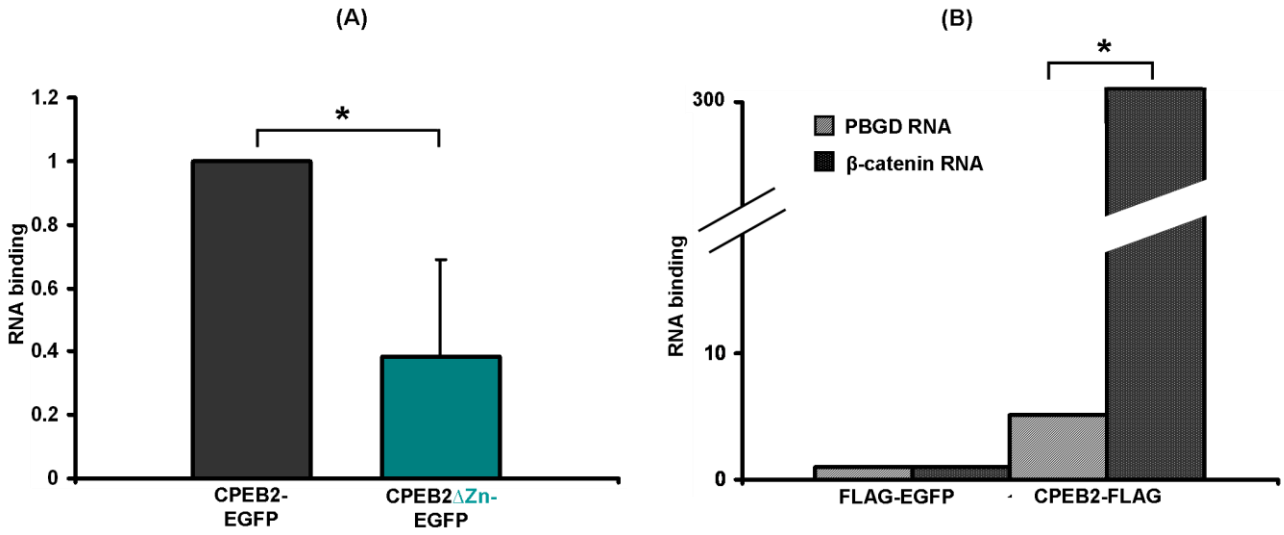

Figure 28: CPEB2- β-catenin co-immunoprecipitation. A) Co-immunoprecipitation of endogenous β-catenin mRNA in HeLa cells transfected with different CPEB2 constructs. The binding was significantly reduced when transfected with CPEB2ΔZn construct (*p < 0.05, student's t-test). B) The binding is mRNA specific as shown by comparing with the binding of CPEB2 to β-catenin and PBGD mRNAs. FLAG-GFP was used as an unspecific control. Experiments were done in triplicates. Error bars represent standard deviation.

4.9.2 CPEB2 represses the basal translation of GluR2 in neurons

GluR2 is an important subunit of the AMPA receptor complex, whose presence makes the AMPA receptors Ca^{2+} impermeable (Liu and Zukin, 2007). The translation of GluR2 is regulated by two members of the CPEB family, CPEB3 and CPEB4 (Huang et al., 2006). To find out if CPEB2 behaves similar to other CPEBs in translational regulation, GluR2 protein levels were analyzed in CPEB2 overexpressing mice. Western blotting of hippocampal protein lysates from both DT animals and their control littermates was performed and the intensity of the bands from both genotypes was quantified using gene tools software (Syngene). The protein values of control animals were set to 100%. GluR2 protein levels were significantly decreased by 66% (*p < 0.05, student's t-test) in DT mice compared to their control littermates (n=3 animals/genotype) (Figures 29 A, B).

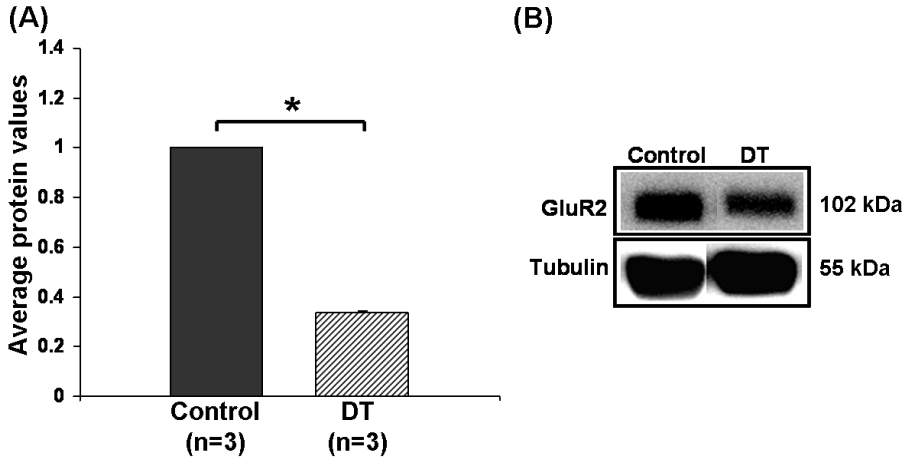

Figure 29: Western blot analysis of GluR2 protein levels in CPEB2 mice. A) Histogram showing decreased GluR2 protein levels in DT animals compared to their control littermates (*p < 0.05, student's t-test). B) Representative Western blot image. n=3 animals/genotype. Error bars represent standard deviation.

4.9.3 GluR1 protein levels were unaltered in CPEB2 overexpressing mice

CPEB2 was found to repress the basal translation of GluR2 in neurons. To find out if CPEB2 also regulates other CPE containing AMPA receptor subunits, protein levels of other AMPA receptor subunits were analyzed. Since GluR1 is the predominant subunit expressed in the CNS along with GluR2 (Sans et al., 2003) and also contains CPEs in its 3'UTR (Figure 30A), the protein levels of GluR1 were analyzed in DT animals compared to their control littermates. No difference in GluR1 protein levels was observed between the genotypes (p = 0.94, student's t-test; Figures 30 B, C).

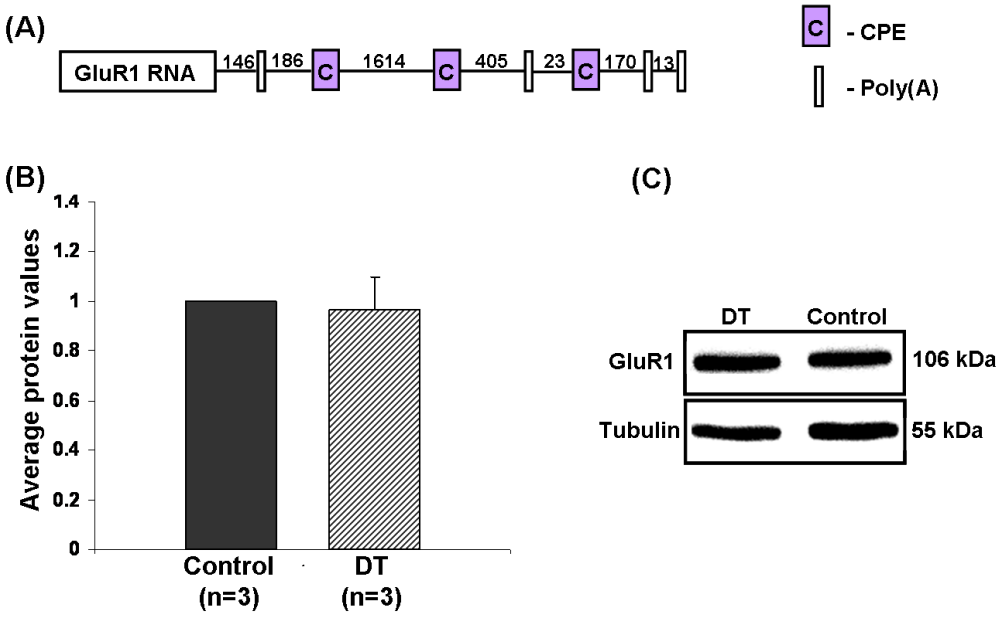

Figure 30: Western blot analysis of GluR1 protein levels in CPEB2 overexpressing mice. A) The 3' UTR of GluR1 with CPEs and poly(A) marked. The numbers indicate the distance in bases between the two elements. B) Histogram showing no significant difference in GluR1 protein levels between the genotypes. C) Representative Western blot image. n=3 animals/genotype. Error bars represent standard deviation.

4.9.4 The protein levels of GluR2 interacting proteins were not altered in CPEB2 overexpressing mice

The C-terminus of GluR2 interacts with several PDZ domain-containing proteins (Braithwaite et al., 2000) and this interaction facilitates the accumulation of functional AMPA receptors at synapses (Srivastava et al., 1998). Among these proteins, ABP/GRIP2 and GRIP1 were analyzed in the present study since both of them contain CPEs in their 3'UTRs (Figure 6). In addition, ABP has been confirmed as a CPEB3 target in neurons (Theis et al., 2011, in revision). Since GluR2 protein levels were decreased in CPEB2 overexpressing mice (Figure 29), it was hypothesized that CPEB2 might interact with the GluR2 interacting partners as well, thereby interfering with AMPA receptor clustering. To find out, immunoblotting was performed and the protein levels were measured.

The protein levels of ABP/GRIP2 were not altered in CPEB2 overexpressing mice ($p = 0.94$, student's t-test; Figures 31 A, B). This could be due to the fact that CPEB mediated translational regulation may vary based on the stoichiometry of CPEs (Pique et al., 2008), and according to this study, at least a cluster of two or more CPEs is required for translational repression to occur. Since ABP contains a single CPE in its 3'UTR, it might have not been repressed by CPEB2.

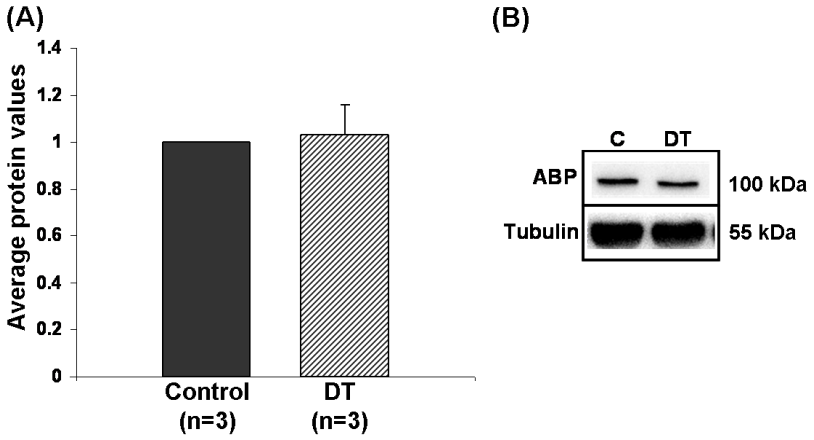

Figure 31: Western blot analysis of ABP/GRIP2 levels in CPEB2 mice. A) Histogram showing no significant difference in ABP/GRIP2 protein levels between the genotypes. B) Representative western blot image. n=3 animals/genotype. Error bars represent standard deviation.

GRIP1 is a PDZ domain-containing protein which interacts with the C-terminus of GluR2 (Dong et al., 1997) and is a splice isoform of ABP/GRIP2 (Wyszynski et al., 1999). WB was performed from both DT animals and their control littermates and the blots were quantified as

above. The protein levels of GRIP1 were not altered in CPEB2 overexpressing mice compared to their control littermates ($p = 0.90$, student's t-test; Figures 32 A, B). This might be due to the fact that even though there are three CPEs in the 3'UTR of GRIP1, the distance between two CPEs might be too far from each other (160 nucleotides) for repression to occur. It is known that cyclin B variants which have more distance between the two CPEs were weakly repressed compared to the other variants (Pique et al., 2008). Hence, it could be speculated that no repression observed in case of GRIP1 might be because of the larger distance present between two CPEs.

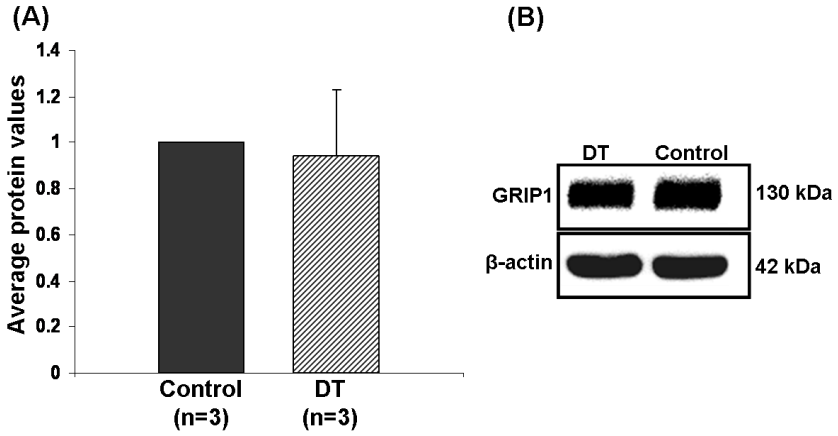

Figure 32: Western blot analysis of GRIP1 protein levels in CPEB2 mice. A) Histogram showing no significant difference in GRIP1 protein levels between the genotypes. B) Representative western blot image. n=3 animals/genotype. Error bars represent standard deviation.

4.9.5 CPEB2 represses basal translation of EphA4 (a new CPEB target) in neurons

4.9.5.1 Decreased EphA4 protein levels in CPEB2 overexpressing mice

The current findings indicate that CPEB2 regulates the translation of two known CPEB targets expressed in neurons (β-catenin and GluR2). In addition to these, several mRNAs were proposed as putative CPEB targets, as they contain CPEs in their 3'UTRs (Du and Richter, 2005). In search of new targets for CPEB2 mediated translational regulation, EphA4 receptor was selected since it contains two CPEs in its 3'UTR (Figure 8; Winter et al., 2008) and was reported to control glial glutamate transport via ephrin-A3 ligand (Filosa et al., 2009). To find out if CPEB2 regulates EphA4 translation, hippocampal protein levels of EphA4 were measured in DT animals in comparison with their control littermates. With immunoblotting, it was found that EphA4 protein levels were decreased by 30% in DT mice compared to their control littermates (Figures 33 A, B) (*$p < 0.05$, student's t-test). Hence, EphA4 can be proposed as a new CPEB2 target from the current findings.

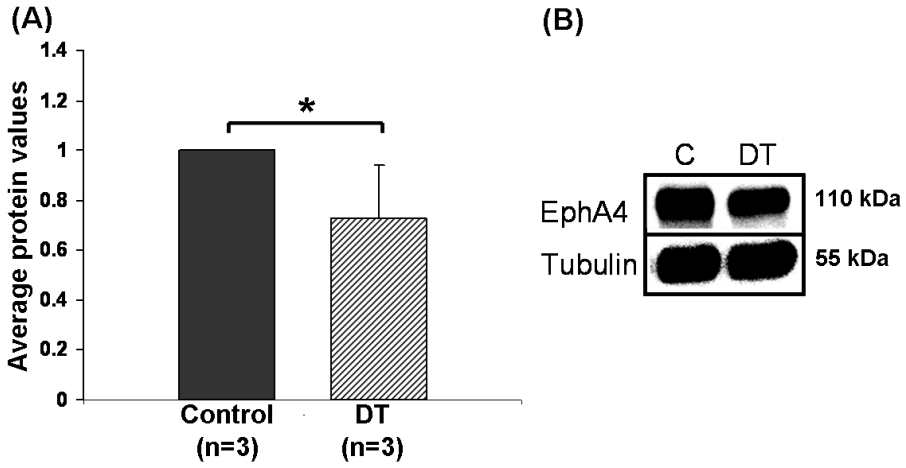

Figure 33: Western blot analysis of EphA4 protein levels in CPEB2 overexpressing mice. A) Histogram showing decreased protein levels in DT animals compared to their control littermates (*p < 0.05, student's t-test). B) Representative Western blot image. n=3 animals/genotype. Error bars represent standard deviation.

As neuronal EphA4 has been shown to participate in neuron-to-glia communication by modulating glial glutamate transport (Filosa et al., 2009), it could be speculated that by regulating the translation of EphA4, CPEB2 might also participate in neuron-glia communication. In addition, EphA4 knockout mice have elevated glutamate transporter levels (Filosa et al., 2009). To find out if CPEB2 regulates glial glutamate transport via EphA4, the protein levels of glial glutamate transporter (GLT-1) were further analyzed in CPEB2 overexpressing mice. No significant changes in GLT-1 protein levels between DT animals and their control littermates were observed (not shown). This could be due to the fact that EphA4 protein levels were reduced only by 30% in CPEB2 mice. As the complete knockout of EphA4 caused 100% elevated glutamate transporter protein levels (Filosa et al., 2009), only 30% of EphA4 deficit might have an insufficient impact on GLT-1 translation. As glial glutamate is transported by two glial transporters (GLT-1 and GLAST), it could be that EphA4, by interacting with GLAST, regulates the glutamate transport in glial cells. To verify this, the translation of GLAST should be analyzed in CPEB2 overexpressing mice.

4.9.5.2 CPEB2 interacts with EphA4 *in vitro*

As immunoblotting results (Figure 33) confirmed that CPEB2 represses the basal translation of EphA4, the physical interaction of CPEB2 with EphA4 was investigated *in vitro*. HeLa cells were transiently transfected with CPEB2-FLAG and EphA4 3'UTR-PGL and the CPEB2 protein that was bound to EphA4 mRNA was co-immunoprecipitated using FLAG antibodies. As a control, FLAG-GFP was used. It was found that CPEB2 specifically interacts with EphA4 mRNA (Figure 34) as no interaction was found with FLAG-GFP. Real time PCR

of transcripts using luciferase primers was done and the results were normalized to PBGD (a housekeeping gene) levels.

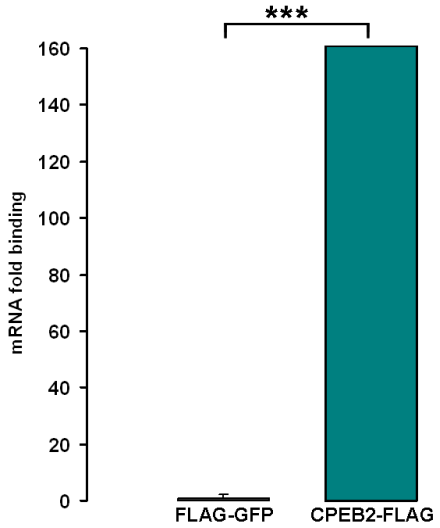

Figure 34: CPEB2-EphA4 co-immunoprecipitation. Co-immunoprecipitation of EphA4 mRNA in HeLa cells transfected with CPEB2-FLAG construct (***$p < 1.5 \times 10^{-9}$, student's t-test). FLAG-GFP was used as an unspecific control. The results were normalized to PBGD. Experiments were done in triplicates. Error bars represent standard deviation.

4.9.6 Synaptophysin protein levels were unaltered in CPEB2 overexpressing mice

Synaptophysin contains no CPEs in its 3'UTR. To validate the results of CPEB2 mediated translational regulation in neurons; synaptophysin was used as a non CPE containing control (negative control). With immunoblotting, protein levels of synaptophysin were measured in CPEB2 overexpressing mice. No changes in the protein levels of synaptophysin ($p = 0.66$, student's t-test) were observed in DT animals compared to their control littermates (Figures 35 A, B). This confirms that CPEB2 binds specifically to CPEs in the 3'UTR of mRNAs.

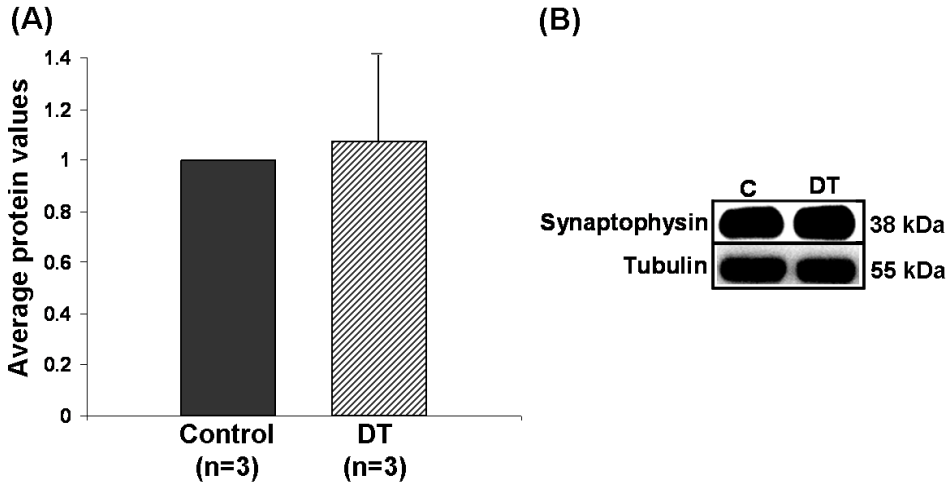

Figure 35: Western blot analysis of synaptophysin protein levels in CPEB2 mice. A) Histogram showing no significant difference in the protein levels between genotypes. B) Representative Western blot image. n=3 animals/genotype. Error bars represent standard deviation.

4.9.7 No change in basal protein levels of β-catenin/GluR2/EphA4 in CPEB2ΔZn overexpressing mice

CPEB2 requires the zinc finger to bind to its target mRNA (Hake et al., 1998; Turimella et al., in revision). To find out if RNA binding has any impact on translational regulation, transgenic mice which overexpress truncated CPEB2 protein that lacks zinc finger (CPEB2ΔZn) in pyramidal neurons were generated. In this set of mice, the protein levels of β-catenin, GluR2 and EphA4 (whose protein levels were decreased in CPEB2 overexpressing mice) were analyzed. It was found that overexpression of CPEB2 protein without the zinc finger (CPEB2ΔZn), did not lead to changes in the protein levels of the above mentioned targets, β-catenin ($p = 0.96$, student's t-test, Figure 36A), GluR2 ($p = 0.59$, student's t-test, Figure 36B) and EphA4 ($p = 0.68$, student's t-test, Figure 36C). This confirms that the zinc finger is essential for CPEB2 in order to bind to target mRNA for regulating its translation.

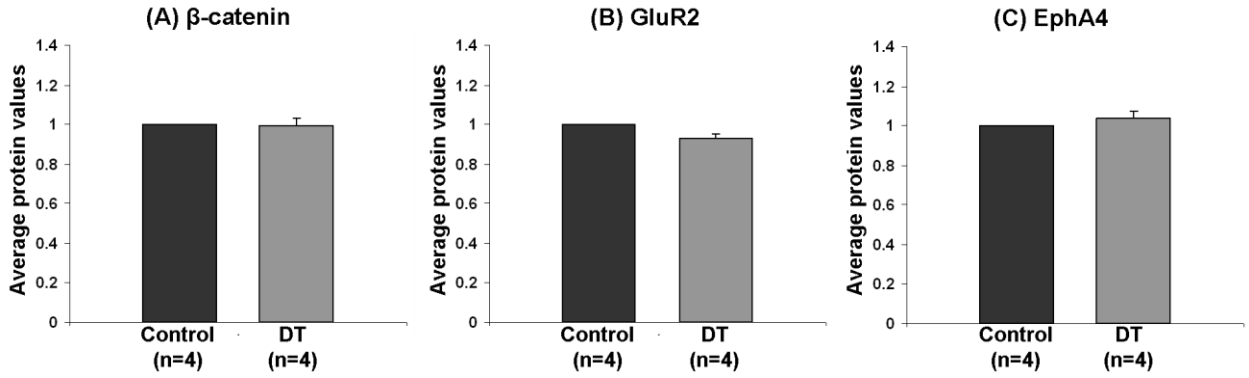

Figure 36: Western blot analysis of β-catenin (A), GluR2 (B) and EphA4 (C) protein levels in CPEB2ΔZn overexpressing mice. n=4 animals/genotype. Student's t-test was done to evaluate the statistical significance. Error bars represent standard deviation.

4.10 Estimating the efficiencies for Real Time PCR primers

From the current findings, it is known that CPEB2 regulates the translation of several targets. To confirm that only the protein levels are changed (exclusive translational regulation), but not the transcript levels, real time PCR was done. The efficiencies of t*aq*man primers used in the present study were estimated using the standard C_T slope method (Liu and Saint, 2002). The C_T values were plotted versus the concentration of cDNA samples. The slopes (R^2 values) for a 10-fold dilution series of the cDNA sample were calculated. The efficiencies of the amplification were calculated from the slope of the graph obtained for each primer set. The following equation was used for estimating the efficiency:

$$E = 10^{(-1/slope)} - 1$$

The efficiencies for EphA4, GluR2 and GAPDH taqman primers were found to be 1.99, 1.86 and 1.86 respectively (Table 26). The efficiencies of both β-catenin and PBGD primers were estimated as 2 (done in the institute before). The standard curves can be found in figures 37 A-C.

T*aq*man primers	**Efficiency (E)**	**Slope (R^2)**
EphA4	1.99	0.99
GluR2	1.86	0.99
GAPDH	1.86	0.99

Table 26: The efficiencies (E) and slope values (R^2) of the t*aq*man primers analyzed.

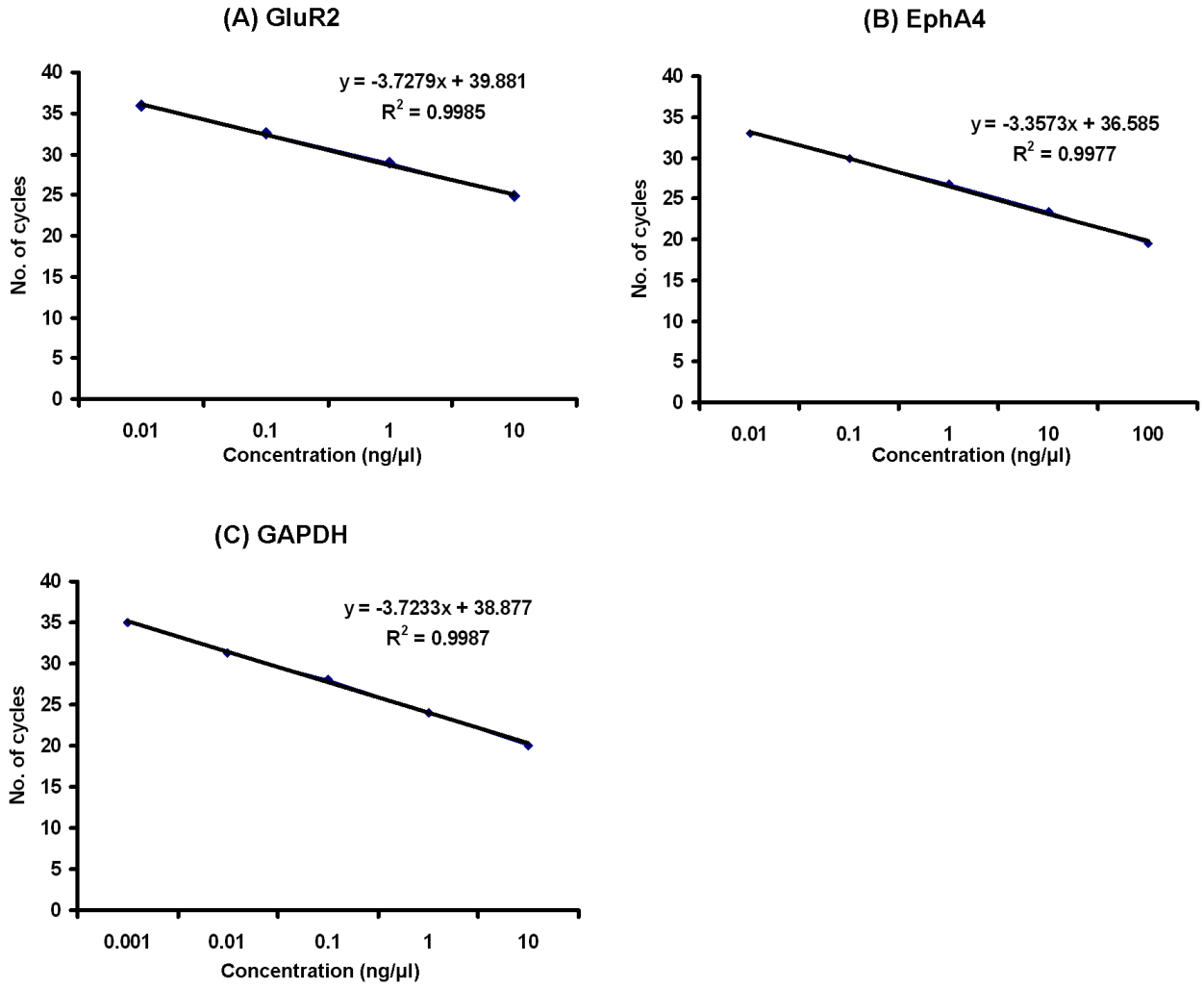

Figure 37: Standard curves for estimating the efficiencies for the following t*aq*man primers: GluR2 (A), EphA4 (B) and GAPDH primers (C).

4.11 Analyzing the transcript levels of putative targets by real time PCR

To confirm the fact that CPEB2 regulates translation but not transcription, the transcript levels of β-catenin, GluR2 and EphA4 were analyzed in CPEB2 overexpressing mice compared to their control littermates. Real time PCR of the above targets revealed no change in either β-catenin or GluR2 or EphA4 transcript levels in DT animals compared to their control littermates (Figure 38 A-D). This suggests the exclusive translational regulation by CPEB2 in neurons. The results were confirmed using two reference genes, β-actin and GAPDH to which the results were normalized. There was a slight decrease observed for transcript levels in DT animals though it was not significant. This could be due to the fact that CPEB2 might be interfering with RNA stability as CPEB3 does (Hosoda et al., 2011).

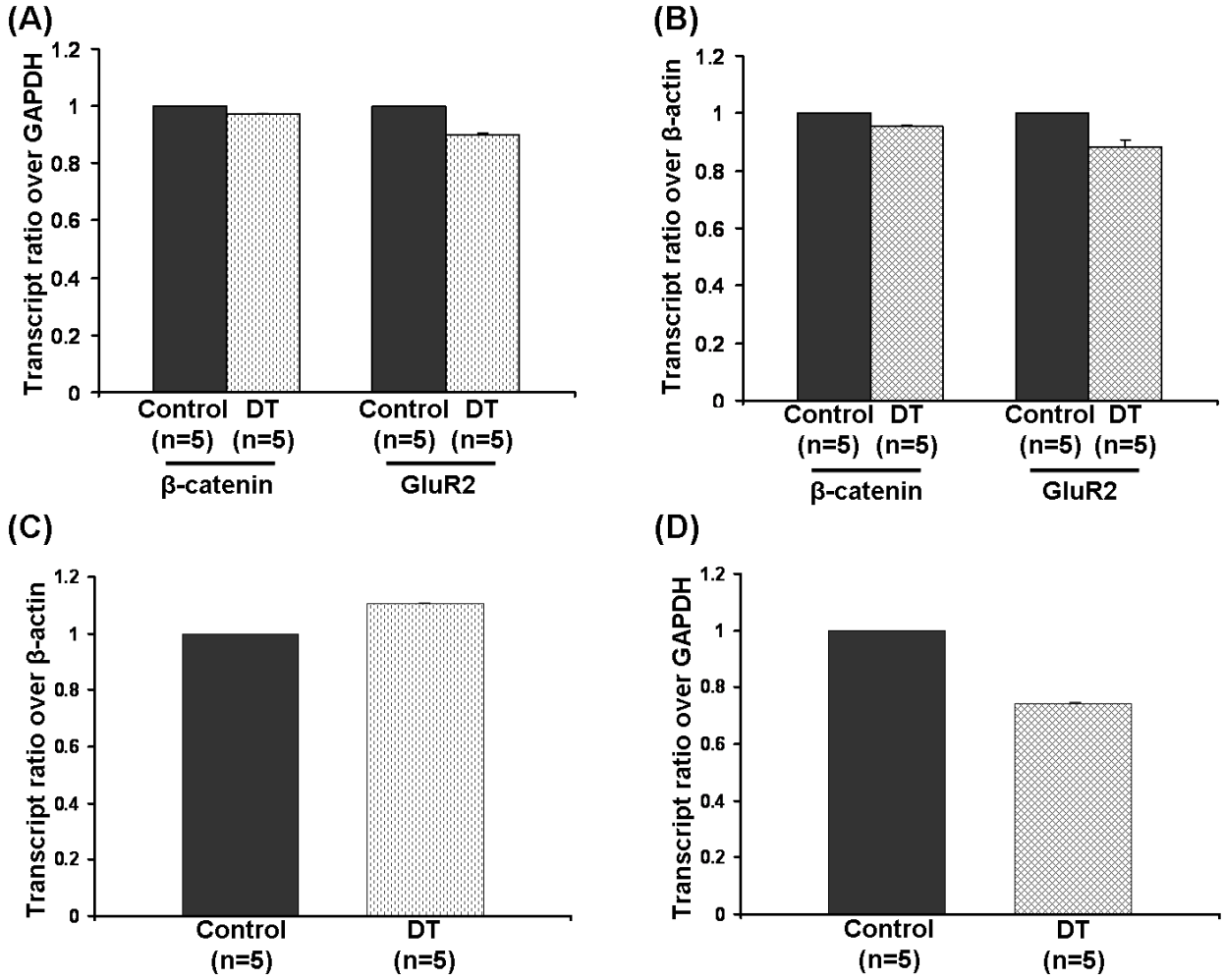

Figure 38: Transcript levels of the putative targets in CPEB2 overexpressing mice. Real Time PCR of β-catenin and GluR2 using GAPDH (A) and β-actin (B) as reference genes. Real Time PCR of EphA4 using β-actin (C) and GAPDH as reference genes (D). The results were normalized to the reference genes used. Experiments were done in triplicates. Student's t-test was done to evaluate the statistical significance. Error bars represent standard deviation.

4.12 Interaction of CPEBs with other target mRNAs

4.12.1 CPEB2 interacts with the CamKIIα 3'UTR

The 3'UTR of CamKIIα contains CPEs and thus could be a potential CPEB target. In deed, CPEB1 regulates the translation of CamKIIα (Wu et al., 1998). To find out whether CPEB2 regulates CamKIIα translation, RNA co-immunoprecipitation was performed from HeLa cell lysates transfected with FLAG tagged CPEB1 or 2 constructs together with the CamKIIα 3'UTR-PGL construct. Both CPEBs (CPEB1 and 2) interacted with CamKIIα 3'UTR, but CPEB1 had significantly higher affinity compared to CPEB2 (Figure 39A; Turimella et al., in revision). The interaction of different CPEB1 isoforms (CPEB1, Δ5, Δ17) with CamKIIα 3'UTR was also analyzed in the present study. It was found that CPEB1 Δ5 had significantly higher affinity for CamKIIα 3'UTR compared to CPEB1 full length and CPEB1 Δ17 isoforms (Figure 39B; Turimella et al., in revision).

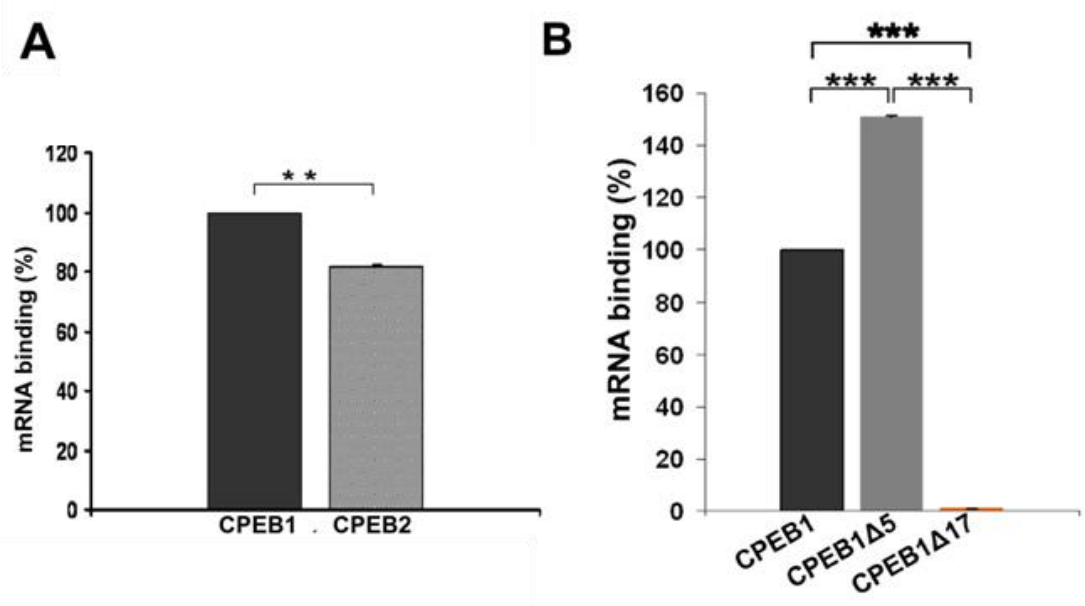

Figure 39: A) Co-immunoprecipitation of CPEB1 and CPEB2 interacting with rat CamKIIα 3'UTR. A) CPEB1 binds to CamKII 3'UTR with significantly higher affinity compared to CPEB2 (**$p < 0.05$, student's t-test). B) Among CPEB1 isoforms, CPEB1 Δ5 binds significantly with higher affinity compared to the CPEB1 full length isoform, CPEB1 (***$p < 0.001$) and CPEB1 Δ17 (***$p < 10^{-9}$). CPEB1 Δ17 has negligible binding when compared to CPEB1 (***$p < 10^{-9}$). Error bars represent standard error of the mean.

4.12.2 CPEB2 interacts with Cx36 3'UTR

The 3'UTR of Cx36 contains CPEs (Figure 40A) and thus could be a CPEB target. By dual luciferase reporter assay, it was found that CPEB2 enhances the translation of Cx36. The translation of Cx36 was impaired when HeLa cells were treated with siRNA against CPEB2, indicating that siRNA knockdown of endogenous CPEB2 impaired the translation process. In

addition, when HeLa cells were transfected with CPEB2-EGFP, the translational efficiency of Cx36 was enhanced by 1.5 fold (Figure 40B), which could be brought back below the control levels upon siRNA knockdown. Altogether, the present study indicates that CPEB2 enhances the translation of Cx36.

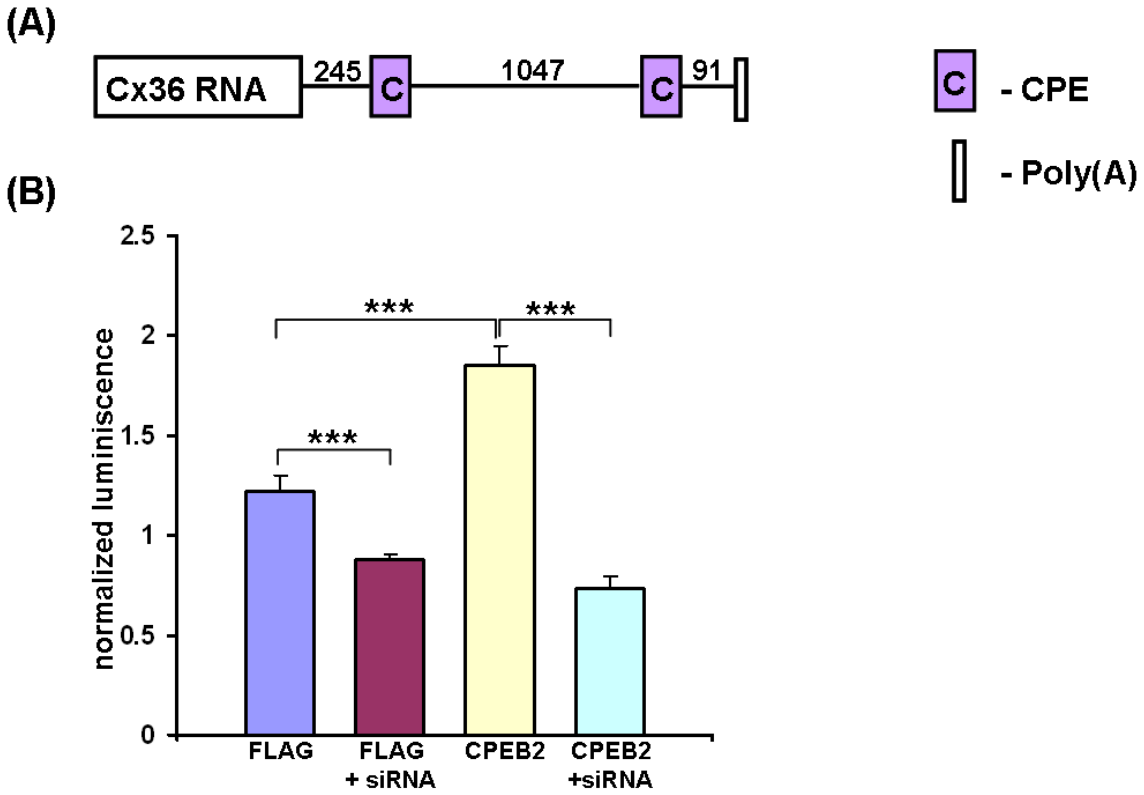

Figure 40: Cx36 luciferase reporter assay. CPEB2 interacts with the Cx36 3'UTR. A) The 3'UTR of Cx36 with CPEs and poly(A) marked. The numbers indicate the distance in bases between the two elements. B) CPEB2 enhances the translation of Cx36, which can be decreased by siRNA against CPEB2. FLAG-EGFP was used as an unspecific control. The translation was also decreased when the endogenous CPEB2 in HeLa cells was knocked down. ***$p < 1.6 \times 10^{-10}$, ANOVA single factor. Error bars represent standard deviation; the experiments were done in triplicates.

4.13 Rapid Amplification of cDNA ends (3' RACE) of CPEB2

It is known that CPEB2 has a major 3'UTR of 3.8 kb in length (Theis et al., 2003), but the sequence information was not available. In the present study, the 3'UTR of CPEB2 was analyzed for potential CPEB binding sites. Mouse brain cDNA was amplified with a gene specific primer that binds within the CPEB2 coding region and an adaptor primer (provided in the kit). Since a smear appeared along with the PCR product (result not shown), a nested PCR was performed as in methods part 3.2.12 using the above PCR product as a template. A PCR product of 3.8 kb was observed which is consistent with the previous findings (Figure 41A;

Theis et al., 2003). This nested PCR product was cloned into the PCR-XL-TOPO vector and the minipreps were digested with *EcoR*I. The digestion of minis revealed several RACE products: 1217 bp, 1647 bp, 2690 bp and 3778 bp (Figure 41B). The sequence analysis of all these different RACE products revealed a number of potential binding sites for CPEBs (as many as 26 CPEs) and several polyadenylation sequences (a total of 6). The presence of these multiple RACE products with different lengths might be due to alternative splicing of the 3'UTR. As a number of poly(A) sequences were found along the 3'UTR of CPEB2, it could be that the different lengths of UTRs might have generated by utilizing different poly(A) sequences. Sequencing of a number of minipreps revealed that the 3.8 kb RACE product is more frequently observed compared to the other.

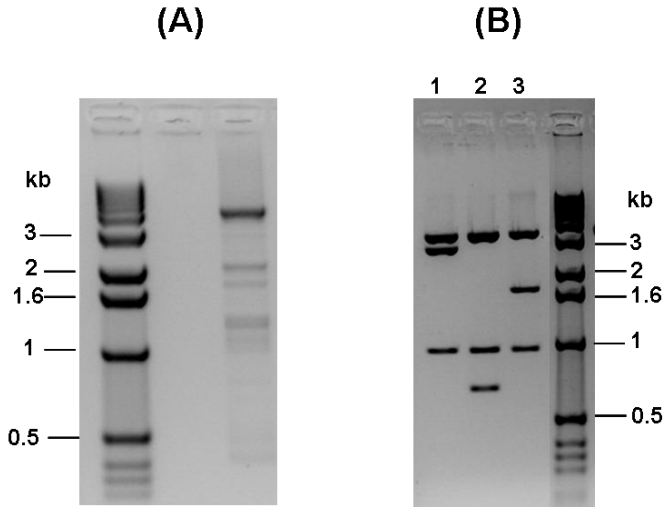

Figure 41: A) 3' RACE of CPEB2. A major PCR product of 3.8 kb was observed along with some minor bands at varying lengths. B) Nested PCR followed by cloning and digestion of minipreps with *EcoR*I revealed several RACE products. PCR-XL-TOPO has an *EcoR*I site, hence after digestion, a 3.5 kb band corresponding to the vector (top most band) and bands corresponding to PCR products were observed. Mini #1 gave 2.8 kb + 1 kb restriction product (together, a 3.8 kb RACE product), mini #2 gave 1 kb + 647 bp restriction products (together, a 1647 bp RACE product), mini #3 gave 1.6 kb and 1 kb restriction product (together a 2690 bp RACE product). All together, these results indicate multiple RACE products with variable lengths: (#1 – 3778 bp, #2 – 1647 bp, #3 – 2690 bp). kb – kilobases.

5 Discussion

5.1 Cell type specific expression of CPEBs: Single-cell RT-PCR

The expression pattern of all CPEBs (1-4) in neurons and glia was analyzed in the present study. Single-cell RT-PCR following electrophysiological characterization of different neural cell types (neurons, astrocytes, NG2 glia and microglia) was performed. CPEBs were more frequently expressed in neurons (Figure 14A) compared to glial cell types. In neurons, the 'sm' isoform (with a small deletion of 5 amino acids in RRM1) was most frequently observed for CPEB1 (Table 22). For CPEB2, the 'a' isoform was the most abundant. All CPEB2 isoforms observed in the present study contained the B-region which harbors a putative phosphorylation site for a number of kinases including PKA, CaMKIIα and p70S6 kinase. Earlier studies (Theis et al., 2003) pointed out that only those isoforms with the B-region are expressed in the principle cell layers of the hippocampus. But in the present study, isoforms lacking the B-region were also observed. For example, in case of CPEB3, although majority of the isoforms contained the B-region, one of the neurons contained 'b' isoform that lacks the B-region. In addition, for CPEB4, 'd' isoform that lacks the B-region was the major isoform observed, in addition to B-region containing isoforms. Multiple splice isoforms were observed within the same cell. This was more frequent in case of CPEB2 and CPEB4 (Figure 14 and Table 22), but can also be seen for CPEB3. This heterogeneity could be related to different activity states of the corresponding neurons at the time of isolation.

The expression pattern of CPEBs in glial subtypes was different from that of neurons. Among glia, CPEBs expression in astrocytes (Figure 14B) was found to be rather infrequent compared to NG2 glia (Figures 14C). For CPEB1, the full length isoform was observed. For CPEB2, isoforms lacking the B-region were observed in all the glial subtypes analyzed (astrocytes, NG2 glia and microglia). For the CPEB 2-4 subfamily, only isoforms containing the B-region are reported in the principal cell layers of the hippocampus (Theis et al., 2003) whereas the B-region lacking isoforms were described in non neuronal tissues, i.e. in testis (Kurihara et al., 2003). This is the first report showing the presence of B-region lacking isoforms (especially for CPEB2) in mouse brain. The presence of CPEBs in astrocytes suggests translational regulation of astrocyte-specific mRNAs which have CPEs in their 3'UTRs. For example, several astrocytic mRNAs including the major gap junction proteins,

Connexin43 (Cx43) and Cx30 (Vangoor et al., in revision); glutamate transporters GLT-1 and GLAST and glutamine synthetase (GS) (an enzyme that converts astrocytic glutamate to glutamine) were found to contain CPEs in their 3'UTRs (Vangoor et al., unpublished). Hence, CPEBs in astrocytes might regulate the translation of one or more of these target mRNAs. Indeed, the translation of Cx43, Cx30, (Vangoor et al., in revision) GLT-1 and GS (Vangoor et al., unpublished) was repressed following overexpression of CPEB3 in astrocytes.

CPEBs were highly expressed in NG2 glia compared to astrocytes (Figure 14 B, C), where they could modulate the translation of NG2 glia-specific mRNAs which contain CPEs in their 3'UTRs. NG2 glia differs from astrocytes not only in pharmacological properties (Matthias et al., 2003), but also in receiving synaptic input from both glutamatergic (Bergles et al., 2000) and GABAergic neurons (Jabs et al., 2005). Even though several astrocytic mRNAs including Cx43 and GLT-1 are expressed in NG2 glia (Matthias et al., 2003; Gerald Seifert, unpublished data), the functional properties of these proteins such as gap junctional coupling and glutamate transporter functions respectively were not observed (Matthias et al., 2003; Wallraff et al., 2004). In addition, the GluR2 subunit of AMPA receptors, which is responsible for restricting the Ca^{2+} entry (Liu and Zukin, 2007) is also expressed in NG2 glia in addition to neurons. Hence, CPEBs in NG2 glia might control the translation of GluR2, Cx43 and GLT-1.

CPEBs were also expressed in microglia (Figure 14D), where they could regulate microglia-specific mRNAs which contain CPEs in their 3'UTRs. For example, tissue plasminogen activator (tPA) is expressed in microglia (Tsirka et al., 1995) and contains CPEs in its 3'UTR (Shin et al., 2004).

5.2 CPEB2/CPEB2ΔZn overexpressing mice

To analyze the role of CPEB2 in neurons, transgenic mice with neuronal overexpression of CPEB2 were generated in the present work. Among the transgenic systems, the conditional tetracycline system (*tet*-OFF system) has been widely used due to its advantage of high temporal control of the transgene (Gossen and Bujard, 1992). The transgene can either be activated, or silenced by the administration of tetracycline or its derivatives such as doxycycline (Figure 9; Lewandoski, 2001). In the present study, *tet*-OFF system (Gossen and Bujard, 1992) and neuron-specific CaMKIIα promoter (Mayford et al., 1997) were used to

drive CPEB2 expression specifically in pyramidal neurons of mouse hippocampus. The CaMKIIα promoter drives the transgene expression specifically in neurons of forebrain and has been successfully used in generating transgenic mouse models for studying various diseases including Alzheimer's disease (Jankowsky et al., 2005), Huntington's disease (Yamamoto et al., 2000), Parkinson's disease (Nuber et al., 2008) and schizophrenia (Pletnikov et al., 2008). The CaMKIIα promoter lines were also used to study synaptic plasticity, learning and memory (Mayford et al., 1997).

Since CPEB2 is tagged with EGFP protein at its C-terminus, the transgene expression was confirmed with GFP fluorescence (Figures 20 and 21). The overexpressed CPEB2 protein was colocalized with the endogenous CPEB2 (Figure 22), in addition, it was often found to localize in the dendrites (Figures 21, 24), where it could modulate the translation of several target mRNAs. This dendritic localization has been described for the other CPEB family members, CPEB3 and CPEB4 in neurons (Huang et al., 2006). CPEB2 has an RNA binding domain, which is conserved among CPEBs (CPEB1, 3 and 4) (Theis et al., 2003). Zinc finger is essential for binding of CPEB1 to the target mRNAs (Hake et al., 1998). To analyze the impact of RNA binding on translational regulation, CPEB2 mutant mice lacking the zinc finger (*tet*O-CPEB2ΔZn-EGFP) were generated using a similar strategy (Figure 18). Using this set of overexpressing mice (CPEB2 and CPEB2ΔZn), the impact of CPEB2 on the translation of different target mRNAs in neurons was investigated, mainly focused on the translation of key players involved in synaptic plasticity such as β-catenin, GluR2 and EphA4.

5.3 CPEB2 regulates β-catenin translation in neurons

β-catenin is an adherens junction (AJ) protein which has multiple roles in cell-cell adhesion, Wnt signalling pathway (Clevers, 2006) and in various stages of neuronal development. It has also been reported as a putative CPEB1 target both in astrocytes (Jones et al., 2008) and in neurons (Kundel et al., 2009). To find out if CPEB2 as well regulates β-catenin translation in neurons, both *in vitro* and *in vivo* approaches were used. The present work indicates that CPEB2 interacts with β-catenin *in vitro* and this interaction was zinc finger mediated, as a CPEB2 mutant without zinc finger showed significantly decreased binding (Figure 28). These results further confirmed the necessity of the zinc finger for CPEB2 for RNA binding. In an *in vivo* approach, the protein levels of β-catenin were analyzed in CPEB2 overexpressing mice in comparison with their control littermates. Overexpression of CPEB2 in neurons has led to a

significant decrease in the basal protein levels of β-catenin by 50% (Figure 27). This negative correlation was also observed at the single cell level *in situ* (Figure 26). As CPEB2 represses the basal translation of β-catenin which is important for dendritic morphogenesis (Yu and Malenka, 2003), and abnormal dendritic spines were associated with β-catenin dysfunction which might contribute to several neurological disorders, CPEB2 might control the morphogenesis of the spines via β-catenin. If this is the fact, there might be abnormal dendritic spines in CPEB2 overexpressing mice which are yet to be investigated. Together, these results suggest that CPEB2 might participate in dendritic morphogenesis or might be involved in neurological disorders associated with abnormal dendritic spines, by modulating the translation of β-catenin.

5.4 CPEB2 might participate in Ca^{2+} permeability by regulating GluR2 translation in neurons

As GluR2 plays a crucial role in synaptic plasticity (Liu and Zukin, 2007), the mechanisms that regulate AMPA receptors were of great interest. Recent observations claim a role of activity-dependent local protein synthesis in regulating AMPA receptor function (Grooms et al., 2006). CPEBs participate in activity-dependent local protein synthesis (Wu et al., 1998). In addition, two members of the CPEB family, CPEB3 and CPEB4 regulate the translation of GluR2 (Huang et al., 2006). To find out whether CPEB2 regulates translation similar to other CPEBs, GluR2 protein levels were analyzed in CPEB2 overexpressing mice. The protein levels of GluR2 were significantly decreased by 66% in CPEB2 overexpressing mice compared to their control littermates (Figure 29). Similarly, in mice overexpressing CPEB3 in neurons, the protein levels of GluR2 were decreased (Kaczmarczyk, PhD thesis). Hence, it can be concluded that CPEB2, similar to CPEB3, represses the basal translation of GluR2. This result is further supporting the notion that CPEBs are translational repressors under basal conditions (Richter, 2007).

Since a major amount of GluR2 was repressed in CPEB2 overexpressing mice, it might lead to excess entry of calcium inside the cell which might cause the neurons to become hyperexcitable (Brusa et al., 1995; Liu and Zukin, 2007). CPEB2 might also participate in LTP by modulating the translation of GluR2. As GluR2 is also expressed in NG2 cells, a glial subpopulation which receives glutamatergic input from neurons (Bergles et al., 2000), CPEB2 might also regulate GluR2 translation in NG2 cells which is yet to be tested. Altogether, it

could be speculated that CPEB2 together with other CPEBs might participate in AMPA receptor function by modulating the translation of GluR2.

5.5 CPEB2 does not regulate the translation of GluR1, an AMPA receptor subunit

The protein levels of GluR2 were decreased in CPEB2 overexpressing mice. As there are four AMPAR subunits which share 70% similarity at the amino acid level (Bettler and Mulle, 1995), bioinformatical analysis was carried out to find out if CPEB2 has binding sites in the 3'UTRs of other AMPA receptor subunits. Among the other AMPA receptor subunits, GluR1 and GluR4 possess CPEs in their 3'UTRs. To find out if CPEB2 regulates the translation of GluR1 or GluR4, Western blotting analysis was performed. GluR1 was selected for analysis due to the following reasons: i) GluR1 (along with GluR2) is the predominant subunit expressed in forebrain (Sans et al., 2003), ii) together with GluR2, it forms the most common combination of AMPA receptor subunits in the CNS (Cull-Candy et al., 2006). The protein levels of GluR1 were not changed in CPEB2 overexpressing mice compared to their control littermates (Figure 30) which means that CPEB2 selectively impairs GluR2 translation. A combinatorial code has been proposed for CPEB1 in *Xenopus* oocytes, according to which at least two CPEs are required for repression to occur (Pique et al., 2008). The authors also found that when two CPEs were far from each other, the repression was weak. In the present study, GluR1 protein levels were unchanged in CPEB2 overexpressing mice; it might be that even though there are three CPEs in GluR1 3'UTR, the distance between two CPEs might be too large for translational repression to occur according to the combinatorial code proposed.

5.6 The GluR2 interacting partners are unaffected by CPEB2 in neurons

GluR2 interacts with many PDZ domain-containing proteins similar to NMDA receptors which bind to PSD-95 family proteins (Kornau et al., 1995). Among those proteins, ABP/GRIP2, GRIP1 and PICK1 were found to be important in AMPA receptor clustering (Srivastava et al., 1998). From this list, ABP (GRIP2) and GRIP1 were chosen in the present study for further analysis because they contain CPEs in their 3'UTRs (Figure 6) and because ABP was shown to be a CPEB target (Theis et al., 2011, in revision). The protein levels of both ABP (GRIP2) and GRIP1 were analyzed in CPEB2 overexpressing mice compared to their control littermates. With immunoblotting, no change in either of the protein levels was

observed (Figures 31, 32). It is widely known that not all the mRNAs containing CPEs in their 3'UTRs are repressed (Barkoff et al., 2000) and the translation of a particular mRNA might depend on the stoichiometry of the regulatory elements present in the 3'UTR. For example, ABP contains a single CPE in its 3'UTR (Figure 6) which might be not enough for repression to occur (Pique et al., 2008). In addition, the CPE is overlapping with the polyadenylation signal which might render the CPE non-functional according to the combinatorial code proposed. GRIP1 protein levels were also found to be unaltered in CPEB2 overexpressing mice. This could be due to the fact that even though there are more than two CPEs present in its 3'UTR (Figure 6), the distance between two CPEs might be too high for repression to occur.

5.7 CPEB2 might participate in neuron to glia communication by regulating EphA4 protein levels

EphA4 has two CPEs in its 3'UTR (Figure 8; Winter et al., 2008). To find out if CPEB2 regulates EphA4 translation in neurons, both *in vitro* and *in vivo* approaches were used. In an *in vitro* approach, cells were transfected with CPEB2-FLAG and EphA4 3'UTR construct and the CPEB2 protein interacting with EphA4 3'UTR was co-immunoprecipitated using FLAG antibodies. It was found that CPEB2 interacts specifically with the EphA4 3'UTR (Figure 34). In an *in vivo* approach, the protein levels of EphA4 were analyzed in CPEB2 overexpressing mice. With the overexpression of CPEB2, EphA4 protein levels were significantly decreased (Figure 33). Thus, from the current findings, EphA4 is identified as a new CPEB2 target in neurons.

Since EphA4 has been shown to interact with astrocytic ephrin-A3 ligand and modulates the glial glutamate transport (Filosa et al., 2009), the impact of neuronal CPEB2 on glutamate transporter, GLT-1 was investigated. The protein levels of GLT-1 were measured in CPEB2 overexpressing mice in comparison with their control littermates, but the protein levels were unaltered (result not shown). This might be due to the fact that the EphA4 protein levels were decreased by only 30% in CPEB2 overexpressing mice. As the complete knockout of EphA4 resulted in 100% elevated GLT-1 protein levels (Filosa et al., 2009), only 30% reduction of EphA4 might have an insufficient impact on GLT-1.

It is also known that either Eph receptors or ephrin ligands can function independent of each other (Pasquale, 2005), hence, in CPEB2 overexpressing mice, EphA4 might be functioning independent of the astrocytic ephrin-A3 ligand. Unlike the other ephrin receptors, EphA4 can interact with both classes of ligands: ephrin-A3 (Carmona et al., 2009; Filosa et al., 2009) and with ephrin-B2 and ephrin-B3 (Yamaguchi and Pasquale, 2004), it is possible that in CPEB2 overexpressing mice, EphA4 might be interacting with other ephrin ligands (other than the classical ephrin-A3 ligand) thereby not interfering with glutamate transport.

EphA4 knockout mice showed distorted spine architecture (Carmona et al., 2009). As EphA4 protein levels were reduced in CPEB2 overexpressing mice, the spine morphology might have been altered in CPEB2 overexpressing mice which needs to be further evaluated. In addition, theta burst (TBS) induced LTP is impaired in EphA4 null mutants (Filosa et al., 2009). So, it can be speculated that CPEB2 overexpressing mice might have deficiencies in TBS-induced LTP. The dysfunction of Eph receptors might lead to neurological disorders such as schizophrenia (Glantz and Lewis, 2000), autism and mental retardation (Kaufmann and Moser, 2000). So, by interfering with the translation of EphA4, CPEB2 might lead to one of the disorders which are yet to be investigated.

5.8 CPEB2 regulates each target mRNA differentially

Although the extent of translational regulation is determined by the phosphorylation status of CPEBs (either repression or activation), it is not known how precisely CPEBs regulate translation. It is also not clear, which factors in combination with CPEBs contribute to either repression or activation of bound mRNA. To better understand the CPEB mediated translational regulation, a combinatorial code has been proposed for cyclin B regulation by CPEB1 in *Xenopus* oocytes (Pique et al., 2008). This code explained that the extent of translational regulation by CPEB1 can be varied depending on the number and position of CPEs along the 3'UTR, the distance between a CPE and the polyadenylation sequence as well as on other elements surrounding the CPE.

In the present study, the impact of CPEB2 on the translation of several mRNAs was investigated. CPEB2 repressed the basal translation of β-catenin (Figure 27), GluR2 (Figure 29) and EphA4 (Figure 33); but it has no impact on the translation of GluR1 (Figure 30), GRIP1 (Figure 32) and ABP/GRIP2 (Figure 31). These results suggest that even though all

target mRNAs that were analyzed in the present study contain CPEs in their 3'UTRs, their translation was not affected in the same way. Among those mRNAs whose translation was repressed, the number and position of CPEs in their 3'UTRs is different. The 3'UTR of β-catenin contains three CPEs (Figure 5; Kundel et al., 2009), GluR2 contains several CPEs (bioinformatics analysis) and EphA4 contains two CPEs (Figure 8; Winter et al., 2008). The smallest distance between two CPEs is 70 nucleotides in EphA4, 71 nucleotides in GluR2 and 73 nucleotides in β-catenin. The translation of all these mRNAs was differentially repressed in CPEB2 overexpressing mice compared to their control littermates.

It was found that those mRNAs which have a single CPE in their 3'UTRs such as ABP, no basal repression of their protein levels was observed (Figure 31). ABP has a single CPE which is overlapping with poly(A) (Figure 6) and this might be making the CPE non-functional for repression according to the combinatorial code proposed. Even though GRIP1 and GluR1 contain two and three CPEs in their 3'UTRs respectively (Figures 6 and 30), their translation was not affected by CPEB2; it could be that the distance between two CPEs (160 nucleotides for GRIP1 and 434 nucleotides for GluR1) might be too big for repression to occur. With the increasing distance between two CPEs, the extent of repression is also getting weakened (Table 27). As CPEBs regulate specifically the translation process, the RNA levels should remain unaltered. To confirm the fact that CPEBs interfere only with translation, quantitative real time PCR was performed to analyze the transcript levels of the aforementioned target mRNAs whose protein levels were decreased in CPEB2 overexpressing mice. None of the transcript levels were changed between CPEB2 overexpressing mice and their control littermates (Figure 38).

In addition, the translation of β-catenin, GluR2 and EphA4 (whose translation was repressed in CPEB2 overexpressing mice) was not affected in CPEB2ΔZn overexpressing mice (Figure 36). This is because of the lack of the zinc finger essential for RNA binding in CPEB2ΔZn overexpressing mice. From these results, it can be concluded that CPEB2 differentially regulates each target mRNA and its regulation is dependent on the zinc finger. A summary of translational regulation of various targets obtained using CPEB2/CPEB2ΔZn overexpressing mice can be found below in table 27.

Target	No. of CPEs	Shortest distance between two CPEs (nucleotides)	Protein levels of respective targets with respect to their control littermates	
			In CPEB2 mice	In CPEB2ΔZn mice
EphA4	2	70	Decreased by 28%	No change
GluR2	14	71	Decreased by 66%	No change
β-catenin	3	73	Decreased by 49%	No change
ABP/GRIP2	1	Overlapping with poly (A)	No change	----
GRIP1	2	160	No change	----
GluR1	3	434	No change	----

Table 27: A summary of translational regulation of various targets using the set of CPEB2/CPEB2ΔZn overexpressing mice. Only in those mRNAs with two or more than two CPEs (GluR2, β-catenin, EphA4) with an optimal distance of ~70 nucleotides, the protein levels were repressed by CPEB2. Even if there are two or more than two CPEs (GRIP1 and GluR1), no repression was observed. The protein levels of GluR2, β-catenin, EphA4 were not changed in CPEB2ΔZn overexpressing mice indicating the importance of the zinc finger for RNA binding.

5.9 The presence of the zinc finger is essential for CPEB2 mediated translational regulation

The zinc finger, which is part of the RNA binding domain, is important for CPEBs in order to bind to target mRNAs, (Hake et al., 1998; Hagele et al., 2009). To investigate if the zinc finger is essential for CPEB2 binding, co-immunoprecipitation experiments were done in HeLa cells. HeLa cells were transfected either with full length or mutant CPEB2 fused to EGFP (CPEB2 or CPEB2ΔZn-EGFP) and the bound β-catenin mRNA was co-immunoprecipitated using CPEB2 serum. The binding of full length CPEB2 to β-catenin was significantly higher than mutant CPEB2 lacking the zinc finger where only residual binding was observed (Figure 28). This residual binding observed might be due to the interaction of CPEB2 with deadenylating enzymes such as pumilio, an RNA binding protein. Pumilio has been reported to interact with CPEB1 in *Xenopus* oocytes (Nakahata et al., 2001).

To confirm the above findings and to study the impact of RNA binding on translational regulation, experiments were done using CPEB2ΔZn overexpressing mice. Since the basal protein levels of all CPEB targets analyzed (β-catenin, GluR2 and EphA4) were decreased in CPEB2 overexpressing mice, the same proteins were analyzed in CPEB2ΔZn overexpressing mice. None of those were changed in these mice (Figure 36). Notably, CPEB2 and CPEB2ΔZn showed comparable expression of the transgenic proteins (Figures 21, 25). Since the zinc finger, which is essential for RNA binding, is not present in these mice, CPEB2 could not bind to any mRNA, hence no translational repression of the mRNAs was observed. Hence it can be concluded that the presence of the zinc finger is essential for CPEB2 for RNA binding.

5.10 CPEB2 might be a putative target for other CPEBs

The 3'UTR of CPEB2 was amplified from mouse brain cDNA and sequenced. In addition to the 3.8 kb long 3'UTR described for CPEB2 (Theis et al., 2003), the present work identified several PCR products with variable lengths (1217 bp, 1647 bp, 2690 bp and 3778 bp) (Figure 41). The sequencing of these PCR products revealed several CPEs as well as polyadenylation sequences. It is known that more than one 3'UTR is present for some of the mRNAs. For example, the AMPA receptor subunit GluR2 contains two transcripts (4 kb and 6 kb in size) which differ in their 3'UTRs (Kohler et al., 1994). Hence, it is possible that CPEB2, similar to GluR2, may have two different UTRs of variable lengths. They might have been generated by utilizing different polyadenylation sequences. But, it is not known which of the CPEs are functional and which polyadenylation element is being used. By cloning different lengths of UTRs and analyzing their functionality *in vitro*, one could find out which CPEs and poly (A)s are functional.

Transgenic mice with neuronal overexpression of dominant negative (DN) CPEB1 were generated (Theis et al., in revision). DN CPEB1 lacks the phosphorylation site in the regulatory domain and can't get activated by phosphorylation. DN-CPEB competes with the classical CPEBs (1-4) and occupies all the CPEs in the 3'UTR of target mRNAs. Hence, neither the translation of bound targets nor the activation of CPEBs by phosphorylation is allowed in these mice. CPEB3 contains CPEs in its 3'UTR and can be a putative target for other CPEBs. In DN-CPEB mice, the translation of both ABP (a CPEB target) and CPEB3 has been impaired (Theis et al., in revision) which indicates that CPEB3 is a target for other CPEBs. In the current study, CPEB2 was found to contain several CPEs, hence, it can be speculated that CPEB2 can be a putative target for other CPEBs. On the other hand, CPEB2 can also bind to other CPE containing CPEBs (CPEB1, 3 and 4) and regulates their translation.

6 Future directions

The present work revealed that CPEB2 represses the basal translation of β-catenin, GluR2 and EphA4 in neurons. In addition to these, many other mRNAs which contain CPEs in their 3'UTRs were proposed as putative CPEB targets (Du and Richter, 2005). Hence, the impact of CPEB2 on the translation of other target mRNAs in neurons should be analyzed; this will give insight into the role played by CPEB2 in neurons.

As CPEBs participate in the polyadenylation induced translation, neurons from hippocampal slices of CPEB2 overexpressing mice can be stimulated with glutamate which might induce phosphorylation of CPEB2. This in turn might result in the activation of translation of the bound mRNAs which can be analyzed by measuring their protein levels in comparison with control littermates. In an independent experiment, kainic acid (a glutamate receptor agonist) should be injected intracortically into mice which might also phosphorylate CPEB2 and enhance the translation of target mRNAs. CPEB1, 3 and 4 were shown to be present in the post synaptic density (PSD) (Huang et al., 2006). But, the subcellular localization of CPEB2 has not yet been investigated. Hence, synaptosomal fractions can be prepared to address this issue. These fractions should be stimulated with glutamate and the activity-induced protein synthesis of target mRNAs by CPEB2 should be studied similar to studies on CPEB1 (Shin et al., 2004).

Since decreased protein levels of GluR2 were observed in CPEB2 overexpressing mice, AMPA receptors might become calcium permeable which might eventually lead to glutamate excitotoxicity. To test this, electrophysiological experiments should be performed to analyze calcium permeability in these mice. Mice deficient in GluR2 were reported to have enhanced LTP (Jia et al., 1996). To find out if CPEB2 has a role in LTP via regulating GluR2 translation, LTP should be induced by stimulating CA1 pyramidal neurons in acute hippocampal slices from CPEB2 overexpressing mice (theta burst stimulations). For this experiment, CPEB2 mutant mice (CPEB2ΔZn) can be used as internal controls since they can't regulate translation due to their inability to bind to target mRNAs. In addition, CPEB2 overexpressing mice should be brought into the epilepsy model by performing intracortical kainate injections (Bedner et al., unpublished) and various parameters such as status epilepticus (SE), spontaneous seizures as well as morphological changes should be analyzed.

This will give a clue if the GluR2 deficiency (observed in CPEB2 overexpressing mice) might cause excess entry of calcium into the cell and thereby making neurons hyperexcitable.

EphA4 in neurons regulate glial glutamate transport via interaction with astrocytic ephrin-A3 ligand and participates in neuron to glia communication (Carmona et al., 2009; Filosa et al., 2009). Since EphA4 protein levels were decreased in CPEB2 overexpressing mice, without altering GLT-1 protein levels, the translation of other glial transporters (such as GLAST) should be analyzed in these mice.

Since the translation of β-catenin, GluR2 and EphA4 was repressed in CPEB2 overexpressing mice which might be linked to neurological disorders, the role of CPEB2 in these disorders should be analyzed thoroughly.

7 Summary

Among four members of the CPEB family, much less information is available for CPEB2. Although the expression of CPEB2 has been reported in mouse brain (Theis et al., 2003; Hagele et al., 2009; Turimella et al., in revision), the functional role of CPEB2 was not reported before. Hence, the present study was aimed to elucidate the functional role of CPEB2 in neurons of mouse hippocampus.

In the first part of my work, I have analyzed the expression pattern of all CPEBs (1-4) in different cells (neurons, astrocytes, NG2 glia and microglia) of the mouse brain by single-cell RT-PCR. The incidence of CPEBs expression was higher in neurons compared to the glial subtypes analyzed. Even though CPEBs were described before in mouse brain, no information is available about which isoforms are present in each cell type and across species. The present study gives detailed information of the isoform distribution across cell types and in different species.

In the second part of my work, I have studied the functional role of CPEB2 in mouse hippocampus. For that purpose, I have generated a set of CPEB2/CPEB2ΔZn transgenic mice using *tet*-OFF system (Lewandoski, 2001). These mice overexpressed either full length or mutant CPEB2 (which lacks the zinc finger essential for RNA binding) in pyramidal neurons of mouse hippocampus. Using immunofluorescence, I have confirmed the transgene expression in pyramidal neurons as well as in dendritic processes where CPEB2 could modulate local protein synthesis. By using this set of overexpressing mice, I have investigated the impact of CPEB2 on the translation of several mRNAs in neurons. CPEB2 was found to repress the basal translation of neuronal mRNAs such as β-catenin, GluR2 and EphA4. By regulating the translation of β-catenin, CPEB2 might regulate dendritic morphogenesis (Yu and Malenka, 2003) and participate in the Wnt signalling cascade (Clevers, 2006). As GluR2 dysfunction is associated with neurodegeneration and epilepsy, CPEB2, by regulating the translation of GluR2, might lead to pathological conditions. CPEB2 also repressed the translation of EphA4, a key player which modulates the glial glutamate transport via interacting with the astrocytic ephrin-A3 ligand (Carmona et al., 2009) and participates in neuron to glia communication. The knockout of EphA4 leads to enhanced glutamate transport (increased GLT-1 and GLAST protein levels) (Filosa et al., 2009), but GLT-1 protein levels were not altered in CPEB2 overexpressing mice. EphA4 protein levels were decreased only

by 30% in CPEB2 overexpressing mice. Since a complete knockout of EphA4 lead to enhanced glutamate transport, it could be that only 30% decrease in EphA4 protein levels might have an insufficient impact on GLT-1. But, it was found that with the astrocytic overexpression of another CPEB family member, CPEB3, the protein levels of GLT-1 were decreased (Vangoor et al., unpublished). Since the transcript levels of all the target mRNAs analyzed in the present study were not changed, it can be concluded that CPEB2 regulation happens at the level of translation.

I have also investigated the impact of RNA binding on the translation of CPEB target mRNAs *in vitro* as well as using CPEB2ΔZn overexpressing mice. By RNA co-immunoprecipitation, I have found that CPEB2 requires the zinc finger for RNA binding since only residual binding was observed with a mutant CPEB2 which lacks the zinc finger. In addition, I have analyzed the protein levels of β-catenin, GluR2 and EphA4 in CPEB2ΔZn overexpressing mice compared to their control littermates. Immunoblot analysis indicated that none of the protein levels were changed, indicating the importance of RNA binding for translational regulation. Since the zinc finger essential for RNA binding is not present in CPEB2ΔZn overexpressing mice, no translational regulation was observed.

In the last part of my work, I have studied the interaction of CPEB2 with other target mRNAs. More than one CPEB can regulate same target mRNA, which means CPEBs have an overlap in the binding specificity of target mRNAs. In the present study, I have investigated the interaction of CPEB2 with CamKIIα (a CPEB1 target) and Cx36 using RNA co-immunoprecipitation or luciferase reporter assays. I found that CPEB2 specifically interacted with CamKIIα, but with less affinity compared to CPEB1. CPEB2 also interacted with Cx36, which could be prevented by knocking down the endogenous as well as overexpressed CPEB2 in HeLa cells.

Taken together, by regulating the translation of several key players in neurons, CPEB2 might participate in synaptic plasticity, learning and memory as well as in neuron to glia communication. From the results obtained in the present study, the following scheme can be proposed for the possible role of CPEB2 in neurons (Figure 42).

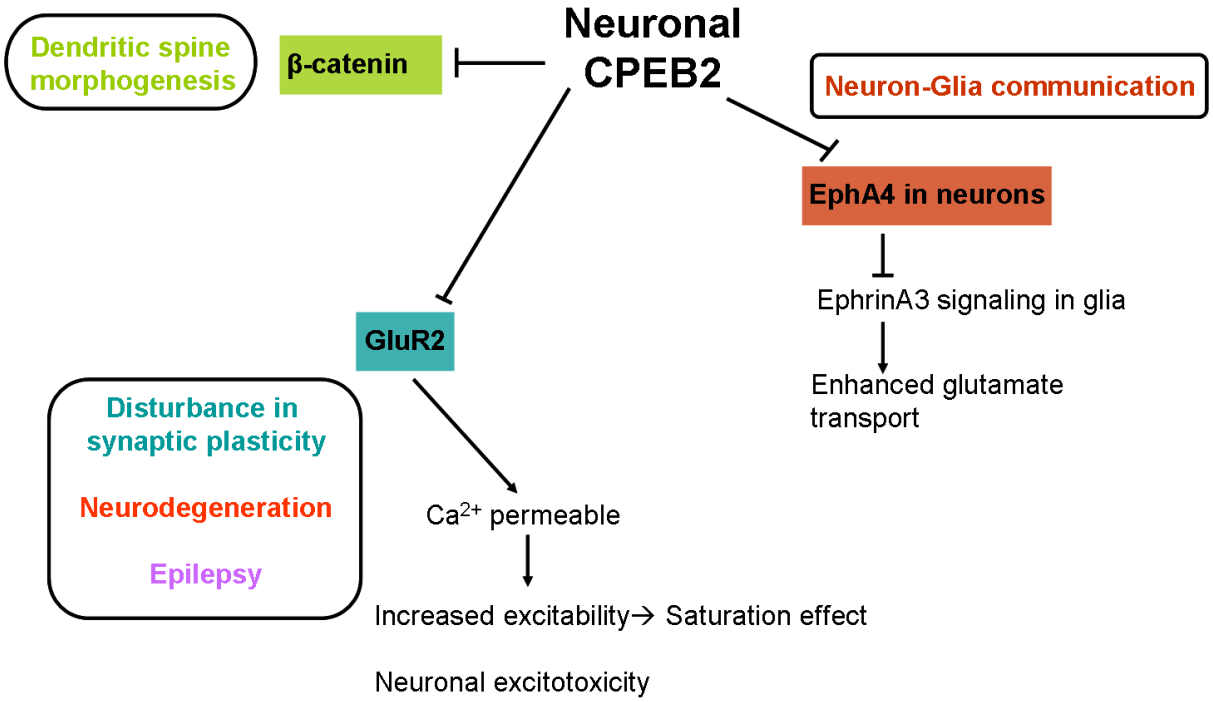

Figure 42: Scheme representing the possible role of CPEB2. By repressing the translation of several target mRNAs (β-catenin, GluR2 and EphA4), CPEB2 might impair various processes such as dendritic spine morphogenesis, neuron to glia communication as well as synaptic plasticity. By repressing the translation of GluR2, it might cause disturbances in synaptic plasticity and make neurons hyperexcitable, thereby leading to epilepsy and neurodegeneration.

8 References

Abel, T., and Lattal, K.M. (2001). Molecular mechanisms of memory acquisition, consolidation and retrieval. Curr Opin Neurobiol *11*, 180-187.

Alarcon, J.M., Hodgman, R., Theis, M., Huang, Y.S., Kandel, E.R., and Richter, J.D. (2004). Selective modulation of some forms of schaffer collateral-CA1 synaptic plasticity in mice with a disruption of the CPEB-1 gene. Learn Mem *11*, 318-327.

Andreassi, C., and Riccio, A. (2009). To localize or not to localize: mRNA fate is in 3'UTR ends. Trends Cell Biol *19*, 465-474.

Antar, L.N., Afroz, R., Dictenberg, J.B., Carroll, R.C., and Bassell, G.J. (2004). Metabotropic glutamate receptor activation regulates fragile x mental retardation protein and FMR1 mRNA localization differentially in dendrites and at synapses. J Neurosci *24*, 2648-2655.

Arikkath, J., and Reichardt, L.F. (2008). Cadherins and catenins at synapses: roles in synaptogenesis and synaptic plasticity. Trends Neurosci *31*, 487-494.

Atkins, C.M., Nozaki, N., Shigeri, Y., and Soderling, T.R. (2004). Cytoplasmic polyadenylation element binding protein-dependent protein synthesis is regulated by calcium/calmodulin-dependent protein kinase II. J Neurosci *24*, 5193-5201.

Bamji, S.X., Shimazu, K., Kimes, N., Huelsken, J., Birchmeier, W., Lu, B., and Reichardt, L.F. (2003). Role of beta-catenin in synaptic vesicle localization and presynaptic assembly. Neuron *40*, 719-731.

Barkoff, A.F., Dickson, K.S., Gray, N.K., and Wickens, M. (2000). Translational control of cyclin B1 mRNA during meiotic maturation: coordinated repression and cytoplasmic polyadenylation. Dev Biol *220*, 97-109.

Belachew, S., and Gallo, V. (2004). Synaptic and extrasynaptic neurotransmitter receptors in glial precursors' quest for identity. Glia *48*, 185-196.

Benson, D.L., and Tanaka, H. (1998). N-cadherin redistribution during synaptogenesis in hippocampal neurons. J Neurosci *18*, 6892-6904.

Berger-Sweeney, J., Zearfoss, N.R., and Richter, J.D. (2006). Reduced extinction of hippocampal-dependent memories in CPEB knockout mice. Learn Mem *13*, 4-7.

Bergles, D.E., Roberts, J.D., Somogyi, P., and Jahr, C.E. (2000). Glutamatergic synapses on oligodendrocyte precursor cells in the hippocampus. Nature *405*, 187-191.

Bettler, B., and Mulle, C. (1995). Review: neurotransmitter receptors. II. AMPA and kainate receptors. Neuropharmacology *34*, 123-139.

Binder, D.K., and Steinhauser, C. (2006). Functional changes in astroglial cells in epilepsy. Glia *54*, 358-368.

Boulter, J., Hollmann, M., O'Shea-Greenfield, A., Hartley, M., Deneris, E., Maron, C., and Heinemann, S. (1990). Molecular cloning and functional expression of glutamate receptor subunit genes. Science *249*, 1033-1037.

Braithwaite, S.P., Meyer, G., and Henley, J.M. (2000). Interactions between AMPA receptors and intracellular proteins. Neuropharmacology *39*, 919-930.

Bramham, C.R., and Wells, D.G. (2007). Dendritic mRNA: transport, translation and function. Nat Rev Neurosci *8*, 776-789.

Brusa, R., Zimmermann, F., Koh, D.S., Feldmeyer, D., Gass, P., Seeburg, P.H., and Sprengel, R. (1995). Early-onset epilepsy and postnatal lethality associated with an editing-deficient GluR-B allele in mice. Science *270*, 1677-1680.

Burnashev, N., Monyer, H., Seeburg, P.H., and Sakmann, B. (1992). Divalent ion permeability of AMPA receptor channels is dominated by the edited form of a single subunit. Neuron *8*, 189-198.

Cadigan, K.M., and Nusse, R. (1997). Wnt signaling: a common theme in animal development. Genes Dev *11*, 3286-3305.

Calo, L., Cinque, C., Patane, M., Schillaci, D., Battaglia, G., Melchiorri, D., Nicoletti, F., and Bruno, V. (2006). Interaction between ephrins/Eph receptors and excitatory amino acid receptors: possible relevance in the regulation of synaptic plasticity and in the pathophysiology of neuronal degeneration. J Neurochem *98*, 1-10.

Cao, Q., and Richter, J.D. (2002). Dissolution of the maskin-eIF4E complex by cytoplasmic polyadenylation and poly(A)-binding protein controls cyclin B1 mRNA translation and oocyte maturation. EMBO J *21*, 3852-3862.

Carmona, M.A., Murai, K.K., Wang, L., Roberts, A.J., and Pasquale, E.B. (2009). Glial ephrin-A3 regulates hippocampal dendritic spine morphology and glutamate transport. Proc Natl Acad Sci U S A *106*, 12524-12529.

Cho, K.O., Hunt, C.A., and Kennedy, M.B. (1992). The rat brain postsynaptic density fraction contains a homolog of the Drosophila discs-large tumor suppressor protein. Neuron *9*, 929-942.

Clevers, H. (2006). Wnt/beta-catenin signaling in development and disease. Cell *127*, 469-480.

Committee, E.N. (1997). Unified nomenclature for Eph family receptors and their ligands, the ephrins. Eph Nomenclature Committee. Cell *90*, 403-404.

Corpet, F. (1988). Multiple sequence alignment with hierarchical clustering. Nucleic Acids Res *16*, 10881-10890.

Cull-Candy, S., Kelly, L., and Farrant, M. (2006). Regulation of Ca2+-permeable AMPA receptors: synaptic plasticity and beyond. Curr Opin Neurobiol *16*, 288-297.

Dingledine, R., Borges, K., Bowie, D., and Traynelis, S.F. (1999). The glutamate receptor ion channels. Pharmacol Rev *51*, 7-61.

Doherty, J., and Dingledine, R. (2001). Reduced excitatory drive onto interneurons in the dentate gyrus after status epilepticus. J Neurosci *21*, 2048-2057.

Dong, H., O'Brien, R.J., Fung, E.T., Lanahan, A.A., Worley, P.F., and Huganir, R.L. (1997). GRIP: a synaptic PDZ domain-containing protein that interacts with AMPA receptors. Nature *386*, 279-284.

Du, L., and Richter, J.D. (2005). Activity-dependent polyadenylation in neurons. RNA *11*, 1340-1347.

Eberhart, D.E., Malter, H.E., Feng, Y., and Warren, S.T. (1996). The fragile X mental retardation protein is a ribonucleoprotein containing both nuclear localization and nuclear export signals. Hum Mol Genet *5*, 1083-1091.

Fiacco, T.A., Agulhon, C., Taves, S.R., Petravicz, J., Casper, K.B., Dong, X., Chen, J., and McCarthy, K.D. (2007). Selective stimulation of astrocyte calcium in situ does not affect neuronal excitatory synaptic activity. Neuron *54*, 611-626.

Filosa, A., Paixao, S., Honsek, S.D., Carmona, M.A., Becker, L., Feddersen, B., Gaitanos, L., Rudhard, Y., Schoepfer, R., Klopstock, T., Kullander, K., Rose, C.R., Pasquale, E.B., and Klein, R. (2009). Neuron-glia communication via EphA4/ephrin-A3 modulates LTP through glial glutamate transport. Nat Neurosci *12*, 1285-1292.

Garner, C.C., Tucker, R.P., and Matus, A. (1988). Selective localization of messenger RNA for cytoskeletal protein MAP2 in dendrites. Nature *336*, 674-677.

Gingras, A.C., Raught, B., and Sonenberg, N. (1999). eIF4 initiation factors: effectors of mRNA recruitment to ribosomes and regulators of translation. Annu Rev Biochem *68*, 913-963.

Gingrich, J.R., and Roder, J. (1998). Inducible gene expression in the nervous system of transgenic mice. Annu Rev Neurosci *21*, 377-405.

Glantz, L.A., and Lewis, D.A. (2000). Decreased dendritic spine density on prefrontal cortical pyramidal neurons in schizophrenia. Arch Gen Psychiatry *57*, 65-73.

Gossen, M., and Bujard, H. (1992). Tight control of gene expression in mammalian cells by tetracycline-responsive promoters. Proc Natl Acad Sci U S A *89*, 5547-5551.

Gossen, M., Freundlieb, S., Bender, G., Muller, G., Hillen, W., and Bujard, H. (1995). Transcriptional activation by tetracyclines in mammalian cells. Science *268*, 1766-1769.

Greger, I.H., Khatri, L., and Ziff, E.B. (2002). RNA editing at arg607 controls AMPA receptor exit from the endoplasmic reticulum. Neuron *34*, 759-772.

Groisman, I., Ivshina, M., Marin, V., Kennedy, N.J., Davis, R.J., and Richter, J.D. (2006). Control of cellular senescence by CPEB. Genes Dev *20*, 2701-2712.

Grooms, S.Y., Noh, K.M., Regis, R., Bassell, G.J., Bryan, M.K., Carroll, R.C., and Zukin, R.S. (2006). Activity bidirectionally regulates AMPA receptor mRNA abundance in dendrites of hippocampal neurons. J Neurosci *26*, 8339-8351.

Gumbiner, B.M. (1996). Cell adhesion: the molecular basis of tissue architecture and morphogenesis. Cell *84*, 345-357.

Hagele, S., Kuhn, U., Boning, M., and Katschinski, D.M. (2009). Cytoplasmic polyadenylation-element-binding protein (CPEB)1 and 2 bind to the HIF-1alpha mRNA 3'-UTR and modulate HIF-1alpha protein expression. Biochem J *417*, 235-246.

Hake, L.E., Mendez, R., and Richter, J.D. (1998). Specificity of RNA binding by CPEB: requirement for RNA recognition motifs and a novel zinc finger. Mol Cell Biol *18*, 685-693.

Hake, L.E., and Richter, J.D. (1994). CPEB is a specificity factor that mediates cytoplasmic polyadenylation during Xenopus oocyte maturation. Cell *79*, 617-627.

Harris, K.M., and Kater, S.B. (1994). Dendritic spines: cellular specializations imparting both stability and flexibility to synaptic function. Annu Rev Neurosci *17*, 341-371.

Higuchi, M., Single, F.N., Kohler, M., Sommer, B., Sprengel, R., and Seeburg, P.H. (1993a). RNA editing of AMPA receptor subunit GluR-B: a base-paired intron-exon structure determines position and efficiency. Cell *75*, 1361-1370.

Higuchi, R., Fockler, C., Dollinger, G., and Watson, R. (1993b). Kinetic PCR analysis: real-time monitoring of DNA amplification reactions. Biotechnology (N Y) *11*, 1026-1030.

Hirai, H., Maru, Y., Hagiwara, K., Nishida, J., and Takaku, F. (1987). A novel putative tyrosine kinase receptor encoded by the eph gene. Science *238*, 1717-1720.

Hosoda, N., Funakoshi, Y., Hirasawa, M., Yamagishi, R., Asano, Y., Miyagawa, R., Ogami, K., Tsujimoto, M., and Hoshino, S. (2011). Anti-proliferative protein Tob negatively regulates CPEB3 target by recruiting Caf1 deadenylase. EMBO J *30*, 1311-1323.

Huang, Y.S., Carson, J.H., Barbarese, E., and Richter, J.D. (2003). Facilitation of dendritic mRNA transport by CPEB. Genes Dev *17*, 638-653.

Huang, Y.S., Kan, M.C., Lin, C.L., and Richter, J.D. (2006). CPEB3 and CPEB4 in neurons: analysis of RNA-binding specificity and translational control of AMPA receptor GluR2 mRNA. EMBO J *25*, 4865-4876.

Huntley, G.W., Gil, O., and Bozdagi, O. (2002). The cadherin family of cell adhesion molecules: multiple roles in synaptic plasticity. Neuroscientist *8*, 221-233.

Isaac, J.T., Ashby, M.C., and McBain, C.J. (2007). The role of the GluR2 subunit in AMPA receptor function and synaptic plasticity. Neuron *54*, 859-871.

Itoh, M., Nagafuchi, A., Yonemura, S., Kitani-Yasuda, T., and Tsukita, S. (1993). The 220-kD protein colocalizing with cadherins in non-epithelial cells is identical to ZO-1, a tight

junction-associated protein in epithelial cells: cDNA cloning and immunoelectron microscopy. J Cell Biol *121*, 491-502.

Jabs, R., Pivneva, T., Huttmann, K., Wyczynski, A., Nolte, C., Kettenmann, H., and Steinhauser, C. (2005). Synaptic transmission onto hippocampal glial cells with hGFAP promoter activity. J Cell Sci *118*, 3791-3803.

Jambhekar, A., and Derisi, J.L. (2007). Cis-acting determinants of asymmetric, cytoplasmic RNA transport. RNA *13*, 625-642.

Jankowsky, J.L., Slunt, H.H., Gonzales, V., Savonenko, A.V., Wen, J.C., Jenkins, N.A., Copeland, N.G., Younkin, L.H., Lester, H.A., Younkin, S.G., and Borchelt, D.R. (2005). Persistent amyloidosis following suppression of Abeta production in a transgenic model of Alzheimer disease. PLoS Med *2*, e355.

Jia, Z., Agopyan, N., Miu, P., Xiong, Z., Henderson, J., Gerlai, R., Taverna, F.A., Velumian, A., MacDonald, J., Carlen, P., Abramow-Newerly, W., and Roder, J. (1996). Enhanced LTP in mice deficient in the AMPA receptor GluR2. Neuron *17*, 945-956.

Jones, K.J., Korb, E., Kundel, M.A., Kochanek, A.R., Kabraji, S., McEvoy, M., Shin, C.Y., and Wells, D.G. (2008). CPEB1 regulates beta-catenin mRNA translation and cell migration in astrocytes. Glia *56*, 1401-1413.

Kahvejian, A., Svitkin, Y.V., Sukarieh, R., M'Boutchou, M.N., and Sonenberg, N. (2005). Mammalian poly(A)-binding protein is a eukaryotic translation initiation factor, which acts via multiple mechanisms. Genes Dev *19*, 104-113.

Kanai, Y., Dohmae, N., and Hirokawa, N. (2004). Kinesin transports RNA: isolation and characterization of an RNA-transporting granule. Neuron *43*, 513-525.

Kandel, E.R. (2001). The molecular biology of memory storage: a dialogue between genes and synapses. Science *294*, 1030-1038.

Kandel, E.R., Schwartz, J.H., and Jessell, T.M. (2000). Principles of neural science. McGraw-Hill, Health Professions Division: New York.

Kang, H., and Schuman, E.M. (1996). A requirement for local protein synthesis in neurotrophin-induced hippocampal synaptic plasticity. Science *273*, 1402-1406.

Karram, K., Goebbels, S., Schwab, M., Jennissen, K., Seifert, G., Steinhauser, C., Nave, K.A., and Trotter, J. (2008). NG2-expressing cells in the nervous system revealed by the NG2-EYFP-knockin mouse. Genesis *46*, 743-757.

Kaufmann, W.E., and Moser, H.W. (2000). Dendritic anomalies in disorders associated with mental retardation. Cereb Cortex *10*, 981-991.

Kiebler, M.A., Hemraj, I., Verkade, P., Kohrmann, M., Fortes, P., Marion, R.M., Ortin, J., and Dotti, C.G. (1999). The mammalian staufen protein localizes to the somatodendritic domain of cultured hippocampal neurons: implications for its involvement in mRNA transport. J Neurosci *19*, 288-297.

Kim, K.C., Oh, W.J., Ko, K.H., Shin, C.Y., and Wells, D.G. (2011). Cyclin b1 expression regulated by cytoplasmic polyadenylation element binding protein in astrocytes. J Neurosci *31*, 12118-12128.

Kistner, A., Gossen, M., Zimmermann, F., Jerecic, J., Ullmer, C., Lubbert, H., and Bujard, H. (1996). Doxycycline-mediated quantitative and tissue-specific control of gene expression in transgenic mice. Proc Natl Acad Sci U S A *93*, 10933-10938.

Klann, E., and Dever, T.E. (2004). Biochemical mechanisms for translational regulation in synaptic plasticity. Nat Rev Neurosci *5*, 931-942.

Kohler, M., Kornau, H.C., and Seeburg, P.H. (1994). The organization of the gene for the functionally dominant alpha-amino-3-hydroxy-5-methylisoxazole-4-propionic acid receptor subunit GluR-B. J Biol Chem *269*, 17367-17370.

Kornau, H.C., Schenker, L.T., Kennedy, M.B., and Seeburg, P.H. (1995). Domain interaction between NMDA receptor subunits and the postsynaptic density protein PSD-95. Science *269*, 1737-1740.

Kosik, K.S. (2006). The neuronal microRNA system. Nat Rev Neurosci *7*, 911-920.

Kullander, K., and Klein, R. (2002). Mechanisms and functions of Eph and ephrin signalling. Nat Rev Mol Cell Biol *3*, 475-486.

Kundel, M., Jones, K.J., Shin, C.Y., and Wells, D.G. (2009). Cytoplasmic polyadenylation element-binding protein regulates neurotrophin-3-dependent beta-catenin mRNA translation in developing hippocampal neurons. J Neurosci *29*, 13630-13639.

Kurihara, Y., Tokuriki, M., Myojin, R., Hori, T., Kuroiwa, A., Matsuda, Y., Sakurai, T., Kimura, M., Hecht, N.B., and Uesugi, S. (2003). CPEB2, a novel putative translational regulator in mouse haploid germ cells. Biol Reprod *69*, 261-268.

Kwak, S., and Weiss, J.H. (2006). Calcium-permeable AMPA channels in neurodegenerative disease and ischemia. Curr Opin Neurobiol *16*, 281-287.

Lee, S.H., Liu, L., Wang, Y.T., and Sheng, M. (2002). Clathrin adaptor AP2 and NSF interact with overlapping sites of GluR2 and play distinct roles in AMPA receptor trafficking and hippocampal LTD. Neuron *36*, 661-674.

Lewandoski, M. (2001). Conditional control of gene expression in the mouse. Nat Rev Genet *2*, 743-755.

Liu, S., Lau, L., Wei, J., Zhu, D., Zou, S., Sun, H.S., Fu, Y., Liu, F., and Lu, Y. (2004). Expression of Ca(2+)-permeable AMPA receptor channels primes cell death in transient forebrain ischemia. Neuron *43*, 43-55.

Liu, S.J., and Zukin, R.S. (2007). Ca2+-permeable AMPA receptors in synaptic plasticity and neuronal death. Trends Neurosci *30*, 126-134.

Liu, W., and Saint, D.A. (2002). A new quantitative method of real time reverse transcription polymerase chain reaction assay based on simulation of polymerase chain reaction kinetics. Anal Biochem *302*, 52-59.

Lyford, G.L., Yamagata, K., Kaufmann, W.E., Barnes, C.A., Sanders, L.K., Copeland, N.G., Gilbert, D.J., Jenkins, N.A., Lanahan, A.A., and Worley, P.F. (1995). Arc, a growth factor and activity-regulated gene, encodes a novel cytoskeleton-associated protein that is enriched in neuronal dendrites. Neuron *14*, 433-445.

Maccaferri, G., and Dingledine, R. (2002a). Complex effects of CNQX on CA1 interneurons of the developing rat hippocampus. Neuropharmacology *43*, 523-529.

Maccaferri, G., and Dingledine, R. (2002b). Control of feedforward dendritic inhibition by NMDA receptor-dependent spike timing in hippocampal interneurons. J Neurosci *22*, 5462-5472.

Malenka, R.C., and Bear, M.F. (2004). LTP and LTD: an embarrassment of riches. Neuron *44*, 5-21.

Martin, K.C., and Zukin, R.S. (2006). RNA trafficking and local protein synthesis in dendrites: an overview. J Neurosci *26*, 7131-7134.

Matthias, K., Kirchhoff, F., Seifert, G., Huttmann, K., Matyash, M., Kettenmann, H., and Steinhauser, C. (2003). Segregated expression of AMPA-type glutamate receptors and glutamate transporters defines distinct astrocyte populations in the mouse hippocampus. J Neurosci *23*, 1750-1758.

Mayford, M., Bach, M.E., Huang, Y.Y., Wang, L., Hawkins, R.D., and Kandel, E.R. (1996). Control of memory formation through regulated expression of a CaMKII transgene. Science *274*, 1678-1683.

Mayford, M., Mansuy, I.M., Muller, R.U., and Kandel, E.R. (1997). Memory and behavior: a second generation of genetically modified mice. Curr Biol *7*, R580-589.

McGrew, L.L., and Richter, J.D. (1990). Translational control by cytoplasmic polyadenylation during Xenopus oocyte maturation: characterization of cis and trans elements and regulation by cyclin/MPF. EMBO J *9*, 3743-3751.

Mendez, R., Murthy, K.G., Ryan, K., Manley, J.L., and Richter, J.D. (2000). Phosphorylation of CPEB by Eg2 mediates the recruitment of CPSF into an active cytoplasmic polyadenylation complex. Mol Cell *6*, 1253-1259.

Mendez, R., and Richter, J.D. (2001). Translational control by CPEB: a means to the end. Nat Rev Mol Cell Biol *2*, 521-529.

Mishra, S., Tripathi, R.D., Srivastava, S., Dwivedi, S., Trivedi, P.K., Dhankher, O.P., and Khare, A. (2009). Thiol metabolism play significant role during cadmium detoxification by Ceratophyllum demersum L. Bioresour Technol *100*, 2155-2161.

Miyashiro, K., Dichter, M., and Eberwine, J. (1994). On the nature and differential distribution of mRNAs in hippocampal neurites: implications for neuronal functioning. Proc Natl Acad Sci U S A *91*, 10800-10804.

Moore, M.J. (2005). From birth to death: the complex lives of eukaryotic mRNAs. Science *309*, 1514-1518.

Morimoto, K., Fahnestock, M., and Racine, R.J. (2004). Kindling and status epilepticus models of epilepsy: rewiring the brain. Prog Neurobiol *73*, 1-60.

Murai, K.K., Nguyen, L.N., Irie, F., Yamaguchi, Y., and Pasquale, E.B. (2003). Control of hippocampal dendritic spine morphology through ephrin-A3/EphA4 signaling. Nat Neurosci *6*, 153-160.

Murai, K.K., and Pasquale, E.B. (2003). 'Eph'ective signaling: forward, reverse and crosstalk. J Cell Sci *116*, 2823-2832.

Murai, K.K., and Pasquale, E.B. (2004). Eph receptors, ephrins, and synaptic function. Neuroscientist *10*, 304-314.

Murase, S., Mosser, E., and Schuman, E.M. (2002). Depolarization drives beta-Catenin into neuronal spines promoting changes in synaptic structure and function. Neuron *35*, 91-105.

Nakahata, S., Katsu, Y., Mita, K., Inoue, K., Nagahama, Y., and Yamashita, M. (2001). Biochemical identification of Xenopus Pumilio as a sequence-specific cyclin B1 mRNA-binding protein that physically interacts with a Nanos homolog, Xcat-2, and a cytoplasmic polyadenylation element-binding protein. J Biol Chem *276*, 20945-20953.

Nicoll, R.A., Tomita, S., and Bredt, D.S. (2006). Auxiliary subunits assist AMPA-type glutamate receptors. Science *311*, 1253-1256.

Nolte, C., Matyash, M., Pivneva, T., Schipke, C.G., Ohlemeyer, C., Hanisch, U.K., Kirchhoff, F., and Kettenmann, H. (2001). GFAP promoter-controlled EGFP-expressing transgenic mice: a tool to visualize astrocytes and astrogliosis in living brain tissue. Glia *33*, 72-86.

Noren, N.K., and Pasquale, E.B. (2004). Eph receptor-ephrin bidirectional signals that target Ras and Rho proteins. Cell Signal *16*, 655-666.

Nuber, S., Petrasch-Parwez, E., Winner, B., Winkler, J., von Horsten, S., Schmidt, T., Boy, J., Kuhn, M., Nguyen, H.P., Teismann, P., Schulz, J.B., Neumann, M., Pichler, B.J., Reischl, G., Holzmann, C., Schmitt, I., Bornemann, A., Kuhn, W., Zimmermann, F., Servadio, A., and Riess, O. (2008). Neurodegeneration and motor dysfunction in a conditional model of Parkinson's disease. J Neurosci *28*, 2471-2484.

Okuda, T., Yu, L.M., Cingolani, L.A., Kemler, R., and Goda, Y. (2007). beta-Catenin regulates excitatory postsynaptic strength at hippocampal synapses. Proc Natl Acad Sci U S A *104*, 13479-13484.

Osten, P., Srivastava, S., Inman, G.J., Vilim, F.S., Khatri, L., Lee, L.M., States, B.A., Einheber, S., Milner, T.A., Hanson, P.I., and Ziff, E.B. (1998). The AMPA receptor GluR2 C

terminus can mediate a reversible, ATP-dependent interaction with NSF and alpha- and beta-SNAPs. Neuron *21*, 99-110.

Pal, R., Agbas, A., Bao, X., Hui, D., Leary, C., Hunt, J., Naniwadekar, A., Michaelis, M.L., Kumar, K.N., and Michaelis, E.K. (2003). Selective dendrite-targeting of mRNAs of NR1 splice variants without exon 5: identification of a cis-acting sequence and isolation of sequence-binding proteins. Brain Res *994*, 1-18.

Pasquale, E.B. (2005). Eph receptor signalling casts a wide net on cell behaviour. Nat Rev Mol Cell Biol *6*, 462-475.

Pasquale, E.B. (2008). Eph-ephrin bidirectional signaling in physiology and disease. Cell *133*, 38-52.

Passafaro, M., Piech, V., and Sheng, M. (2001). Subunit-specific temporal and spatial patterns of AMPA receptor exocytosis in hippocampal neurons. Nat Neurosci *4*, 917-926.

Pickering, B.M., and Willis, A.E. (2005). The implications of structured 5' untranslated regions on translation and disease. Semin Cell Dev Biol *16*, 39-47.

Pique, M., Lopez, J.M., Foissac, S., Guigo, R., and Mendez, R. (2008). A combinatorial code for CPE-mediated translational control. Cell *132*, 434-448.

Pletnikov, M.V., Ayhan, Y., Nikolskaia, O., Xu, Y., Ovanesov, M.V., Huang, H., Mori, S., Moran, T.H., and Ross, C.A. (2008). Inducible expression of mutant human DISC1 in mice is associated with brain and behavioral abnormalities reminiscent of schizophrenia. Mol Psychiatry *13*, 173-186, 115.

Racca, C., Gardiol, A., and Triller, A. (1997). Dendritic and postsynaptic localizations of glycine receptor alpha subunit mRNAs. J Neurosci *17*, 1691-1700.

Richter, J.D. (2007). CPEB: a life in translation. Trends Biochem Sci *32*, 279-285.

Rouach, N., Byrd, K., Petralia, R.S., Elias, G.M., Adesnik, H., Tomita, S., Karimzadegan, S., Kealey, C., Bredt, D.S., and Nicoll, R.A. (2005). TARP gamma-8 controls hippocampal AMPA receptor number, distribution and synaptic plasticity. Nat Neurosci *8*, 1525-1533.

Rozen, S., and Skaletsky, H. (2000). Primer3 on the WWW for general users and for biologist programmers. Methods Mol Biol *132*, 365-386.

Sans, N., Vissel, B., Petralia, R.S., Wang, Y.X., Chang, K., Royle, G.A., Wang, C.Y., O'Gorman, S., Heinemann, S.F., and Wenthold, R.J. (2003). Aberrant formation of glutamate receptor complexes in hippocampal neurons of mice lacking the GluR2 AMPA receptor subunit. J Neurosci *23*, 9367-9373.

Sarkissian, M., Mendez, R., and Richter, J.D. (2004). Progesterone and insulin stimulation of CPEB-dependent polyadenylation is regulated by Aurora A and glycogen synthase kinase-3. Genes Dev *18*, 48-61.

Seifert, G., Huttmann, K., Schramm, J., and Steinhäuser, C. (2004). Enhanced relative expression of glutamate receptor 1 flip AMPA receptor subunits in hippocampal astrocytes of epilepsy patients with Ammon's horn sclerosis. J Neurosci *24*, 1996-2003.

Seifert, G., Schilling, K., and Steinhäuser, C. (2006). Astrocyte dysfunction in neurological disorders: a molecular perspective. Nat Rev Neurosci *7*, 194-206.

Seifert, G and Steinhäuser, C (2007). Structural and functional analyses of single cells by combining patch-clamp techniques with reverse transcription-polymerase chain reaction in Neuromethods, Vol 38: 373-409 (ed. Walz, Humana Press, Totowa, NJ, USA).

Shin, C.Y., Kundel, M., and Wells, D.G. (2004). Rapid, activity-induced increase in tissue plasminogen activator is mediated by metabotropic glutamate receptor-dependent mRNA translation. J Neurosci *24*, 9425-9433.

Shockett, P.E., and Schatz, D.G. (1996). Diverse strategies for tetracycline-regulated inducible gene expression. Proc Natl Acad Sci U S A *93*, 5173-5176.

Si, K., Giustetto, M., Etkin, A., Hsu, R., Janisiewicz, A.M., Miniaci, M.C., Kim, J.H., Zhu, H., and Kandel, E.R. (2003). A neuronal isoform of CPEB regulates local protein synthesis and stabilizes synapse-specific long-term facilitation in aplysia. Cell *115*, 893-904.

Song, I., and Huganir, R.L. (2002). Regulation of AMPA receptors during synaptic plasticity. Trends Neurosci *25*, 578-588.

Srivastava, S., Osten, P., Vilim, F.S., Khatri, L., Inman, G., States, B., Daly, C., DeSouza, S., Abagyan, R., Valtschanoff, J.G., Weinberg, R.J., and Ziff, E.B. (1998). Novel anchorage of GluR2/3 to the postsynaptic density by the AMPA receptor-binding protein ABP. Neuron *21*, 581-591.

Stebbins-Boaz, B., Cao, Q., de Moor, C.H., Mendez, R., and Richter, J.D. (1999). Maskin is a CPEB-associated factor that transiently interacts with elF-4E. Mol Cell *4*, 1017-1027.

Steward, O., and Levy, W.B. (1982). Preferential localization of polyribosomes under the base of dendritic spines in granule cells of the dentate gyrus. J Neurosci *2*, 284-291.

Sun, Y., Chen, X., and Xiao, D. (2007). Tetracycline-inducible expression systems: new strategies and practices in the transgenic mouse modeling. Acta Biochim Biophys Sin (Shanghai) *39*, 235-246.

Swanson, G.T., Kamboj, S.K., and Cull-Candy, S.G. (1997). Single-channel properties of recombinant AMPA receptors depend on RNA editing, splice variation, and subunit composition. J Neurosci *17*, 58-69.

Takeichi, M., and Abe, K. (2005). Synaptic contact dynamics controlled by cadherin and catenins. Trends Cell Biol *15*, 216-221.

Tang, S.J., and Schuman, E.M. (2002). Protein synthesis in the dendrite. Philos Trans R Soc Lond B Biol Sci *357*, 521-529.

Tay, J., and Richter, J.D. (2001). Germ cell differentiation and synaptonemal complex formation are disrupted in CPEB knockout mice. Dev Cell *1*, 201-213.

Theis, M., Si, K., and Kandel, E.R. (2003). Two previously undescribed members of the mouse CPEB family of genes and their inducible expression in the principal cell layers of the hippocampus. Proc Natl Acad Sci U S A *100*, 9602-9607.

Tiedge, H., and Brosius, J. (1996). Translational machinery in dendrites of hippocampal neurons in culture. J Neurosci *16*, 7171-7181.

Tiruchinapalli, D.M., Oleynikov, Y., Kelic, S., Shenoy, S.M., Hartley, A., Stanton, P.K., Singer, R.H., and Bassell, G.J. (2003). Activity-dependent trafficking and dynamic localization of zipcode binding protein 1 and beta-actin mRNA in dendrites and spines of hippocampal neurons. J Neurosci *23*, 3251-3261.

Togashi, H., Abe, K., Mizoguchi, A., Takaoka, K., Chisaka, O., and Takeichi, M. (2002). Cadherin regulates dendritic spine morphogenesis. Neuron *35*, 77-89.

Tongiorgi, E., Righi, M., and Cattaneo, A. (1997). Activity-dependent dendritic targeting of BDNF and TrkB mRNAs in hippocampal neurons. J Neurosci *17*, 9492-9505.

Tsirka, S.E., Gualandris, A., Amaral, D.G., and Strickland, S. (1995). Excitotoxin-induced neuronal degeneration and seizure are mediated by tissue plasminogen activator. Nature *377*, 340-344.

Tsuzuki, K., Lambolez, B., Rossier, J., and Ozawa, S. (2001). Absolute quantification of AMPA receptor subunit mRNAs in single hippocampal neurons. J Neurochem *77*, 1650-1659.

Uchida, N., Honjo, Y., Johnson, K.R., Wheelock, M.J., and Takeichi, M. (1996). The catenin/cadherin adhesion system is localized in synaptic junctions bordering transmitter release zones. J Cell Biol *135*, 767-779.

Wallraff, A., Odermatt, B., Willecke, K., and Steinhauser, C. (2004). Distinct types of astroglial cells in the hippocampus differ in gap junction coupling. Glia *48*, 36-43.

Wang, X.P., and Cooper, N.G. (2009). Characterization of the transcripts and protein isoforms for cytoplasmic polyadenylation element binding protein-3 (CPEB3) in the mouse retina. BMC Mol Biol *10*, 109.

Wilczynska, A., Aigueperse, C., Kress, M., Dautry, F., and Weil, D. (2005). The translational regulator CPEB1 provides a link between dcp1 bodies and stress granules. J Cell Sci *118*, 981-992.

Winter, J., Roepcke, S., Krause, S., Muller, E.C., Otto, A., Vingron, M., and Schweiger, S. (2008). Comparative 3'UTR analysis allows identification of regulatory clusters that drive Eph/ephrin expression in cancer cell lines. PLoS One *3*, e2780.

Woods, D.F., and Bryant, P.J. (1991). The discs-large tumor suppressor gene of Drosophila encodes a guanylate kinase homolog localized at septate junctions. Cell *66*, 451-464.

Wu, L., Wells, D., Tay, J., Mendis, D., Abbott, M.A., Barnitt, A., Quinlan, E., Heynen, A., Fallon, J.R., and Richter, J.D. (1998). CPEB-mediated cytoplasmic polyadenylation and the regulation of experience-dependent translation of alpha-CaMKII mRNA at synapses. Neuron *21*, 1129-1139.

Wyszynski, M., Valtschanoff, J.G., Naisbitt, S., Dunah, A.W., Kim, E., Standaert, D.G., Weinberg, R., and Sheng, M. (1999). Association of AMPA receptors with a subset of glutamate receptor-interacting protein in vivo. J Neurosci *19*, 6528-6537.

Xia, J., Zhang, X., Staudinger, J., and Huganir, R.L. (1999). Clustering of AMPA receptors by the synaptic PDZ domain-containing protein PICK1. Neuron *22*, 179-187.

Yamaguchi, Y., and Pasquale, E.B. (2004). Eph receptors in the adult brain. Curr Opin Neurobiol *14*, 288-296.

Yamamoto, A., Lucas, J.J., and Hen, R. (2000). Reversal of neuropathology and motor dysfunction in a conditional model of Huntington's disease. Cell *101*, 57-66.

Yu, X., and Malenka, R.C. (2003). Beta-catenin is critical for dendritic morphogenesis. Nat Neurosci *6*, 1169-1177.

Zagulska-Szymczak, S., Filipkowski, R.K., and Kaczmarek, L. (2001). Kainate-induced genes in the hippocampus: lessons from expression patterns. Neurochem Int *38*, 485-501.

Zhou, R. (1998). The Eph family receptors and ligands. Pharmacol Ther *77*, 151-181.

Zoidl, G., Meier, C., Petrasch-Parwez, E., Zoidl, C., Habbes, H.W., Kremer, M., Srinivas, M., Spray, D.C., and Dermietzel, R. (2002). Evidence for a role of the N-terminal domain in subcellular localization of the neuronal connexin36 (Cx36). J Neurosci Res *69*, 448-465.

9 Appendix

A 9.1 Preparation of TOP10 chemically competent E. *coli*

Glycerol stocks were made from commercial TOP10 competent E. *coli* (Invitrogen). Equal volume of E. *coli* and sterile glycerol (for example, 50 µl TOP10 E. *coli* + 50 µl of sterile glycerol) were mixed and stored at -80^{o}C. From this stock, a loop full of E. *coli* was inoculated in 2.5 ml of LB broth with additives (20 mM $MgSO_4$ and 10 mM KCl). For preparing 100 ml of LB broth with additives, 10 ml of 20 mM $MgSO_4$ and 10 ml of 10 mM KCl were added to 80 ml of LB broth. The bacteria were grown at 37^{o}C overnight with 250 rpm shaking. From this overnight culture, 200 µl was taken and added to 5 ml of LB with additives and incubated at 37^{o}C for 1 h 30 min. During this time, 100 ml of LB with additives was prewarmed in a sterile flask at 37^{o}C for further use. After the incubation time, the OD was checked at 600 nm. The bacteria were grown until the OD was in the range of 0.7 – 0.8. When it reached the above range, the culture (5 ml) was poured into the 100 ml of prewarmed medium and grown for another 2 h and the OD checked. When the OD_{600nm} was ≥ 0.5, the growth was stopped by placing the flask on ice for 5 min. After 5 min, the culture was aliquoted into two 50 ml falcon tubes and centrifuged at 3,500 rpm for 5 min. The supernatant was discarded and each pellet was resuspended in 10 ml of TFBI buffer (30 mM K^+ acetate, 50 mM $MnCl_2$, 100 mM RbCl, 10 mM $CaCl_2$, 15% glycerol in dH_2O. The solution was sterile filtered and stored at 4^{o}C), incubated on ice for 10 min and then centrifuged at 3,500 rpm for 5 min. The supernatant was discarded and the pellets were resuspended each in 2 ml of TFBII buffer (10 mM morpholino propanesulfonic acid (MOPS) Na^+ salt, 75 mM $CaCl_2$, 10 mM RbCl, 15% glycerol in dH_2O. The solution was sterile filtered and stored at 4^{o}C). These competent E. *coli* were aliquoted (50 µl each) in sterile 1.5 ml eppendorf tubes and were immediately placed in liquid nitrogen for few minutes and then stored at -80^{o}C.

A 9.2 Single-cell RT-PCR

A 9.2.1 Expression of CPEB1 in neurons

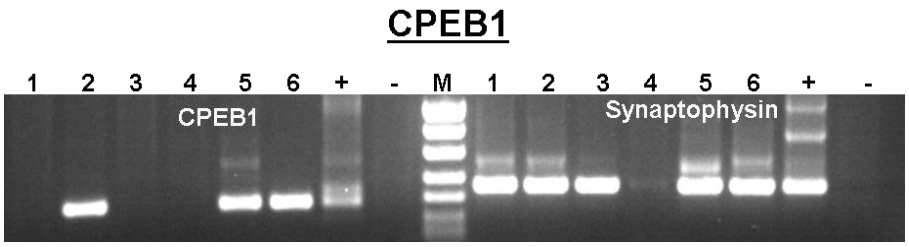

A 9.2.2 Expression of CPEB3 in neurons (A), astrocytes (B), NG2 glia (C) and microglia (D).

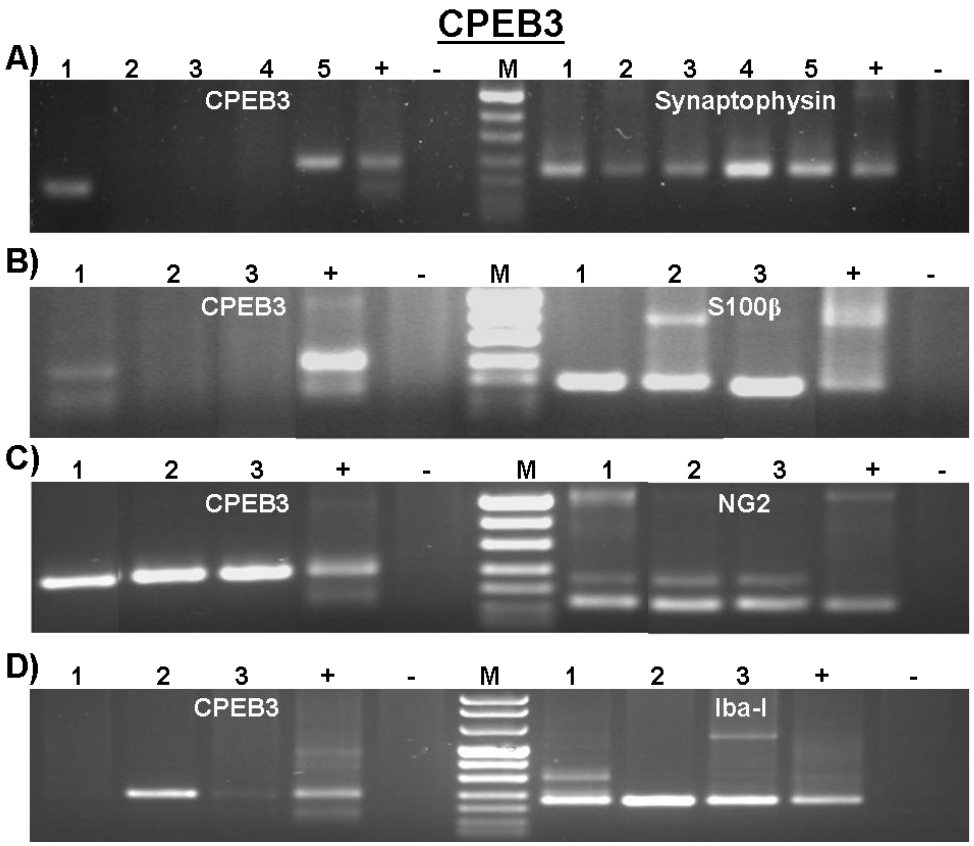

A 9.2.3 Expression of CPEB4 in neurons (A), astrocytes (B), NG2 glia (C) and microglia (D).

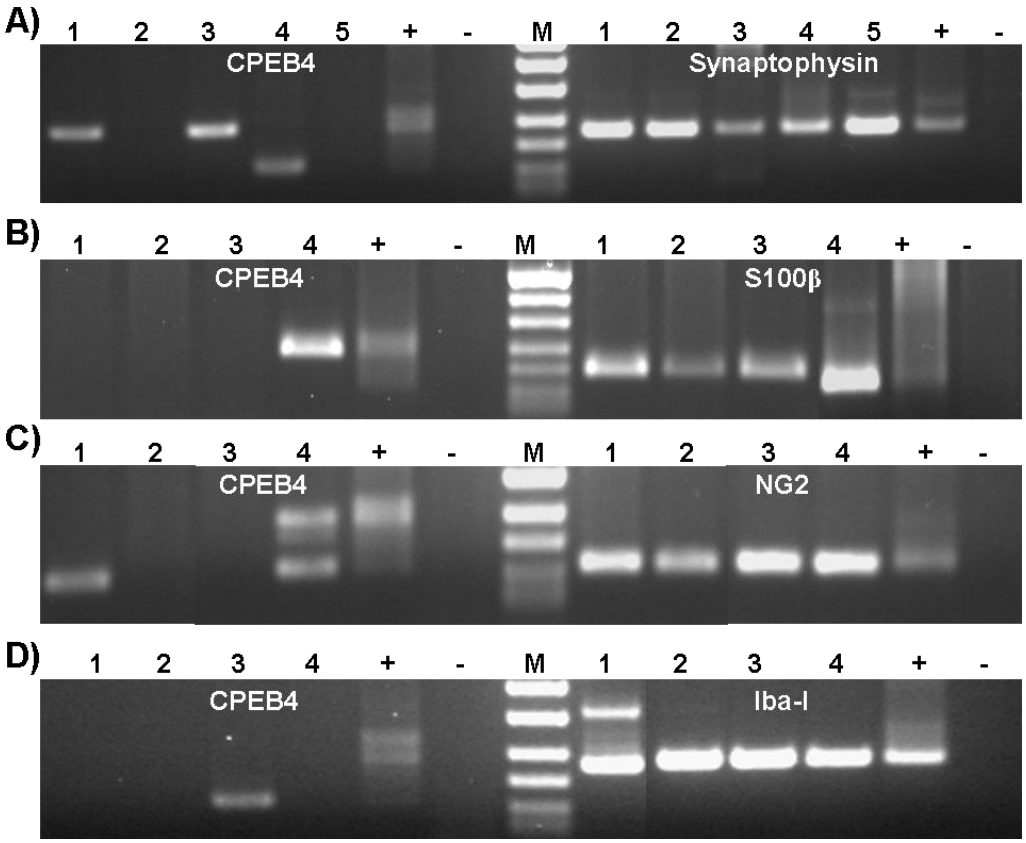

List of Figures

Fig 1: An experimental model to study activity-dependent synaptic plasticity in the rodent hippocampus
Fig 2: A schematic showing both early and late LTP
Fig 3: General protein structure of all four CPEBs
Fig 4: CPEB1 mediated translational regulation in neurons
Fig 5: The 3'UTR of β-catenin with CPEs and poly(A) marked
Fig 6: The 3'UTRs of ABP/GRIP2 and GRIP1 with CPEs and poly(A) marked
Fig 7: EphA4-ephrin-A3 bidirectional signalling
Fig 8: The 3'UTR of EphA4 with CPEs and poly(A) marked
Fig 9: Two variants of *tet*-inducible conditional transgenic system
Fig 10: The typical current patterns of different neural cells analyzed
Fig 11: The procedure of two round multiplex PCR.
Fig 12: CPEBs in rat and human brain hippocampus
Fig 13: CPEBs (1-4) in Primary Hippocampal Cultures (PHCs)
Fig 14: Single cell RT-PCR
Fig 15: Representative gel pictures showing CPEB2 expression across cell types
Fig 16: Infusion cloning of CPEB2/CPEB2ΔZn into pMM403-400.
Fig 17: Restriction digestion of CPEB2-pMM and CPEB2ΔZn-pMM minis with *Not*I
Fig 18: Constructs of CPEB2/CPEB2ΔZn-pMM for generating transgenic mice
Fig 19: Genotyping of new born mice: tTA and *tet*O PCRs
Fig 20: Expression pattern of CPEB2-EGFP in mouse hippocampus
Fig 21: Expression pattern of CPEB2-EGFP in CA1 region of mouse hippocampus
Fig 22: Analysis of CPEB2 transgene expression
Fig 23: Histogram showing extent of CPEB2 transgene expression
Fig 24: Colocalization of CPEB2 and MAP2
Fig 25: Immunofluorescence of CPEB2ΔZn-EGFP
Fig 26: β-catenin downregulation *in situ* in CPEB2 mice
Fig 27: Western blot analysis of β-catenin protein levels in CPEB2 mice
Fig 28: CPEB2- β-catenin Co-immunoprecipitation
Fig 29: Western blot analysis of GluR2 protein levels in CPEB2 mice
Fig 30: Western blot analysis of GluR1 protein levels in CPEB2 mice
Fig 31: Western blot analysis of ABP (GRIP2) levels in CPEB2 mice

Fig 32: Western blot analysis of GRIP1 protein levels in CPEB2 mice
Fig 33: Western blot analysis of EphA4 protein levels in CPEB2 mice
Fig 34: CPEB2-EphA4 Co-immunoprecipitation
Fig 35: Western blot analysis of Synaptophysin protein levels in CPEB2 mice
Fig 36: Western blot analysis of β-catenin, GluR2 and EphA4 protein levels in CPEB2ΔZn mice
Fig 37: Standard curves for estimating the efficiencies for real time PCR primers
Fig 38: Transcript levels of the putative targets in CPEB2 mice
Fig 39: Co-immunoprecipitation of CPEB1 and CPEB2 interacting with CamKIIα 3'UTR
Fig 40: Cx36 luciferase reporter assay
Fig 41: 3'RACE of CPEB2
Fig 42: Scheme representing the possible role of CPEB2 in neurons

List of tables

Table 1: A summary of multiple splice isoforms identified for each CPEB
Table 2: A list of proven CPEB targets in different cell types and their functions
Table 3: Neurological disorders associated with altered GluR2 expression and function
Table 4: A summary of proteins interacting with the C-terminus of GluR2
Table 5: Reaction mix used for reverse transcription reaction
Table 6: Master mix used for the first round of PCR
Table 7: PCR program used for the first round of PCR
Table 8: List or primers used for Single-cell RT-PCR
Table 9: Master mix used for nested PCR
Table 10: PCR program used for nested PCR
Table 11: Restriction digestion of pMM403-400 vector
Table 12: PCR reaction mix for amplification of CPEB2/CPEB2ΔZn-EGFP
Table 13: Infusion cloning of CPEB2/CPEB2ΔZn-EGFP into pMM403-400 vector
Table 14: Restriction digestion of CPEB2/CPEB2ΔZn-pMM minis with *Not*I
Table 15: Primers used for tTA and *tet*O PCRs
Table 16: Genotyping PCR master mix
Table 17: Reverse transcription master mix for mouse brain hippocampal RNA samples
Table 18: List of T*aq*man primers and probes used for real time PCR
Table 19: PCR master mix used for 3'RACE of CPEB2
Table 20: Touchdown PCR program used for 3'RACE of CPEB2
Table 21: Nested PCR program used for 3'RACE of CPEB2
Table 22: Summary of different isoforms observed for each CPEB
Table 23: Analysis of *tet*O-CPEB2-EGFP mice lines
Table 24: Analysis of *tet*O-CPEB2ΔZn-EGFP mice lines
Table 25: CPEB2 target mRNAs with their CPEB binding sites and polyadenylation sequences.
Table 26: The efficiencies (E) and slope values (R^2) of the T*aq*man primers analyzed
Table 27: A summary of translational regulation of various targets using the set of CPEB2/CPEB2ΔZn transgenic mice.

Curriculum Vitae

NAME	Sada Lakshmi Turimella
BORN IN	Guntur, India
MARITAL STATUS	married

.....

EDUCATION

Since 2007	PhD in the Institute of Cellular Neurosciences at the University of Bonn. Title of the thesis: "Impact of neuronal CPEB2 on the translation of mRNAs involved in synaptic plasticity". Scientific supervisor: Prof. Dr. Martin Theis.
2006 – 2007	Masters in Molecular Biology from University of Skövde, Sweden. Title of the thesis: "Characterization of CPEB-2, a translational regulator expressed in brain".
2002 – 2004	Masters in Biotechnology from Acharya Nagarjuna University, India. Title of the thesis: "Radiation processing to ensure microbiological safety of sprouts".
1999 – 2002	Bachelors in Microbiology from Acharya Nagarjuna University, India.
1987 – 1999	Secondary School education from B.S.S.S. High School, Repalle, India.

.....

PRESENTATION AT SCIENTIFIC MEETINGS

Turimella *et al*., 2011, 8th World Congress of Neuroscience, Florence, Italy.

Turimella *et al*., 2011, 9th Goettingen meeting of the German Neuroscience Society.

Turimella *et al*., 2010, Bonner Forum Biomedicine annual meeting, Bonn, Germany.

Turimella *et al*., 2010, Society For Neuroscience, San Diego, USA.

Turimella *et al*., 2009, 8th Goettingen meeting of the German Neuroscience Society.

Turimella *et al*., 2009. Advances in qPCR symposium, Berlin, Germany.

Turimella *et al*., 2008, 6th Federation of European Neuroscience Meeting (FENS), Geneva, Switzerland.

.....

PUBLICATIONS

Frinchi, M., Di Liberto, V., **Turimella, S.,** D'Antoni, F., Theis, M., Belluardo, N and Mudo, G. Connexin36 (Cx36) expression and protein detection in the mouse carotid body and myenteric plexus. *Acta Histochemica*, 2012 Aug 13.

Vangoor, VR., **Turimella, SL.,** Zhang, J., Kaczmarczyk, L., Bedner, P., Degen, J., Passlick, S., von Staden, E., Willecke, K., Derouiche, A., Jabs, R., Seifert, G., Steinhaeuser, C., and Theis, M. CPEB3 regulates the translation of Cx43 and Cx30, interasctrocytic coupling and adult neurogenesis (*PNAS*, in revision).

Turimella, SL., Vangoor, VR., Kaczmarczyk, L., Bedner, P., Karl, K., Zoidl, G., Seifert, G., Steinhaeuser, C., Kandel, ER and Theis, M. Expression of new CPEB1 and CPEB2 splice isoforms in hippocampal neurons and their RNA binding activities (*Journal of Comparative Neurology*, in revision).

Turimella, SL*., Vangoor, VR*., Bedner, P., Kaczmarczyk, L., Borojerdi, A., Karram, K., Trotter, J and Theis, M. Expression of Cytoplasmic Polyadenylation Element Binding Proteins 3 and 4 in neurons, microglial cells and NG2 glia (*Brain Research*, in revision).

Bedner, P., Dublin, P., **Turimella, SL.,** Vangoor, VR., Hüttmann, K., Kandel, ER., Steinhaeuser, C and Theis, M. The impact of Cytoplasmic Polyadenylation Element Binding Protein (CPEB)-mediated translational regulation on development and progression of temporal lobe epilepsy: Evidence from mice expressing a dominant negative CPEB in forebrain neurons (manuscript in preparation).